



รายงานการวิจัย

**Absorption and Luminescence Spectra of Transition Metal
Ions/Rare Earth Ions Containing Transparent Glass-Ceramics for
Electronic Devices**

ได้รับทุนอุดหนุนการวิจัยจาก
มหาวิทยาลัยเทคโนโลยีสุรนารี

ผลงานวิจัยเป็นความรับผิดชอบของหัวหน้าโครงการวิจัยแต่เพียงผู้เดียว

รหัสโครงการ SUT7-708-48-12-58



รายงานการวิจัย

**Absorption and Luminescence Spectra of Transition Metal
Ions/Rare Earth Ions Containing Transparent Glass-Ceramics for
Electronic Devices**

หัวหน้าโครงการ

Dr. Shigeki Morimoto

School of Ceramic Engineering

Institute of Engineering

Suranaree University of Technology

ได้รับทุนอุดหนุนการวิจัยจากมหาวิทยาลัยเทคโนโลยีสุรนารี ปีงบประมาณ 2548

ผลงานวิจัยเป็นความรับผิดชอบของหัวหน้าโครงการวิจัยแต่เพียงผู้เดียว

พฤศจิกายน 2549

Acknowledgement

This research was supported by Special Coordination Funds of Suranaree University of Technology, to which the author indebted. The author would like to thank Prof. Dr. Setsuhisa Tanabe, Kyoto University Japan, for emission measurement and also Dr. Hiroshi Nakajima, National Synchrotron Research Center (NSRC) in Thailand, for ligand field analysis. The author also thank Mrs Waraporn Emem and Mr. Chokchai Yatongchai for some part of sample preparation and measurement and Mrs. Pantipar Namsawangrungrueng for the preparation of this report.

Dr. Shigeki Morimoto

บทคัดย่อ

เป็นการศึกษาการเตรียมกลาสเซรามิกโปร่งใส (transparent glass-ceramics) ชนิดใหม่ลักษณะเฉพาะการดูดกลืนแสง (absorption) และการเปล่งแสง (emission) ของธาตุที่มีสภาพไวต่อแสง (active ion) เช่น ไอออนของธาตุทรานซิชัน (transition metal ion) และไอออนของธาตุแรร์เอิร์ท (rare earth ion) ที่อยู่ในกลาสเซรามิกโปร่งใส

กลาสเซรามิกโปร่งใสชนิดใหม่นี้จะแตกต่างกันขึ้นอยู่กับผลึกที่อยู่ในโครงสร้าง ได้แก่ $\text{Li}_2\text{O}\cdot\text{SiO}_2$, $\text{Li}_2\text{O}\cdot 2\text{SiO}_2$, BPO_4 และ AlPO_4 ซึ่งสามารถเตรียมได้จากอัตราส่วนที่เหมาะสม ขนาดและปริมาณของผลึกเหล่านี้จะอยู่ในช่วง 20-40 นาโนเมตรและ 30-70 % ตามลำดับ กลาสเซรามิกโปร่งใสที่มีความโปร่งใสสูงจะได้รับการควบคุมกระบวนการเกิดนิวเคลียสผลึก (nucleation) และการเกิดผลึก (crystallization) ที่เหมาะสม ซึ่งความโปร่งใสสามารถเทียบได้กับความโปร่งใสของแก้ว

กลาสเซรามิกที่มีความโปร่งใสสูงจะมีขนาดของผลึกที่เล็กมากทำให้ความแข็งแรงทางกลไม่แตกต่างจากแก้วมากนัก ซึ่งโดยปกติจะอยู่ที่ 50-100 MPa สำหรับงานที่ต้องการความแข็งแรงทางกลสูง จึงมีความจำเป็นอย่างยิ่งที่ต้องมีการปรับปรุงคุณสมบัติของกลาสเซรามิกโปร่งใสให้มีความแข็งแรงทางกลที่เพิ่มมากขึ้น กระบวนการ แลก เปลี่ยน ไอออน (ion exchange) เป็นวิธีที่มีความเหมาะสมในการเพิ่มความแข็งแรงทางกลและยังสามารถรักษาผิวของกลาสเซรามิกให้เรียบ แต่พบว่ากระบวนการนี้ไม่สามารถใช้ได้กับแก้วและกลาสเซรามิกที่มี Li_2O เป็นส่วนประกอบ

การศึกษาลักษณะเฉพาะการดูดกลืนแสงและการเปล่งแสงของ Cr ไอออนในกลาสเซรามิกโปร่งใสในกลาสเซรามิกชนิด spinel glass-ceramics พบว่า Cr^{3+} ions จะอยู่ที่ octahedral site ทำให้เกิดเป็นสี่ขมพูและเปล่งแสงสีแดง (R-line) ออกมา สำหรับ AlPO_4 glass-ceramics, Cr^{3+} ions มีความแรงของ ligand field อยู่ในระดับปานกลางเป็นผลทำให้สีไม่เปลี่ยนแปลงและเกิดการเปล่งแสงในช่วง NIR สำหรับกลาสเซรามิกโปร่งใสที่มีผลึกของ $\text{Li}_2\text{O}\cdot\text{SiO}_2$ และ $\text{Li}_2\text{O}\cdot 2\text{SiO}_2$ จะแสดงลักษณะที่พิเศษ คือ Cr^{3+} ไอออนจะอยู่ที่ tetrahedral site ในผลึกของ $\text{Li}_2\text{O}\cdot\text{SiO}_2$ ทำให้แก้วที่มีสีเขียวเปลี่ยนไปเป็นสีขมพูและเกิดการเปล่งแสงในช่วง NIR เมื่อถูกกระตุ้นด้วยแสงที่มีความยาวคลื่น 500 นาโนเมตร ในกลาสเซรามิกที่มีผลึกของ $\text{Li}_2\text{O}\cdot 2\text{SiO}_2$ จะมี Cr^{4+} เกิดขึ้น ซึ่ง Cr^{4+} เกิดขึ้นจากการลดลงของ Cr^{6+} ในระหว่างกระบวนการเกิดผลึกของ $\text{Li}_2\text{O}\cdot 2\text{SiO}_2$ และ Cr^{4+} จะอยู่ที่ tetrahedral site ในเฟสของแก้ว (SiO_2 glassy phase) และเกิดการเปล่งแสงในช่วง NIR (1000-1500 นาโนเมตร) เมื่อถูกกระตุ้นด้วย Laser diode ที่ให้ความยาวคลื่น 792 นาโนเมตร

สำหรับการศึกษาลักษณะการดูดกลืนแสงและการเปล่งแสงของไอออนของธาตุแรร์เอิร์ท เช่น Nd^{3+} , Er^{3+} และ Pr^{3+} ในกลาสเซรามิกโปร่งใส พบว่าความเข้มในการดูดกลืนแสงและตำแหน่งของไอออนในกลาสเซรามิกไม่มีการเปลี่ยนแปลงซึ่งต่างจากไอออนของธาตุทรานซิชัน และยังพบว่าเกิด up-conversion emission ขึ้นกับไอออนของธาตุเหล่านี้ในกลาสเซรามิก

Abstract

The preparation of new type transparent glass-ceramics was investigated, and the absorption and emission characteristics of active ions such as transition metal ions and rare earth ions in transparent glass-ceramics were also investigated.

The new type transparent glass-ceramics based on $\text{Li}_2\text{O}\cdot 2\text{SiO}_2$, $\text{Li}_2\text{O}\cdot \text{SiO}_2$, BPO_4 and AlPO_4 crystals can be prepared using corresponding base glass composition. The size and amount of these crystals are 20-40 nm and 30-70 %, respectively. Highly transparent glass-ceramics also were obtained by controlling heat treatment for nucleation and crystallization condition, and their transparency is comparable with that of glass.

However, the mechanical strength of very fine grained transparent glass-ceramics is not so different from that of conventional glass, usually 50-100 MPa. Higher mechanical strength of transparent glass-ceramics is required for certain application area. Although ion exchange method is a favorable method to increase the mechanical strength keeping surface flatness of transparent glass-ceramics, it is found that this method can not be applied for Li_2O -containing glass and glass-ceramics.

The absorption and emission characteristics of Cr ion in various transparent glass-ceramics were investigated. The Cr^{3+} ion in spinel glass-ceramics occupies strong octahedral site and appears to be pink color, and emits strong sharp red light(R-line). On the contrary, in AlPO_4 glass-ceramics, Cr^{3+} ion is in intermediate ligand field strength, and hence color does not change and an usual emission is observed in NIR region. It should be noted that Cr ion in $\text{Li}_2\text{O}\cdot \text{SiO}_2$ and $\text{Li}_2\text{O}\cdot 2\text{SiO}_2$ crystals based transparent glass-ceramics exhibits anomalous behavior. It is found that Cr^{3+} ion occupies tetrahedral site in $\text{Li}_2\text{O}\cdot \text{SiO}_2$ crystal, the color changes from green of glass to pink. The emission near NIR is observed under the excitation of around 500 nm light. In $\text{Li}_2\text{O}\cdot 2\text{SiO}_2$ transparent glass-ceramics, the existence of Cr^{4+} ion is confirmed. The Cr^{4+} ion was formed by the reduction of Cr^{6+} during crystallization of $\text{Li}_2\text{O}\cdot 2\text{SiO}_2$ crystal, and it occupies tetrahedral site in residual high SiO_2 glassy phase. The characteristic emission around NIR region(1000-1500 nm) was observed under the excitation of 792 nm laser diode.

The absorption and emission characteristics of rare earth ions such as Nd^{3+} , Er^{3+} , Pr^{3+} in transparent glass-ceramics were investigated. The absorption intensity and position of these ions in glass-ceramics do not change unlike transition metal ions. The up-conversion emission was observed for these ions in glass-ceramics.

Contents

	page
Acknowledgement	i
Abstract(Thai)	ii
Abstract(English)	iii
Contents	iv
Tables	v
Figures	vi
I. Introduction	1
II. Preparation of highly transparent AlPO ₄ system glass-ceramics	3
III. Preparation and properties of highly transparent Li ₂ O·2SiO ₂ system glass-ceramics	14
3.1. Strength of Li ₂ O·2SiO ₂ transparent glass-ceramics	14
3.2. Strengthening of Li ₂ O·2SiO ₂ transparent glass-ceramics by ion exchange	23
IV. Absorption and emission characteristics of Cr ions in transparent glass-ceramics	30
4.1. Cr ³⁺ ion in spinel transparent glass-ceramics	30
4.2. Optical properties of Cr ³⁺ ions in Li ₂ O·SiO ₂ transparent glass-ceramics	36
4.3. Cr ³⁺ in AlPO ₄ system transparent glass-ceramics	48
4.4. Cr ⁴⁺ in Li ₂ O·2SiO ₂ system transparent glass-ceramics	53
V. Absorption and emission behavior of rare-earth ions in transparent glass-ceramics	61
5.1. Nd ³⁺ and Er ³⁺ ions in Li ₂ O·2SiO ₂ and AlPO ₄ system transparent glass-ceramics	61
5.2. Pr ³⁺ ion in Li ₂ O·2SiO ₂ transparent glass-ceramics	68
VI. Summary	72
References	
Appendix A	
Appendix B	
Appendix C	
Appendix D	

Tables

	page
Table 1. Thermal properties of glasses studied.	7
Table 2. Properties of glass-ceramics.	11
Table 3. properties of glass and glass-ceramics.	17
Table 4. Fracture strength of glass and glass-ceramics before and after ion exchange.	25
Table 5. Calculated density, molar volume and thermal expansion coefficient of Li-, Na- and K-glasses.	27
Table 6. Crystalline phase, percent crystallinity and crystal size of transparent glass-ceramics.	39
Table 7. Ligand field parameters of Cr ³⁺ ions in glass and glass-ceramics.	44
Table 8. Ligand field parameters of Cr ³⁺ ions in various hosts.	49
Table 9. Multi -peak fitting for absorption spectrum of Cr ⁴⁺ ions in transparent glass-ceramics.	58
Table 10. Composition of glasses in Li ₂ O·2SiO ₂ and AlPO ₄ transparent glass-ceramics.	62

Figures

	page
Figure 1. Thermal expansion curves of glasses. Heating rate: 5°C/min.	4
Figure 2. SEM photos of glasses after heat treatment.	6
(A). No.1 glass: 550°C—10h, 800°C—5h.	
(B). No.2 glass: 550°C—10h, 750°C—5h.	
Figure 3. XRD patterns of No.3 and No.4 glass-ceramics.	8
Insert denotes heat treatment condition: °C—h.	
Figure 4. Relationship between crystal size and percent crystallinity and heat treatment temperature of No.3 and No.4 glasses. 1st heat treatment: 510°C—10h for No.3 glass, 520°C—5h for No.4 glass.	9
Figure 5. SEM photos of No.3 glass.	10
(A). 510°C—10h, 550°C—20h (B). 510°C—10h, 600°C—10h (C). 510°C—10h, 650°C—50h.	
Figure 6. Transmission curves of glass and glass-ceramics.	12
Sample thickness: 3 mm.	
Figure 7. XRD patterns of glass-ceramics.	16
Figure 8. Effect of percent crystallinity on the fracture strength.	18
Figure 9. Effect of crystal size on the fracture strength of glass and glass-ceramics.	20
Figure 10. Fracture strength of glass and glass-ceramics after ion exchange.	26
Figure 11. SEM photos of glass and glass-ceramics after ion exchange.	28
Figure 12. Absorption and differential spectra of glass and glass-ceramics.	32
$\Delta[\text{O.D.}(\text{cm}^{-1})] = [\text{O.D.}(\text{cm}^{-1})]_{\text{glass-ceramics}} - [\text{O.D.}(\text{cm}^{-1})]_{\text{glass}}$	
Figure 13. Emission spectra of glass and glass-ceramics under the excitation of 532 and 632 nm.	33
Figure 14. XRD patterns of Li ₂ O·SiO ₂ transparent glass-ceramics.	37
Figure 15. Absorption spectra of glass and glass-ceramics.	40
Glass-ceramics: 1st heat treatment: 510°C—10h.	
Figure 16. Differential spectra of glass and glass-ceramics.	41
Glass-ceramics: 1st heat treatment: 510°C—10h.	
$\Delta[\text{O.D.}(\text{cm}^{-1})] = [\text{O.D.}(\text{cm}^{-1})]_{\text{glass-ceramics}} - [\text{O.D.}(\text{cm}^{-1})]_{\text{glass}}$	
Figure 17. Relation between absorption intensity of new bands and % crystallinity.	43
Figure 18. Emission spectra of glass and glass-ceramics at room temperature.	46

	page
Figure 19. Absorption and differential spectra of glass and glass-ceramics.	50
$\Delta[\text{O.D.}(\text{cm}^{-1})] = [\text{O.D.}(\text{cm}^{-1})]_{\text{glass-ceramics}} - [\text{O.D.}(\text{cm}^{-1})]_{\text{glass}}$	
Figure 20. Emission spectra of glass and glass-ceramics at room temperature.	51
Glass-ceramics: 510°C–10h, 650°C–50h.	
Figure 21. Absorption and differential spectra of glass and glass-ceramics.	55
Glass-ceramics: 1st heat treatment: 510°C–10h.	
$\Delta[\text{O.D.}(\text{cm}^{-1})] = [\text{O.D.}(\text{cm}^{-1})]_{\text{glass-ceramics}} - [\text{O.D.}(\text{cm}^{-1})]_{\text{glass}}$	
Figure 22. Relationship between absorption intensity and heating temperature.	56
Heating time: 5h at various temperature.	
1st heat treatment: 510°C–10h., Cr ₂ O ₃ =0.4%.	
Figure 23. Emission spectra of glass and glass-ceramics under the excitation of 792 nm laser diode.	57
Figure 24. Relation between decrease in [Cr ⁶⁺] and increase in [Cr ⁶⁺] in Li ₂ O·SiO ₂ transparent glass-ceramics.	59
Figure 25. Transmission spectra of Nd ³⁺ doped Li ₂ O·2SiO ₂ [L·2S] and AlPO ₄ transparent glass-ceramics.	63
Figure 26. Transmission spectra of Er ³⁺ doped Li ₂ O·2SiO ₂ [L·2S] and AlPO ₄ transparent glass-ceramics.	64
Figure 27. Up-conversion spectra of Nd ³⁺ doped Li ₂ O·2SiO ₂ [L·2S] and AlPO ₄ transparent glass-ceramics.	65
Figure 28. Up-conversion spectra of Er ³⁺ doped Li ₂ O·2SiO ₂ [L·2S] and AlPO ₄ transparent glass-ceramics.	66
Figure 29. Absorption and emission spectra of Pr ³⁺ doped glass and transparent glass-ceramics.	69
(a). Absorption spectra.	
(b). Emission spectra.	
Figure 30. Emission spectra of Pr ³⁺ doped glass and transparent glass-ceramics at room temperature.	70

Chapter I

Introduction

There has been some interesting exploratory research in recent years on the luminescent behavior of transparent glasses and glass-ceramics doped with chromium^(1,2). Because Cr^{3+} absorbs broadly in the visible wavelength range yet can fluoresce in the near infrared (1 μm or 1000 nm) when incorporated in certain inorganic phases, it has been considered as a key luminescent ion for potential application in tunable lasers and in solar collector applications⁽³⁾.

Glasses have an enough wavelength gap between Cr^{3+} absorption and fluorescence (Stokes shift), but the quantum efficiency is generally poor, below 15 %. Certain crystalline phases like aluminum phosphate (AlPO_4) and Alexandrite (BeAl_2O_4) have similar shift, but are highly efficient-near 90 %. Transparent glass-ceramics, polycrystalline materials with very fine grain size, often less than 100 nm, are currently being considered as hosts for luminescent ions^(1,4). These materials can be formed as glasses into flat sheet, and clearly warrant further study. Because a number of different crystal structure can be developed in highly transparent glass-ceramics with a wide variety of potential fluorescent doping ions and combinations available.

Here, the preparation of special transparent glass-ceramics is investigated and the emission and absorption spectra of transition metal ions and rare-earth ions are also investigated in transparent glass-ceramics in order to study the process of production of glass-ceramics for opt-electronics or photonics devices and substrate, especially, to obtain the desired materials, highly transparent glass-ceramics, by controlling phase separation and crystallization. Next topics are investigated.

(1). Preparation of highly transparent AlPO_4 system glass-ceramics.

(2). Preparation and properties of highly transparent $\text{Li}_2\text{O}\cdot 2\text{SiO}_2$ system glass-ceramics.

(1). Strength of $\text{Li}_2\text{O}\cdot 2\text{SiO}_2$ transparent glass-ceramics.

(2). Strengthening of $\text{Li}_2\text{O}\cdot 2\text{SiO}_2$ transparent glass-ceramics by ion exchange.

(3). Absorption and emission characteristics of Cr^{3+} ions in transparent glass-ceramics.

(1). Cr^{3+} ions in Spinel type transparent glass-ceramics.

(2). Optical properties of Cr^{3+} ions in lithium metasilicate ($\text{Li}_2\text{O}\cdot \text{SiO}_2$) transparent glass-ceramics.

(3). Cr^{3+} in AlPO_4 system transparent glass-ceramics.

(4). Cr^{4+} in $\text{Li}_2\text{O}\cdot 2\text{SiO}_2$ system transparent glass-ceramics.

(4). Absorption and emission characteristics of rare-earth ions in transparent glass-ceramics.

(1). Nd^{3+} and Er^{3+} ions in $\text{Li}_2\text{O}\cdot 2\text{SiO}_2$ and AlPO_4 systems transparent glass-ceramics.

(2). Pr³⁺ ions in Li₂O·2SiO₂ transparent glass-ceramics.

Chapter II

Preparation of highly transparent AlPO_4 system glass-ceramics

1. Introduction

Glass-ceramics can be defined as a two-phase system comprising crystals that have been controllably grown from a parent glass by precise heat treatment. Optical properties of glass-ceramics have been impaired by the scattering losses. However, the ability some crystalline phases to partition rare-earth or transition metal ions into the crystal phase during crystallization has suggested that these materials could provide efficient lasing hosts⁽⁵⁻⁹⁾. Such systems would be capable of properties that are glass-like in most respects, except for the spectroscopy, which can be crystal-like.

In the early 1960s, transparency which was sufficiently good, so that imaging through short path length was possible, was observed in certain glass-ceramic materials⁽¹⁰⁾ and this eventually led to a commercial cookware application. This work was instrumental in the subsequent discovery of many new transparent glass-ceramic systems⁽¹¹⁻¹⁴⁾.

From the structure of glass point of view, network mixed glasses in the system $\text{SiO}_2\text{-Al}_2\text{O}_3\text{-P}_2\text{O}_5\text{(-B}_2\text{O}_3\text{+Na}_2\text{O)}$ are also special interest because all these may act as glass former⁽¹⁵⁾. It is well known that AlPO_4 crystal readily precipitates from glasses containing relatively large amount of Al_2O_3 and P_2O_5 ^(16,17). AlPO_4 crystal has all the three normal silica structures and has a characteristic functions^(18,19).

In order to obtain transparent glass-ceramics based on AlPO_4 crystal, the phase separation and crystallization behavior of glasses in the system $\text{SiO}_2\text{-Al}_2\text{O}_3\text{-P}_2\text{O}_5\text{(-B}_2\text{O}_3\text{+Na}_2\text{O)}$ was investigated, and highly transparent glass-ceramics could be successfully obtained.

2. Experimental

2.1. Sample preparation

Five glasses were prepared, and their compositions were expressed by $(80-X)\text{SiO}_2 \cdot X(\text{Al}_2\text{O}_3 + \text{P}_2\text{O}_5) \cdot 5\text{B}_2\text{O}_3 \cdot 15\text{Na}_2\text{O}$ (mol%, $X=20,30,40,45,50$). High purity silica sand, alumina and reagent grade chemicals of $(\text{NaPO}_3)_6$, $(\text{NH}_4)_2\text{HPO}_4$, H_3BO_3 and Na_2CO_3 (Carlo Erba) were used as raw materials. Batches corresponding to 200 g of glass were mixed thoroughly and pre-calcined at 400°C overnight to remove NH_3 . then they were melted in 100 ml Pt/Rh10 crucible according to melting schedule, $1550^\circ\text{C} - 3 \text{ h} \rightarrow 1500^\circ\text{C} - 1 \text{ h}$, in an electric furnace in air, and poured onto iron plate and pressed by another iron plate.

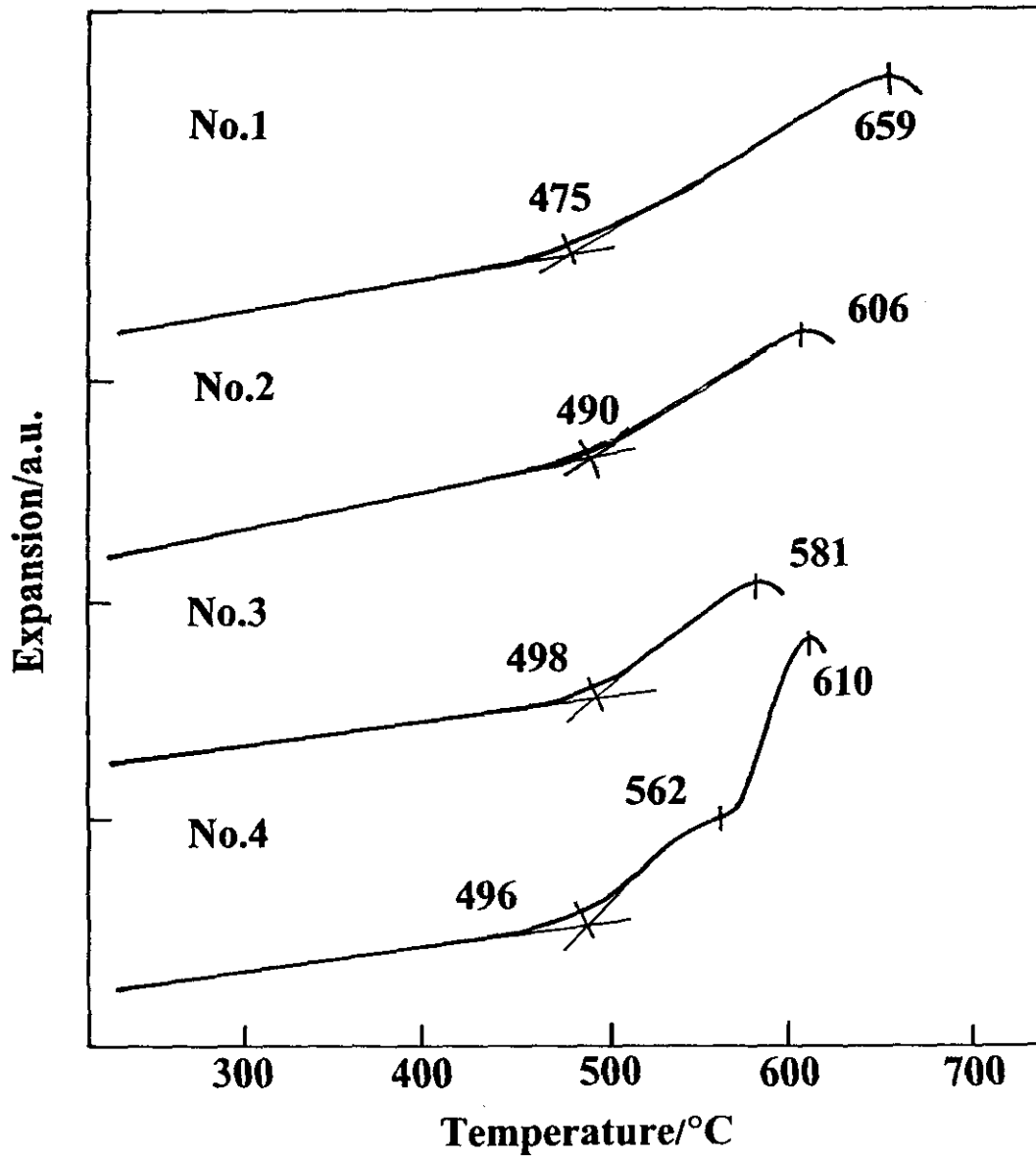


Fig. 1. Thermal expansion curves of glasses. Heating rate: 5°C/min.

They were then annealed at 510°C for 30 min and cooled to room temperature in the furnace.

The glasses were heat treated at just above the glass transition temperature (T_g) for 5 h to 10 h for nucleation and subsequently heat treated under various conditions for crystallization.

2.2. TDA and DTA

Glass transition temperature (T_g), dilatometric softening point (Y_p) and thermal expansion coefficient (α) of glasses were measured routinely using fused silica single push rod type dilatometer (Netzsch 402EP) at the heating rate of 5°C/min. The differential thermal analysis (DTA) was carried out using Perkin Elmer DTA-7 at the heating rate of 10°C/min.

2.3. XRD and SEM

Crystalline phases, percent crystallinity and crystalline size were examined by powder X-ray diffraction analysis (XRD, Bruker, AXS Model D5005) with Cu-K α radiation⁽²⁰⁾. The fine structure of glasses and glass-ceramics was observed by scanning electron microscope (SEM, JEOL JSM 6400). The fracture surface of sample was etched by 0.5% HF solution for 1 min at room temperature for SEM observation.

2.4. Optical spectroscopy

The transmission spectra of glass and glass-ceramics were measured using UV-VIS spectrometer (Varian, Carry 1E) in the range of 200 to 800 nm. The sample thickness was about 3 mm.

3. Results and discussion

3.1. Properties of glass

Transparent, bubble free glasses were obtained for No.1~4 composition ($X=20,30,40$ and 45), while No.5 composition ($X=50$) crystallized during casting.

Figure 1 shows the thermal expansion curves of glasses. T_g increases slightly with increases in X , while Y_p decreases markedly with increase in X . The temperature interval between T_g and Y_p of No.1, No.2 and No.3 glasses is very wide, 184°C, 116°C and 83°C, respectively. This abnormal expansion phenomenon is often observed in phase separated Na₂O-B₂O₃-SiO₂ glass. This suggests that the phase separation might occur in these glasses. For No.4 glass, on the other hand, two peaks of Y_p can be observed, lower one shows the true Y_p and higher one might indicate the starting of crystallization. Thermal expansion coefficient decreases with increase in X .



Fig. 2. SEM photos of glasses after heat treatment.

(A): No.1 glass, 550°C – 10 h and 800°C – 5 h.

(B): No.2 glass: 550°C – 10 h and 750°C – 5 h

DTA runs of No. 1 and No.2 glasses shows no exothermic or endothermic peaks, whilst in No.3 and No.4 glasses, the exothermic peaks due to crystallization appear. Thermal properties are summarized in Table 1. The crystallization temperature decreases significantly with increase in X.

3.2. Phase separation and crystallization

The appearance of phase separation was suggested in No.1 and No.2 glasses by thermal expansion measurement. Figure 2 shows the SEM photomicrographs of these glasses after heat treatment. The phase separation can be observed clearly in both glasses, and the size of which is about 100 nm. The matrix phase (continuous phase) might be $\text{Al}_2\text{O}_3\text{-P}_2\text{O}_5(\text{SiO}_2)^{(16)}$.

On the other hand, No.3 and No.4 glasses readily crystallize resulted in transparent to opaque glass-ceramics depending on the heat treatment condition. Figure 3 shows XRD patterns of these glasses Table 1. Thermal properties of glasses studied.

Glass		Dilatometer			DTA		
No.	X	$T_g/^\circ\text{C}$	$Y_p/^\circ\text{C}$	$\alpha/10^{-7}\text{K}^{-1}$	$T_g/^\circ\text{C}$	$T_{\text{onset}}/^\circ\text{C}$	$T_{\text{peak}}/^\circ\text{C}$
1	20	475	659	77.8	460	—	—
2	30	490	606	77.8	501	—	—
3	40	498	606	74.1	503	653	716
4	45	496	581	70.4	498	600	619
5	50	Crystallized during casting					

after heat treatment under various conditions, and only AlPO_4 crystal(tridymite type) was detected. Transparent glass-ceramics can be obtained by the heat treatment at relatively low temperature. Figure 4 shows the percent crystallinity (%C) and crystallite size (D, nm) of No.3 and No.4 glass-ceramics against heating temperature. The percent crystallinity increases gradually with increase in heating temperature, and reaches to about 50% for No.3 glass and about 60% for No.4 glass after the heat treatment of 700°C —5 h (1st heat treatment: 520°C —5 h). If all of P_2O_5 and Al_2O_3 would be spent for the formation of AlPO_4 crystal, the amount of AlPO_4 being precipitating is expected to be 57% for No.3 and 62% for No.4, respectively. Thus, the experimental results are thought to be reasonable (see Appendix).

The crystallite size increases rapidly with increase in temperature, and its size exceeds 100 nm by the heat treatment at above 700°C for No.3 glass and above 650°C for No.4 glass. The glass-ceramics

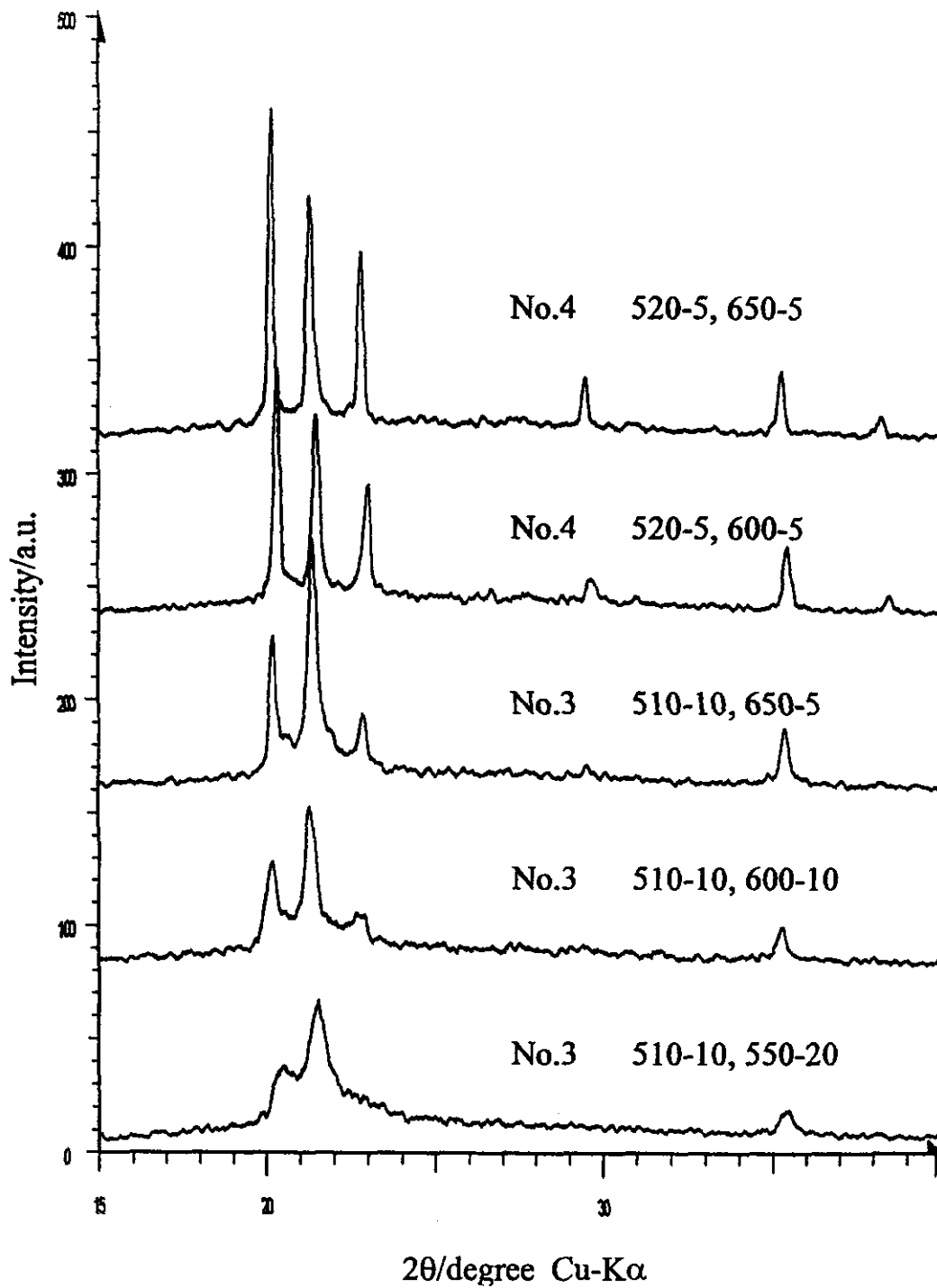


Fig. 3. XRD patterns of No.3 and No.4 glass-ceramics.
Insert denotes heat treatment condition: °C – h.

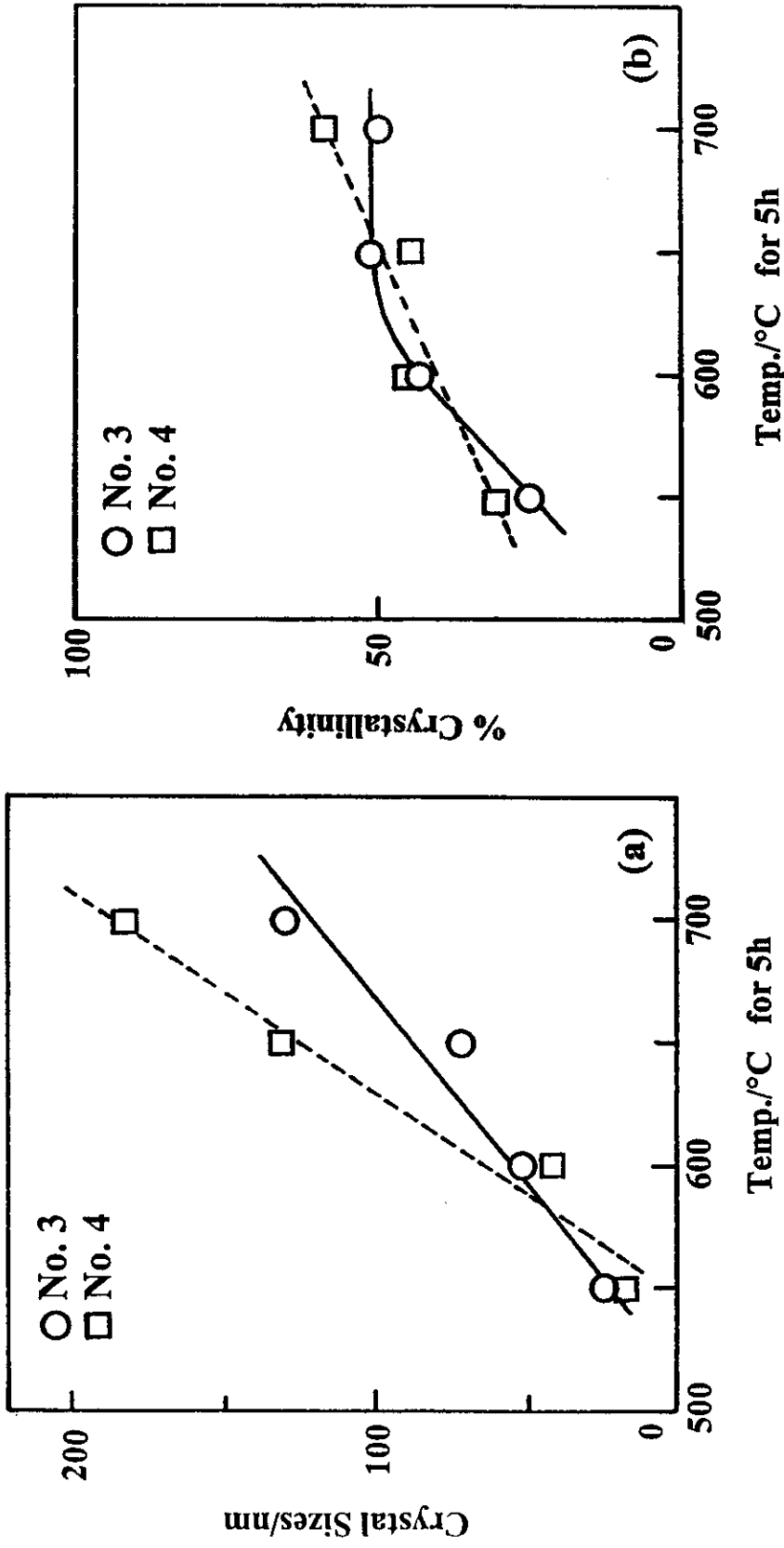


Fig. 4. Relationship between crystal size and percent crystallinity and heat treatment temperature of No.3 and No.4 glasses.

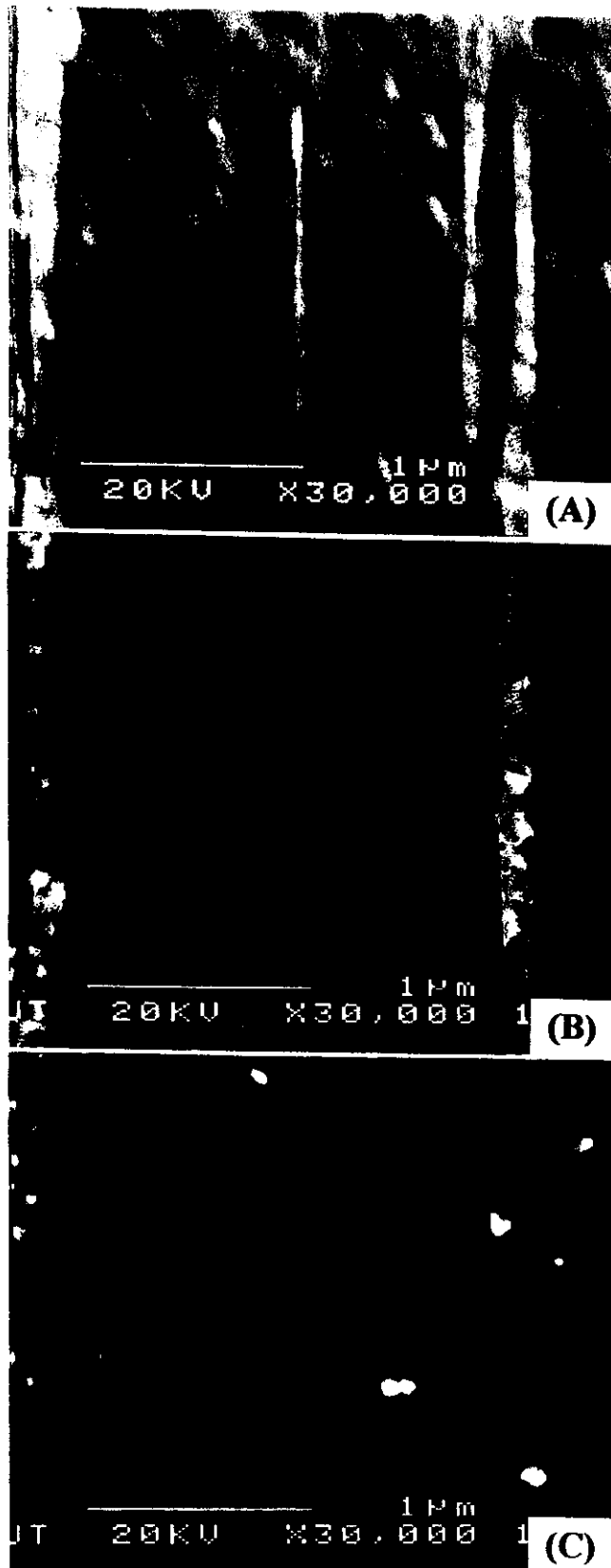


Fig. 5. SEM photos of No.3 glass-ceramics.

(A). $510^{\circ}\text{C}-10\text{h}$, $550^{\circ}\text{C}-20\text{h}$. (B). $510^{\circ}\text{C}-10\text{h}$, $550^{\circ}\text{C}-10\text{h}$.

(C). $510^{\circ}\text{C}-10\text{h}$, $650^{\circ}\text{C}-5\text{h}$.

containing over 100 nm of AlPO_4 crystal shows opaque in appearance, whilst glass-ceramics having smaller than 50 nm of crystal appears to be transparent. Figure 5 shows the SEM photomicrographs of No.3 transparent glass-ceramics. This glass was pre-heat treated at 510°C for 10 h and subsequently heat treated at higher temperature. Although an individual crystal can not be found, a phase separation-like structural change is observed in sample A. A very fine continuous and interconnected-like structure consisting of fine crystals can be observed in the sample B heat treated 600°C —10 h. In the sample C heat treated at 650°C for 5 h, an individual AlPO_4 crystal can be observed clearly. The percent crystallinity and crystallite size of these glass-ceramics are 34% and 21 nm for A sample, 48% and 34 nm for B sample and 50% and 60 nm for C sample, respectively. From SEM observation, the mechanism of crystallization might be thought as follows: 1). phase separation into two phases, one of which is rich in $\text{Al}_2\text{O}_3\text{-P}_2\text{O}_5(\text{SiO}_2)$ and forms a continuous phase. 2). AlPO_4 crystal starts to precipitate in this continuous phase, 3). AlPO_4 crystal grows in this phase resulting in individual crystal⁽¹⁶⁾.

Table 2 shows the properties of glass-ceramics. Thermal expansion coefficient of glass-ceramics increases with increase in the amount of AlPO_4 crystal.

Table 2. Properties of glass-ceramics.

Glass No.	Heat treatment ($^\circ\text{C}$ -h)	Appearance	Crystalline phases	α^* (10 ⁻⁷ /K)	%C	D (nm)
3	—	Transparent	Glassy	74.1	—	—
	510-10	"	"	—	—	—
	510-10, 550-20	"	AlPO_4	—	34	21
	510-10, 600-10	"	"	—	48	34
	510-10, 650-5	Slightly translucent	"		50	60
	520-5, 600-10	"	"	110**	44	42
	520-5, 650-5	Translucent	"	140**	50	70
4	—	Transparent	Glassy	70.4	—	—
	520-5, 550-5	"	AlPO_4	"	30	18
	520-5, 600-10	Translucent	"	125**	50	106

*: $30^\circ\text{--}300^\circ\text{C}$, **: $100^\circ\text{--}300^\circ\text{C}$

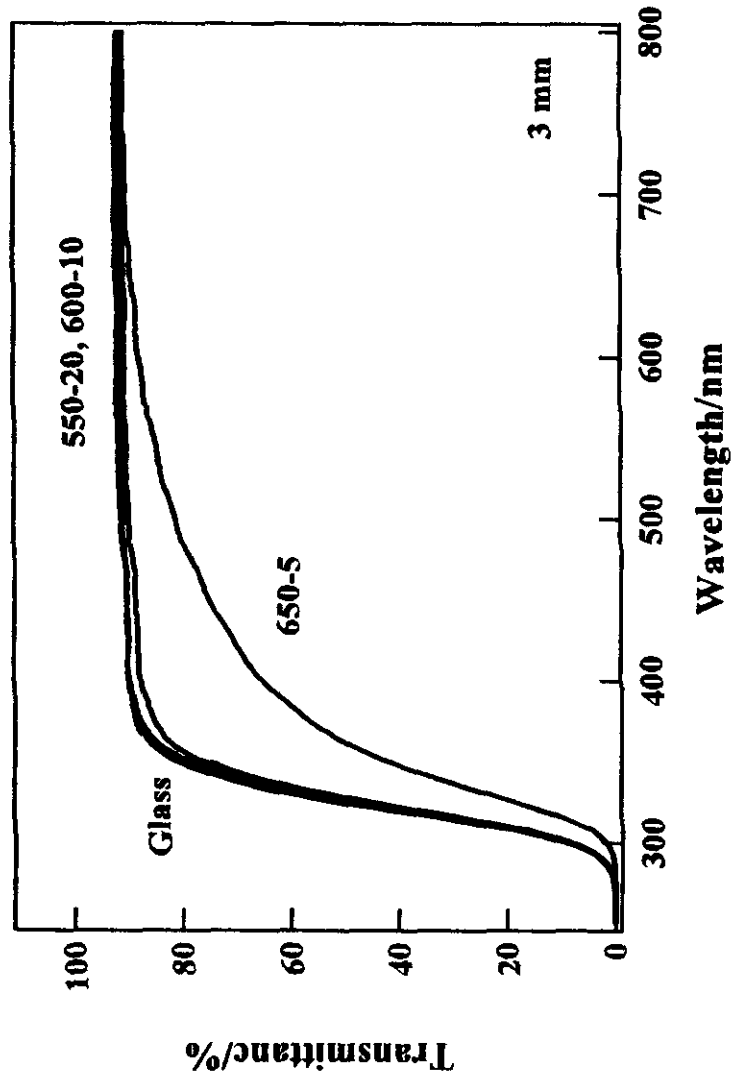


Fig. 6. Transmission curves of glass and glass-ceramics.
Sample thickness: 3 mm.

3.4. Transparency

The transparency of glass and glass-ceramics was compared. Figure 6 shows the transmission spectra of No.3 glass and glass-ceramics. Both A(510-10, 550-20) and B(510-10, 600-10) glass-ceramics have a very high transparency comparable with parent glass. However, C(510-10, 650-5) sample shows a lower transmittance due to scattering in 25-800 nm range.

According to scattering theory, the coefficient of scattering (σ) is governed by the particle size (R) embedded in matrix, $[\sigma \propto R^3]$, and the refractive index difference between particle (n) and matrix (n_0), $[\sigma \propto \{(n^2 - n_0^2)/(n^2 + n_0^2)\}^2]$. Therefore, the smaller particles and the smaller refractive index difference provide lower scattering. The transparency of the transparent glass-ceramics is achieved by the smaller particle size⁽¹²⁾. Though AlPO_4 crystal (trydimite type) has birefringence, its mean refractive index is about 1.46⁽²¹⁾. The refractive index of residual glassy phase is estimated to be about 1.51, the difference in refractive index between them may be 0.05. This value is sufficient too low, and the crystalline size is also too small by 20-30 nm, thus the lower scattering can be achieved.

4. Conclusion

The phase separation and crystallization behavior in $(80-X)\text{SiO}_2 \cdot X(\text{Al}_2\text{O}_3 + \text{P}_2\text{O}_5) \cdot 5\text{B}_2\text{O}_3 \cdot 15\text{Na}_2\text{O}$ (mol%, $X=20,30,40,45,50$) glasses were investigated. The phase separation was observed in all glasses, especially in $X=20$ and 30 composition, and the continuous phase is estimated to be rich in $\text{Al}_2\text{O}_3\text{-P}_2\text{O}_5(\text{SiO}_2)$. The crystallization tendency increases with increase in X , and the precipitation of trydimite type AlPO_4 crystal was observed in $X=40$ and 45 glasses. The amount of AlPO_4 crystal is about 50 to 60%. It is concluded that the phase separation occurs at first, forming continuous $\text{Al}_2\text{O}_3\text{-P}_2\text{O}_5(\text{SiO}_2)$ rich phase and then trydimite type AlPO_4 crystal precipitates and grows in this phase.

A highly transparent glass-ceramics comparable with glass can be obtained successfully by controlling heat treatment precisely. The crystallite size and percent crystallinity of these transparent glass-ceramics are 20-30 nm and about 50%.

Chapter III

Preparation and properties of $\text{Li}_2\text{O}\cdot 2\text{SiO}_2$ system transparent glass-ceramics

3.1. Strength of $\text{Li}_2\text{O}\cdot 2\text{SiO}_2$ transparent glass-ceramics

1. Introduction

One of the significant characteristics of glass-ceramics is that they are stronger than that of glass. Although glass is a typical brittle material that readily fractures, its theoretical strength is quite high (≈ 10 GPa). However, the practical strength of glass is below 50-100 MPa. Griffith⁽²²⁾ introduced the "Griffith flaw theory" to explain this phenomena. On the reason is that various kind of flaw existing on the surface act as stress concentrator. A higher close to the theoretical strength could be obtained by thin fiber or by removing surface flaws.

Generally, the high strength of glass-ceramics represents practical strength. It is recognized that crystals dispersed in glass-ceramics prevent flaw generation or crack propagation.

Many researches on the relationship between fracture strength and crystal size have been carried out for glass-ceramics^(23,24), and sintered polycrystalline materials^(25,26). It is confirmed that fracture strength increases with decreasing crystal size on the basis of Griffith's equation assuming that the crystal size is equal to the crack size in a micrometer-order crystal [$\sigma \propto d^{-1/2}$]⁽²⁷⁾. According to this idea, the fracture strength of very fine grained sintered polycrystalline materials and glass-ceramics, e.g. transparent glass-ceramics, should be very high. However, the fracture strength of very fine grained transparent glass-ceramics is not so different from that of conventional glass, hence, this idea is not applicable to these materials.

We investigated the relationship between fracture strength and crystal size of $\text{Li}_2\text{O}\cdot 2\text{SiO}_2$ system transparent glass-ceramics and found that fracture strength increases with increasing crystal size up to 100 nm.

2. Experiment

2.1. Sample preparation

The composition of the glass used is $80\text{SiO}_2\cdot 4\text{Al}_2\text{O}_3\cdot 13\text{Li}_2\text{O}\cdot 3\text{P}_2\text{O}_5$ (mass%)[$73.0\text{SiO}_2\cdot 2.15\text{Al}_2\text{O}_3\cdot 23.7\text{Li}_2\text{O}\cdot 1.15\text{P}_2\text{O}_5$, mol%]. High purity silica sand, alumina and reagent grade chemicals of Li_2CO_3 and $(\text{NH}_4)_2\text{HPO}_4$ (Carlo Erba) were used as raw materials. A batch corresponding to 200 g of glass was mixed thoroughly and pre-calcined at 300°C overnight to remove NH_3 . Then it was melted in a 100

ml Pt/Rh10 crucible at 1450°C for 3h in an electric furnace.

A rod about 5 mm diameter was freshly drawn and cut into about 7 cm long sample for strength measurement. The samples were then annealed at 450°C for 30 min and cooled to room temperature in the furnace. They were then heat treated for crystallization under various conditions.

The densities of glass and glass-ceramics were measured by the He-gas substitution method using Accupyc 1330 (Micromeritics).

2.2. DTA, XRD, SEM

A differential thermal analysis (DTA) was carried out routinely to determine the crystallization temperature at a heating rate of 10K/min using a Perkin-Elmer DTA-7.

Crystalline phases were examined by powder X-ray diffraction analysis (XRD, Bruker, AXS Model D5005). Crystalline sized was calculated using Scherrer's equation.

$$D = 0.9 \cdot \lambda / \beta \cdot \cos \theta \quad (1)$$

Where D is the crystalline size (Å), λ the wavelength of X-ray (1.54Å), β the true half width (radian) and θ the diffraction angle (degree). True half width was determined by the Jones method⁽²⁸⁾, and α -Quartz was used as a standard.

Percent crystallinity was determined using Ohlberg and Strickler's method⁽²⁹⁾, and was calculated using by:

$$\text{Percent crystallinity (\%C)} = 100x(I_g - I_x) / (I_g - I_c) \quad (2)$$

Where I_g is the background intensity of glass, I_x that of specimens and I_c that of the crystal at $2\theta = 23^\circ$. The calibration curve was obtained using mixtures α -Quartz and a parent glass at various ratio, and showed good linearity.

The surface structures of the non-abraded and abraded specimens were observed by scanning electron micrograph (SEM, JEOL JSM 6400).

2.3. Strength measurement

The fracture strength of annealed glass and glass-ceramics were measured using Instron Model 5569 according to ASTM C-158. The three-point bending method was employed and the surface of the specimens was abraded with #180 SiC abrasive paper before the measurement, and the strength of non-abraded specimens was also measured. The span length and loading rate were 50 mm and 10 mm/min, respectively.

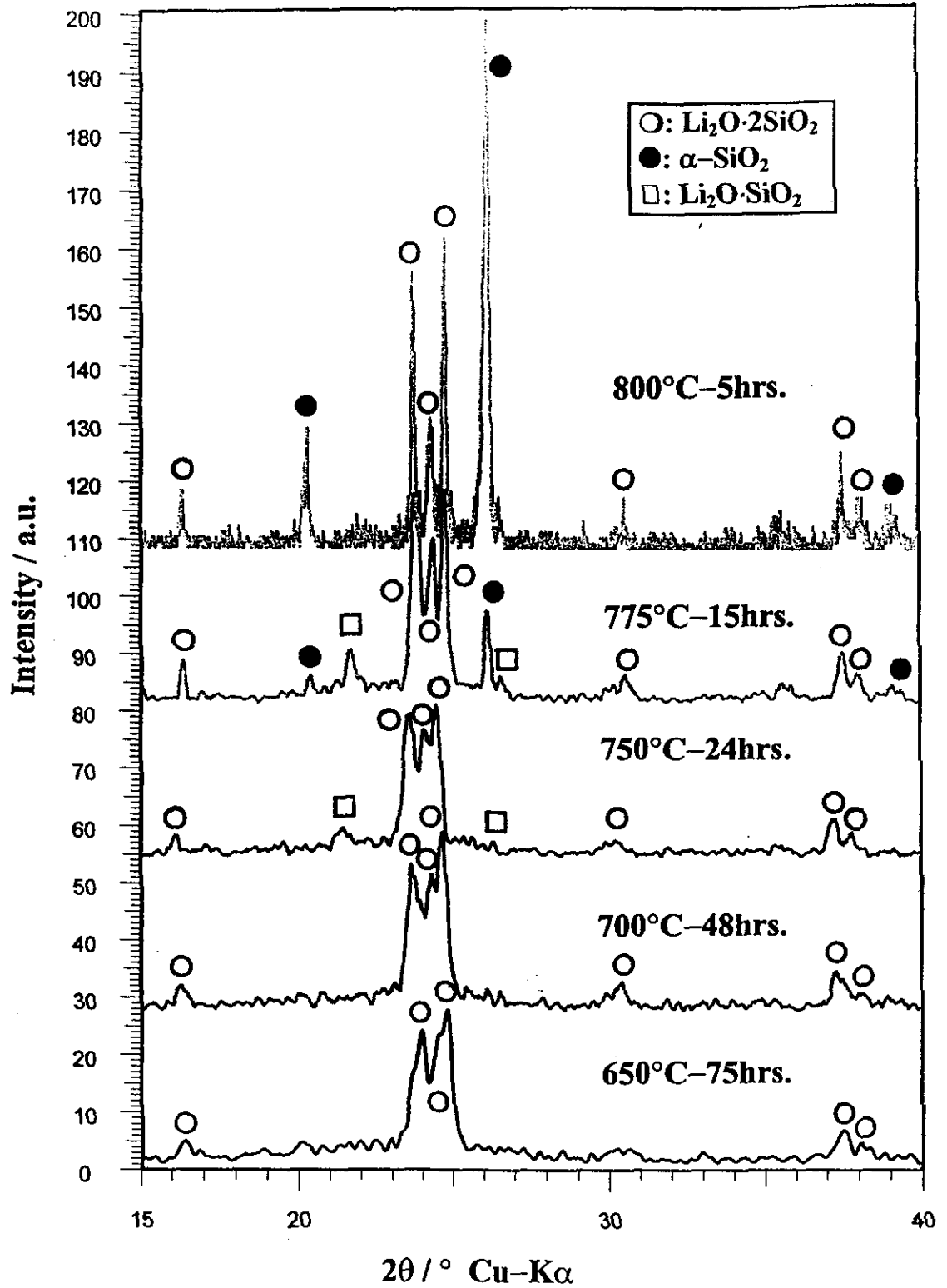


Fig. 7. XRD patterns of glass-ceramics.

Table 3. Properties of glass and glass-ceramics.

Heat treatment (°C - h)	Appearance	Density (g/cm ³)	Crystalline phase (XRD)**	Percent crystallinity	Crystal size (nm)	Fracture strength MPa***
Glass	Transparent	2.3541	-	-	-	122.8±21.7 56.8±6.4
600	Transparent	2.3810	L-2S	59	22.6	68.7±6.7
144	Transparent	2.3907	L-2S	60	24.3	-
650	Transparent	2.3880	L-2S	67	24.2	67.7±5.6
75	Slightly translucent	2.4096	L-2S	66	27.1	78.5±5.6 151.8±36.2 78.3±6
700	Slightly translucent	2.4161	L-2S	72	28	187.9±41.3 82.7±10.5
48	Slightly translucent	2.4114	L-2S	74	31.2	161.7±29.8 90.6±6.5
750	Slightly translucent	2.4213	L-2S	75	34.0	176.9±49.7 90.6±9.8
24	Slightly translucent	2.4385	L-2S L-S(very slight)	72	35.8	179.1±30.3 96.5±6.5
775	Weakly translucent	2.4385	L-2S, L-S(very slight) α-Quartz(very slight)	77	42.1	205.6±14.4 98.9±9.4
15	Weakly translucent	2.4358	L-2S, L-S(very slight) α-Quartz(slight)	77	60.2	238.8±49.6 113.3±12.8
800	Translucent	2.5053	L-2S, α-Quartz	-	-	-

*: 1st heat treatment: 500°C - 15 h, **: L-S = Li₂O-SiO₂, L-2S = Li₂O-2SiO₂, ***: upper: non-abraded, lower: abraded

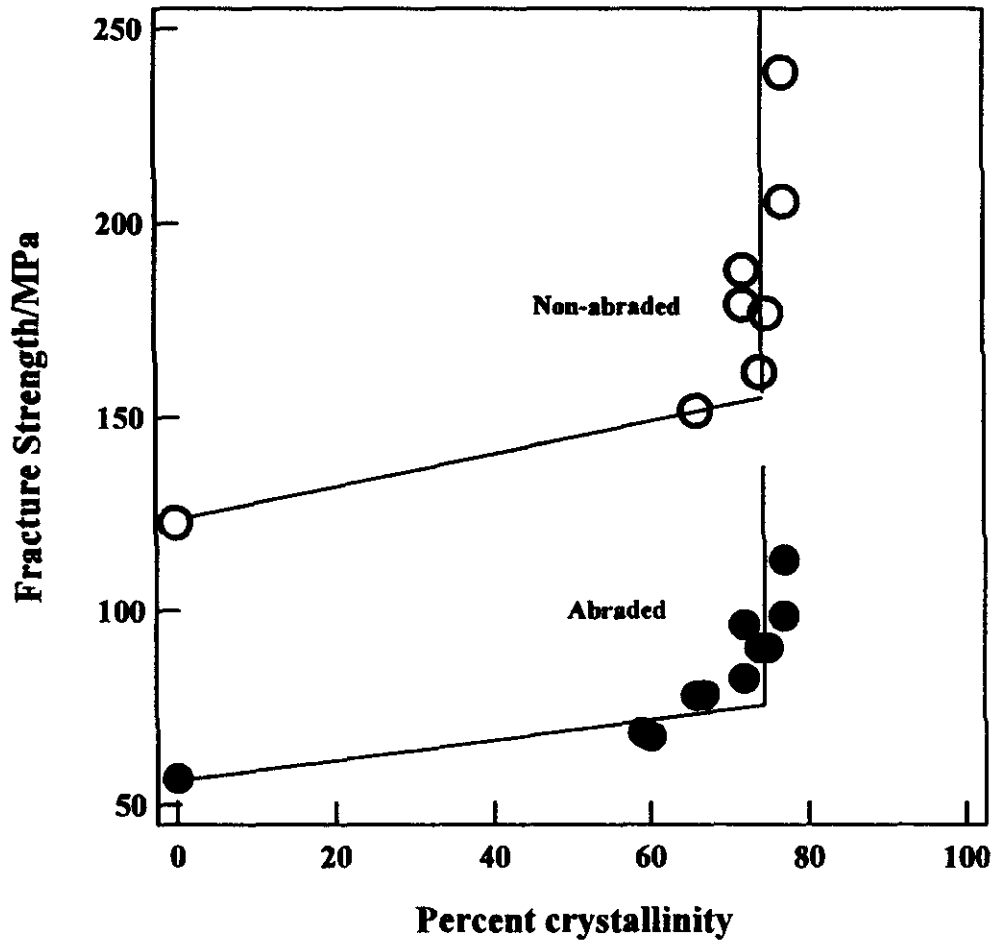


Fig. 8. Effect of percent crystallinity on the fracture strength.

3. Results

3.1. Properties of glass-ceramics

Two exothermic peaks appeared at around 600°C and 800°C in DTA run; the former peak corresponds to the precipitation of $\text{Li}_2\text{O}\cdot 2\text{SiO}_2$ crystal and the latter corresponds to α -Quartz. Figure 7 shows the XRD patterns of glass-ceramics. The main crystalline phase is $\text{Li}_2\text{O}\cdot 2\text{SiO}_2$ at lower temperature and for a shorter time of crystallization. However, a considerable amount of α -Quartz crystal precipitates at a higher temperature for longer time, particularly above 800°C. The percent crystallinity and crystal size ranged from 60 to 75% and from 20 to 60 nm, respectively. The transparent glass-ceramics can be obtained by heat treatment below 800°C. The density of glass-ceramics increases with increasing heating temperature and time of crystallization.

Table 3 summarizes the heat treatment conditions, appearance, density, precipitated crystalline phases, percent crystallinity, crystal size, non-abraded and abraded fracture strength of glass-ceramics.

3.2. Effect of percent crystallinity on strength

Figure 8 shows the relationship between fracture strength and percent crystallinity. Both the non-abraded and abraded fracture strength increases with increasing percent crystallinity up to 75-80%. However, the strength does not depend on the percent crystallinity at this region; it depends on another factor, namely, crystal size.

3.3. Effect of crystal size on strength

Figure 9 shows the relationship between fracture strength and crystal size of non-abraded and abraded specimens. The non-abraded specimen has a very smooth surface, while scratches of various types and sizes in all directions can be observed on the surface of the abraded specimen.

Although the fracture strength is slightly low for the sample with lower percent crystallinity, it is found that fracture strength increases linearly with increasing crystal size for both non-abraded and abraded specimens, and it can be expressed by the following equation as a function of crystal size, d (nm). The fracture strength of the abraded specimens is about one half that of non-abraded specimens.

$$\sigma = 100.5 + 2.32d \text{ (MPa) [Non-abraded]}$$

$$\sigma = 56.3 + 0.99d \text{ (MPa) [Abraded]}$$

These calculations were carried out without glass and glass-ceramics of low percent crystallinity.

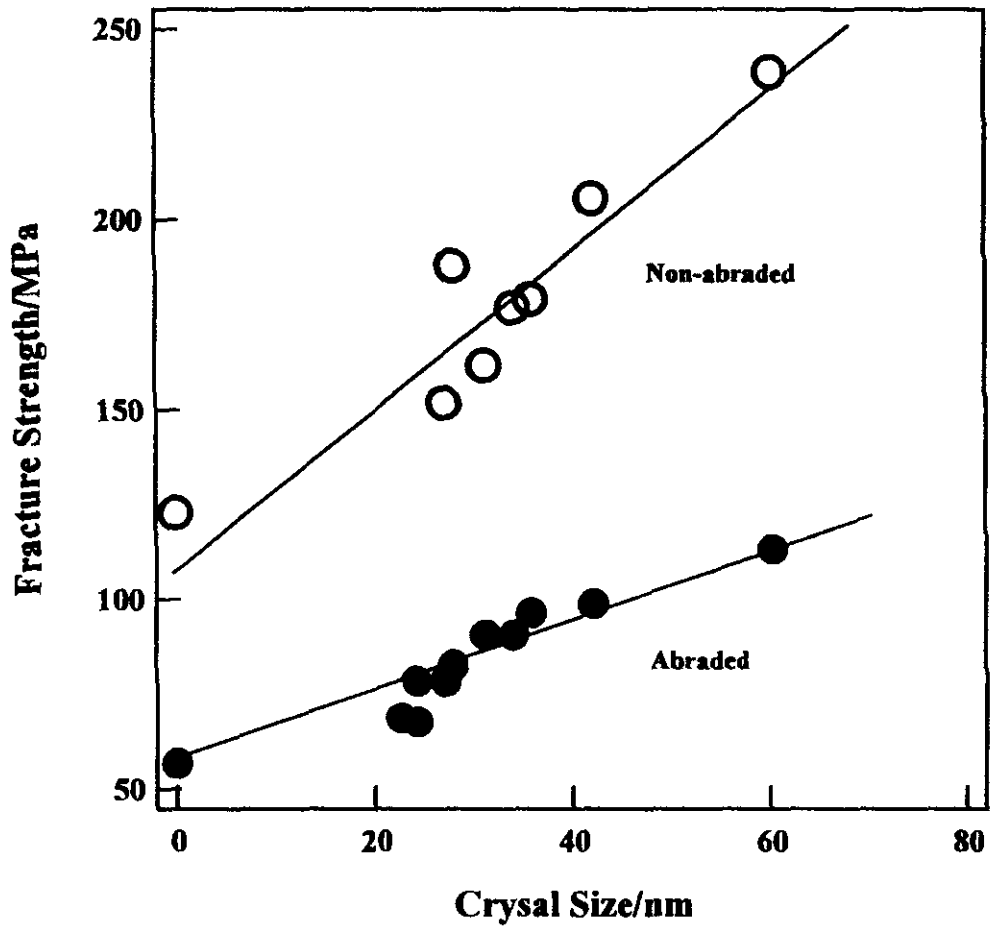


Fig. 9. Effect of crystal size on the fracture strength of glass and glass-ceramics.

4. Discussion

As observed above, the abraded and non-abraded fracture strength of $\text{Li}_2\text{O}\cdot 2\text{SiO}_2$ system transparent glass-ceramics increases with increasing crystal size ranging from 20 to 60 nm.

There are many factors affecting the strength of glass and glass-ceramics, and they may be classified into internal and surface structure⁽³⁰⁾. The factors resulting from the internal structure are void (pore), difference in thermal expansion coefficient, percent crystallinity and crystal size. In glass-ceramics, the influence void and the difference in thermal expansion coefficient may be disregarded, and also the effect of surface structure can also be disregarded. Therefore, only the influence of percent crystallinity and crystal size should be regarded as affecting fracture strength.

Concerning the fracture strength of polycrystalline materials and glass-ceramics, two mechanisms have been proposed. One is the intergranular fracture in which the crack propagates along with the grain boundary and another is the transgranular fracture in which the crack propagates in the grain. The higher strength of glass-ceramics can be explained by the term of interruption of crack propagation by crystal grain. When the crack propagates along with grain boundary in polycrystalline or glass-ceramics materials, crack front runs into crystals, which changes the direction of crack propagation. In this case, higher stress is required to maintain crack propagation. For example, as the crack propagation direction changes by 60° , a stress of 1.8 times higher than that of normal direction may be required, and 4 times larger stress is required for 90° . This is the reason glass-ceramics exhibits higher strengths. In this situation, the crystal size can be accounted for by Griffith's crack size, and thus, fracture strength is proportional to the reciprocal of crystal size ($\sigma \propto d^{-1/n}$). Many experimental results⁽²³⁻²⁶⁾ confirmed this relation for sintered polycrystalline materials and glass-ceramics of micrometer-order of crystal size; however, the n term differs among researchers. This equation clearly indicates that fracture strength increases with decreasing crystal size.

By assuming the limitations of $d \rightarrow 0$ (glass), the fracture strength must reach the theoretical strength according to the above theory. However, as is well known, the practical fracture strength of glass is quite low compared to the theoretical strength. The present result also indicates that fracture strength increases with increasing crystal size of nanometer-order of crystal. This implies that the above principle is not applicable to a very fine grained glass-ceramics.

The present result shows that very fine crystals can not effectively interrupt the crack propagation. Because a crack propagates along with the grain boundary, the change in direction of crack propagation may be much smaller than that for larger grain, and hence, the stress required for the change in direction may be small. Consequently, the fracture strength of very fine grained glass-ceramics is

estimated to be small. It should also be noted that a critical crystal size may exist for attaining the maximum fracture strength of polycrystalline and glass-ceramics materials based on above results.

5. Conclusion

The relationship between fracture strength and crystal size of the $\text{Li}_2\text{O}\cdot 2\text{SiO}_2$ system transparent glass-ceramics was investigated and following results were obtained.

(1). The precipitated crystalline phases, percent crystallinity and crystal size were $\text{Li}_2\text{O}\cdot 2\text{SiO}_2$, 60-80% and 20-60 nm, respectively, following heat treatment below 800°C for 5-144 h.

(2). Fracture strength increases linearly with increasing crystal size ranging 20-60 nm. This can be expressed by

$$\sigma = 100.5 + 2.32d \text{ (MPa) [Non-abraded]}$$

$$\sigma = 56.3 + 0.99d \text{ (MPa) [Abraded]}$$

(3). Very fine crystals can not effectively interrupt crack propagation. Therefore, the stress required for changing the direction of propagation may be small.

(4). It can be considered that a critical crystal size may be exist for the attainment of maximum strength.

3. 2. Strengthening of $\text{Li}_2\text{O}\cdot 2\text{SiO}_2$ transparent glass-ceramics by ion exchange

1. Introduction

Transparent glass-ceramics comprises the essential group in glass-ceramics, is composed of fine-grained crystallites, usually nano-scale size, and residual glassy phase. The transparent glass-ceramics has been developed and used for many applications, such as transparent cookware, precision optical instruments, ring-laser gyroscope, large telescope mirror blanks, etc. Further, recently, active ions, transition metal ion and rare-earth ion, doped transparent glass-ceramics are developed and many researches on this materials have been carried out⁽³¹⁻³⁴⁾.

$\text{Li}_2\text{O}\text{-SiO}_2$ system of glass has well been known as a base glass for glass-ceramics, such as chemically machinable glass-ceramics and high strength glass-ceramics. And also, transparent glass-ceramics based on lithium metasilicate [$\text{Li}_2\text{O}\cdot\text{SiO}_2$] and lithium disilicate [$\text{Li}_2\text{O}\cdot 2\text{SiO}_2$] crystals can be obtained easily in this system of glass^(35,36). However, the mechanical strength of transparent glass-ceramics is not so high⁽³⁷⁾, similar to that of glass, and hence the higher mechanical strength is required in special application area.

There are two methods to increase mechanical strength of glasses and glass-ceramics, thermal strengthening and chemical strengthening. The latter is called as ion exchange strengthening method and has many advantages over thermal strengthening, such as easy processing, available for any shapes of articles, available for thin articles, available to maintain the surface flatness and smoothness, capable of applying for low thermal expansion materials, etc. $\text{Li}^+\text{-Na}^+$ and $\text{Li}^+\text{-K}^+$ ion exchange is expected to increase mechanical strength of these transparent glass-ceramics.

Here the chemical strengthening of $\text{Li}_2\text{O}\cdot 2\text{SiO}_2$ transparent glass-ceramics was investigated.

2. Experiments

2.1. Sample preparation

The composition of glass used is $\text{SiO}_2\cdot 4\text{Al}_2\text{O}_3\cdot 13\text{Li}_2\text{O}\cdot 3\text{P}_2\text{O}_5$ (wt%) [$72.9\text{SiO}_2\cdot 2.15\text{Al}_2\text{O}_3\cdot 23.8\text{Li}_2\text{O}\cdot 1.15\text{P}_2\text{O}_5$ (mol %)]. High purity silica sand, alumina and reagent grade chemicals of Li_2CO_3 and $(\text{NH}_4)_2\text{HPO}_4$ (Aldrich) were used as raw materials. A batch corresponding to 200 g of glass was mixed thoroughly and pre-calcined at 300°C for overnight to remove NH_3 . Then it was melted in a 100 ml Pt/Rh10 crucible at 1450°C for 2h in an electric furnace. The molten glass was poured onto iron plate and crushed, and then it was melted at the same condition to improve homogeneity.

A rod about 5 mm diameter was freshly drawn and cut into about 7 cm long. The samples were annealed at 450°C for 30 min and cooled to room temperature in the furnace.

The samples were heat treated at 500°C for 15h for nucleation and 700°C for 10 h for crystallization.

2.2. Ion exchange

The samples were ion exchanged in NaNO₃ and KNO₃ molten bath under various conditions (Salt/glass ratio is 10 by wt).

2.3. XRD and SEM

Crystalline phases and lattice constant were determined by powder X-ray diffraction analysis (XRD) (Bruker, AXS Model D5005). Si powder was used as an internal standard for the measurement of the lattice constant. The surface structure of glasses and glass-ceramics after ion exchange were observed by scanning electron microscopy (SEM) (JEOL JSM 640).

2.4. Strength measurement

The fracture strength was measured using Instron Model 5569 according to ASTM C-158. The three point bending method was employed, and the span length and loading rate were 50 mm and 1 mm/min, respectively.

3. Results and discussion

The glass transition temperature (T_g), dilatometric softening point (Y_p), thermal expansion coefficient (α) and density of glass were 473°C, 541°C, $88.9 \times 10^{-7}/K$ (30-300°C) and 2.354 g/cm³, respectively. The main crystal, percent crystallinity and crystallite size of glass-ceramics were Li₂O·2SiO₂ crystal (JCPDS 40-0376), about 70 % and 40 nm respectively. The thermal expansion coefficient and density of transparent glass-ceramics were $90 \times 10^{-7}/K$ (30-300°C) and 2.414 g/cm³.

Table 4 shows the fracture strength and appearance of glass and glass-ceramics before and after ion exchange, $Li^+ \leftrightarrow Na^+$ and $Li^+ \leftrightarrow K^+$.

Figure 10 shows the relation between fracture strength and ion exchange time. In the case of glass, the fracture strength increases first and then decreases markedly, and a crack generation was observed by naked eye with progress of ion exchange for $Li^+ \leftrightarrow Na^+$ and $Li^+ \leftrightarrow K^+$ exchange. The rate of

ion exchange for $\text{Li}^+ \leftrightarrow \text{Na}^+$ is greater than that for $\text{Li}^+ \leftrightarrow \text{K}^+$ exchange.

The change in fracture strength of glass-ceramics with time shows the similar tendency to that of glass. However, the rate of ion exchange is much slower compared with that of glass. The fracture strength of glass-ceramics increases significantly for both the $\text{Li}^+ \leftrightarrow \text{Na}^+$ and $\text{Li}^+ \leftrightarrow \text{K}^+$ exchange at 450°C . At higher temperature (550°C), the fracture strength increases at

Table 4. Fracture strength of glass and glass-ceramics before and after ion exchange.

Ion exchange condition ($^\circ\text{C}\text{-h}$)		Fracture strength/MPa and appearance*	
		$\text{Li}^+ \leftrightarrow \text{Na}^+$	$\text{Li}^+ \leftrightarrow \text{K}^+$
Glass	—	146.4	146.4
	450-0.4	243	—
	450-1	156	—
	450-4	34.7(crack)	250.9
	450-9	—	154.9
	450-16	—	82(crack)
	Glass-Ceramics	—	166.5
450-1		345	—
450-4		376.3	—
450-16		—	288
550-1		189(peeling)	—
550-4		200(peeling)	—
550-9		236(peeling)	246
550-16		178(peeling)	333
550-25		—	256

*: determined by naked eye

first and then decreases gradually. The peeling off of ion exchanged layer was observed for $\text{Li}^+ \leftrightarrow \text{Na}^+$ exchange by naked eye.

Figure 11 shows the SEM photos of the surface of glass and glass-ceramics after ion exchange. It is interesting to note that the ion exchanged layer of glass and glass-ceramics peels off from the surface by $\text{Li}^+ \leftrightarrow \text{Na}^+$ exchange. The surface of glass is smooth, but that of glass-ceramics appears to be wrinkling. A

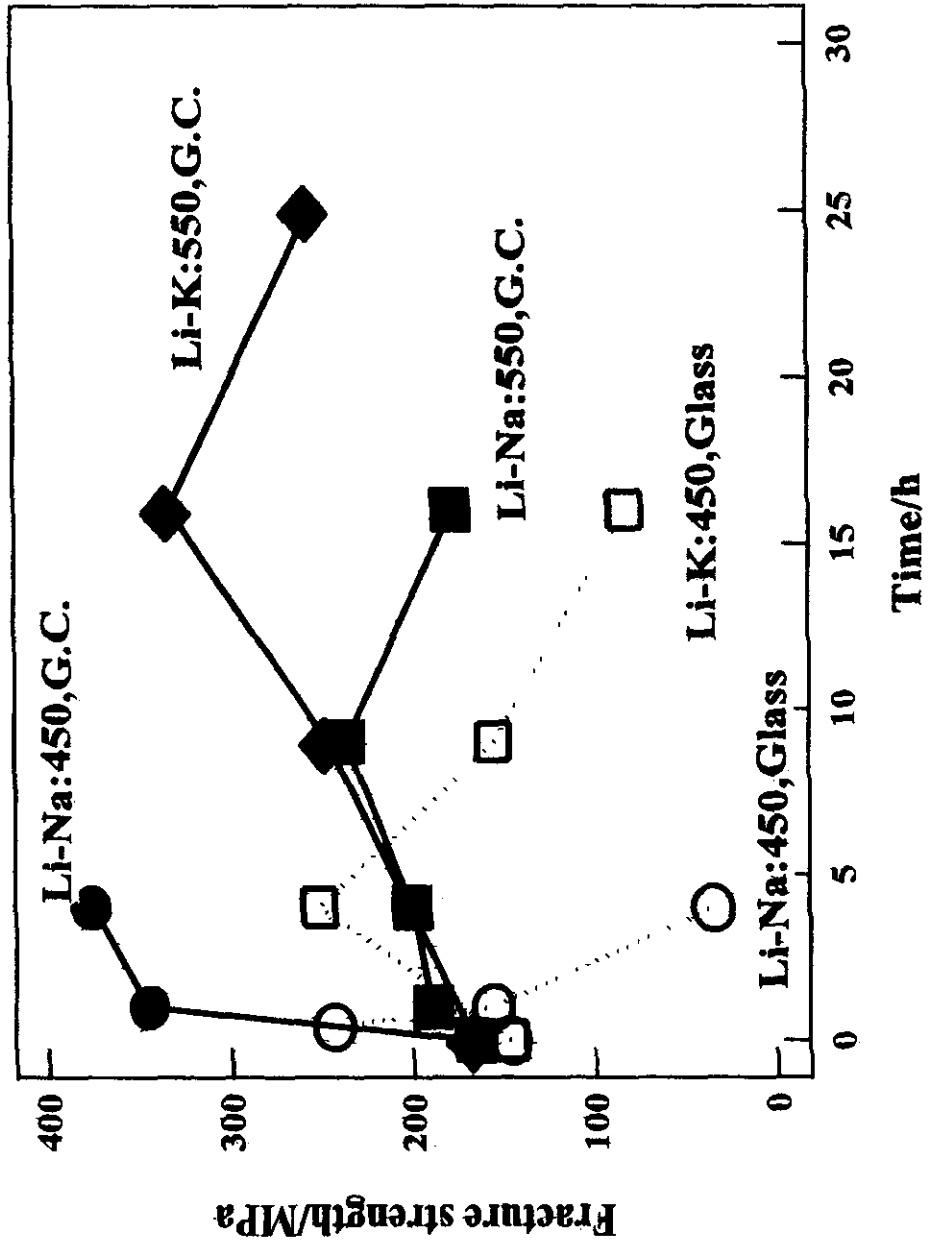


Fig. 10. Fracture strength of glass and glass-ceramics after ion exchange.

hair-like crack can be observed on the surface just below the peeled off layer for glass and glass-ceramics. On the contrary for $\text{Li}^+ \leftrightarrow \text{K}^+$ exchange, cracks can be observed on the surface of glass-ceramics and some irregular spots and cracks emerge for glass. Thus the surface of glass and glass-ceramics shows the abnormal behavior after ion exchange. The relation between this abnormal behavior of surface and the strength will be discussed below.

Generally, it is well known that the brittle materials like glasses are weak in tensile stress, and the ion exchange strengthening can be achieved due to the compressive stress arisen in the surface layer by the replacement of smaller ions in glass by larger foreign ions. This method is called "Crowding"[8]. The maximum compressive stress arisen by this mechanism may be given:

$$\sigma_c = (1/3) \cdot [E/(1-\mu)] \cdot (\Delta V/V) \quad 3)$$

where V is the volume of glass, ΔV the volume change by ion exchange without stress at room temperature, E the Young's modulus and μ the Poisson's ratio. This equation indicates that the larger ΔV gives the larger compressive stress.

Table 2 shows the calculated density, molar volume and thermal expansion coefficient of Li-, Na- and K-glasses⁽³⁹⁾. Assuming that $E=70\text{GPa}$, $\mu=0.2$, $\Delta V/V=2.78/23.10=0.12$, then $\sigma_c = 3.5\text{GPa}$ for $\text{Li}^+ \leftrightarrow \text{Na}^+$ exchange. And $\Delta V/V=0.22$ and $\sigma_c = 6.5\text{GPa}$ for $\text{Li}^+ \leftrightarrow \text{K}^+$ exchange. The volume change of glass-ceramics is much larger than that of glass by ion exchange because of higher density of glass-ceramics.

Table 5. Calculated density, molar volume and thermal expansion coefficient of Li-, Na- and K- glasses.

Glass	Density(g/cm^3)	Molar volume (cm^3/mol)	$\Delta V^*/\%$ ($\text{Li}^+ - \text{M}^+$)	$\alpha (\times 10^{-7}/\text{K})$
Li-glass	2.36	23.20	—	89.5
Na-glass	2.41	25.88	11.6	119.1
K-glass	2.48	28.22	21.6	135.7

*: change in molar volume after ion exchange(calculated value)

It should be noted here that $\text{Li}_2\text{O} \cdot 2\text{SiO}_2$ crystal in the ion exchanged layer of glass-ceramics was destroyed and disappeared with progress of ion exchange(This phenomena will be discussed elsewhere⁽⁴⁰⁾). However, the volume and thermal expansion coefficient of this glassy phase is much larger than those of glass-ceramics, and therefore the same treatment as glass might be possible.

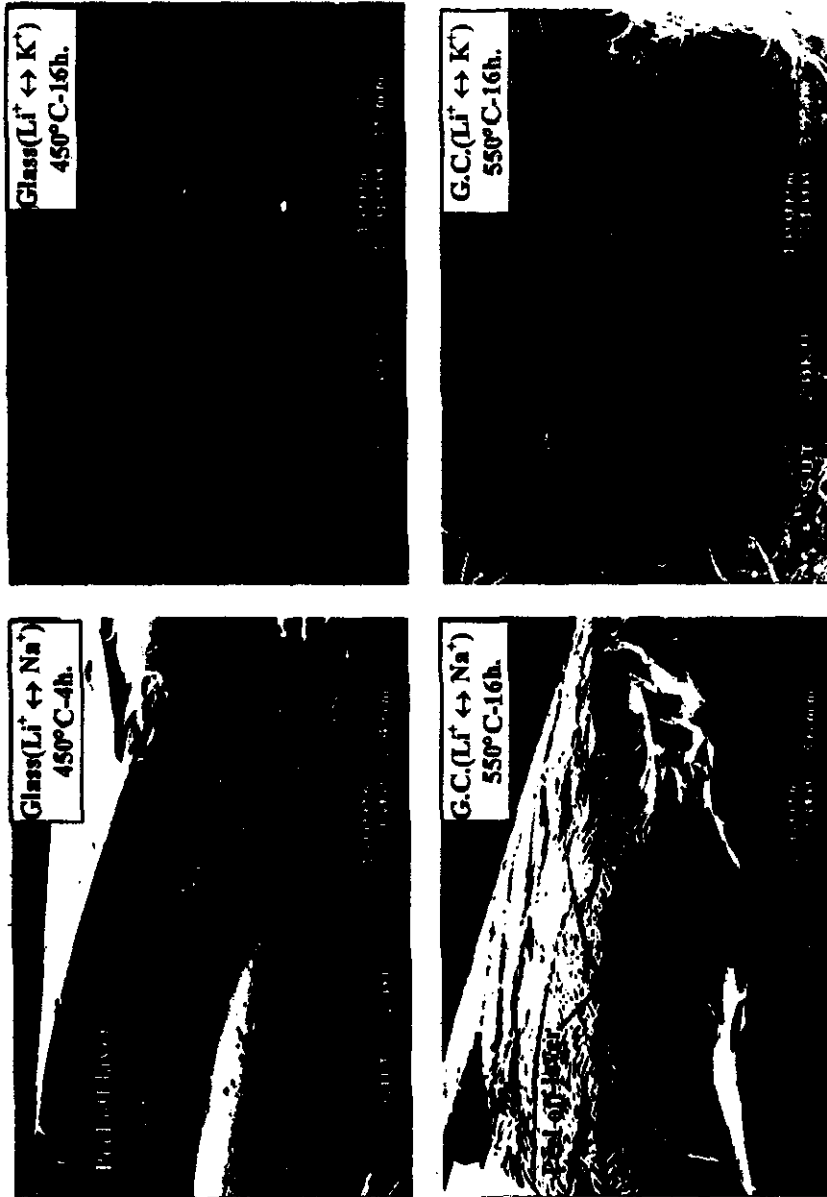


Fig. 11. SEM photos of glass and glass-ceramics after ion exchange.

The calculated volume change of this glass, $\Delta V/V$, is very large, however, this value must be much smaller actually, and hence the compressive stress arisen is estimated to be much lower, 800~1,000MPa. It is very interesting to note that the peeling and crack formation occur despite a large compressive stress arise in ion exchanged layer. The peeling and crack formation are not observed in a usual ion exchange process. In the early stage of ion exchange discussed here, peeling and crack formation were not observed for glass and glass-ceramics, therefore, the compressive stress arisen affects effectively on the increase in strength. However, as increase in the thickness of ion exchanged layer, the volume change of ion exchanged layer can not be neglected, and crack and peeling may generate in that layer. It is considered that this large volume change anyhow causes the peeling and crack formation of ion exchange layer. With progress of ion exchange, the peeling and crack formation take place and the submicroscopic crack(hair-like crack in Figure 11), which acts as stress concentrator, generates perpendicular to the surface and finally the fracture strength decreases.

The volume change of ion exchanged layer strongly depends on the alkali content in the base glass. The glass discussed here contains about 24 mol% of Li_2O . These peeling and crack formation seems to be the characteristics of high alkali containing glasses by ion exchange.

4. Conclusion

The chemical strengthening of $\text{Li}_2\text{O}\cdot 2\text{SiO}_2$ transparent glass-ceramics was investigated. The fracture strength of glass and glass-ceramics increased first and then decreased, and the crack formation and peeling of ion exchanged layer were observed for both $\text{Li}^+ \leftrightarrow \text{Na}^+$ and $\text{Li}^+ \leftrightarrow \text{K}^+$ ion exchange. This suggests that the submicroscopic crack generates perpendicular to the surface when the ion exchanged layer peels off from the surface.

The calculated volume change by $\text{Li}^+ \leftrightarrow \text{Na}^+$ and $\text{Li}^+ \leftrightarrow \text{K}^+$ ion exchange is very large, over 10%, this large volume change causes the peeling and crack formation of ion exchanged layer despite in which the large compressive stress arise. In the early stage of ion exchange, the compressive stress arisen affects effectively on the increase in strength. However, as increase in the thickness of ion exchanged layer, the volume change of ion exchanged layer can not be neglected, and crack and peeling may generate in that layer. Finally, the fracture strength decreases.

Chapter IV

Absorption And Emission Characteristics of Cr Ions in Transparent Glass-Ceramics

4. 1. Cr³⁺ ion in spinel transparent glass-ceramics

1. Introduction

Many researches are devoted to optical properties of transition metal ions in solids for laser applications. Especially, Cr²⁺, Cr³⁺ and Cr⁴⁺ centers give rich spectroscopic data, which are now already used in laser transitions.

Glasses as laser hosts have many advantages such as mass production at low cost and fabrication for any shapes more easily than single crystals⁽⁴¹⁾. However, due to the disorder of glass structure the inhomogeneous line-broadening of transition metal ions is caused by site multiplicity. Thus the characteristic emission such as single crystals can usually not be observed. In the present, the stimulated emission of lasers is limited to rare earth ions for glasses in which the transition between 4fⁿ state is oscillating. The stimulated emission of lasers of 3dⁿ transition metal ions in glass has not been achieved yet, unlike single crystals.

The transparent glass-ceramics contains nanometer-order crystallite, and hence they have the potential to exhibit the emission behavior similar to single crystals. Furthermore, the transparent glass-ceramics is produced through glass route, they have many advantages for fabrication compared with single crystals⁽⁴¹⁾.

Here the absorption and emission spectra of Cr³⁺ ions-containing spinel type transparent glass-ceramics was investigated and the characteristic emission of Cr³⁺ ions in strong octahedral field was observed. These results are presented.

2. Experiments

2.1. Sample preparation

The base glass composition used is 54.2SiO₂·30.6Al₂O₃·9.1MgO·6.1ZnO·1TiO₂·7ZrO₂·0.5Cr₂O₃ (mass%). ZrO₂, TiO₂ and Cr₂O₃ are introduced as nucleating agents and coloring agent by excess mass percent.

High purity silica sand, alumina, acid washed zircon sand and reagent grade chemicals of MgO, ZnO, Cr₂O₃ and TiO₂ (Carlo Erba) are used as raw materials. A batch corresponding to about 60g of glass was mixed thoroughly and melted in 60cc Pt/RH10 crucible at 1570°C for 2 h in an electric furnace in air. They are then poured onto iron plate and pressed by another iron plate.

The glasses are heat treated at 800°C for 10 h for nucleation and cooled in the furnace, and subsequently heat treated at 1050°C for 3.5 h for crystallization. They are optically polished into about 1.6mm in thickness.

2.2. XRD

The crystalline phases precipitated, crystalline size and percent crystallinity are determined by XRD.

2.3. Absorption and emission spectra

The absorption spectra are measured with Cary 5E UV-VIS-NIR spectrometer in the range of 300~800 nm at room temperature.

The emission spectra are measured with Perkin-Elmer Luminescence Spectrometer LS50B in the range of 300~900 nm at room temperature.

3. Results and Discussion

The glass obtained is dark green in color and changes to red-purple upon crystallization. The color is also accompanied by faint red fluorescence which is stimulated by ordinary artificial light (incandescent light bulb) or sunlight.

Glass-ceramics consists of spinel[(Mg,Zn)Al₂O₄] crystal of about 25 nm in size and the crystallinity is about 40%.

Fig. 12 shows the absorption spectra of glass and glass-ceramics. In glasses, two absorption bands centered at 450 nm and 650 nm appear, and the latter band splits into three peaks. They are ascribed to d-d transition of Cr³⁺ ion, and correspond to ⁴A_{2g}(F)→⁴T_{1g}(F) and ⁴A_{2g}→⁴T_{2g}(F) transitions, respectively. It seems that only Cr³⁺ ions exist in glass. The general feature of spectrum is quite similar to that reported previously⁽⁴²⁾, and the peak positions are almost the same as those. This indicates that the ligands field parameter, 10Dq and Racah B parameter, might be the same as those⁽⁴²⁾. They are, 10Dq ≈ 15,300cm⁻¹ and B ≈ 750cm⁻¹ (Dq/B=2.04).

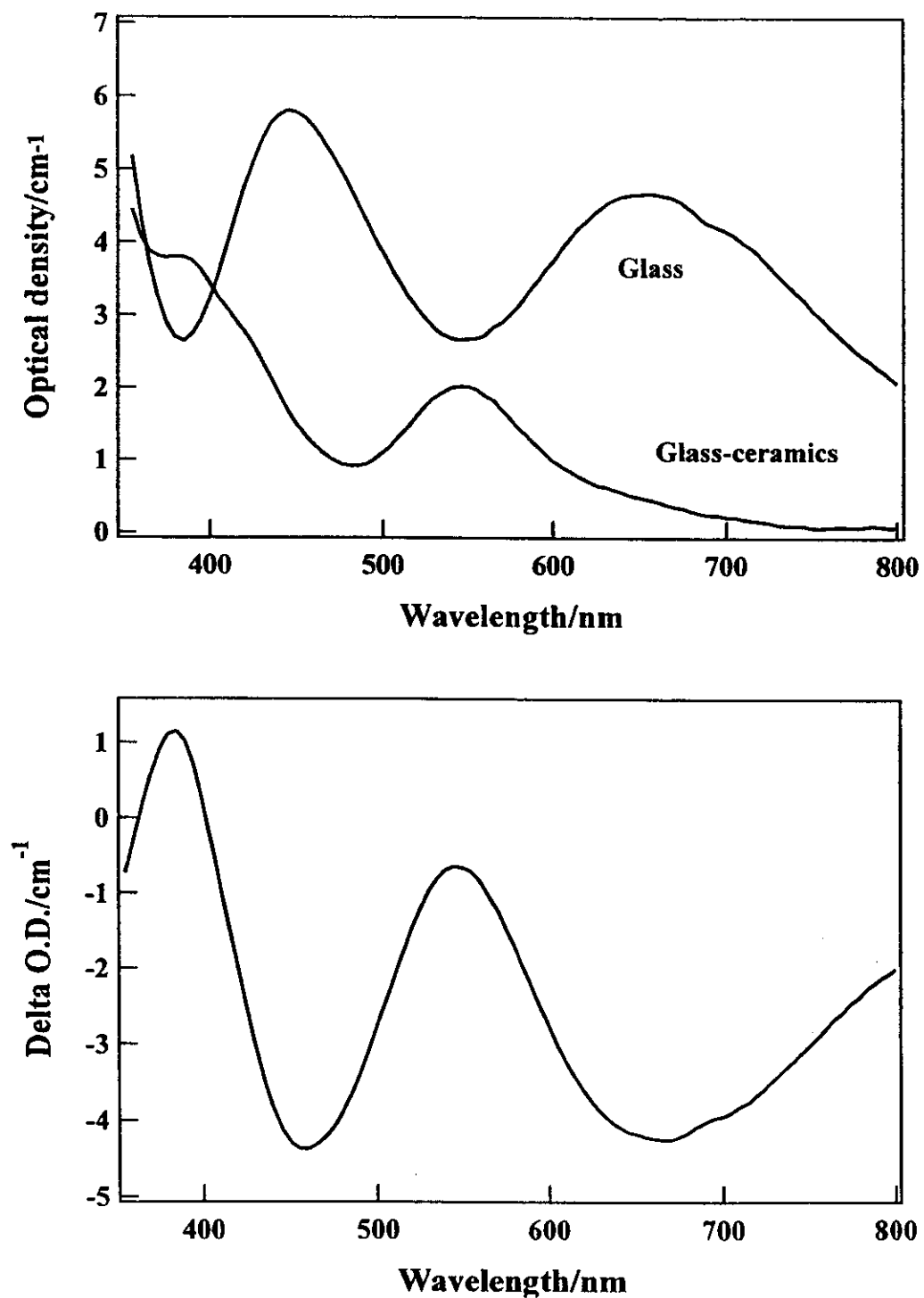


Fig. 12. Absorption and differential spectra of glass and glass-ceramics.

$$\Delta[\text{O.D.}(\text{cm}^{-1})] = [\text{O.D.}(\text{cm}^{-1})]_{\text{glass-ceramics}} - [\text{O.D.}(\text{cm}^{-1})]_{\text{glass}}$$

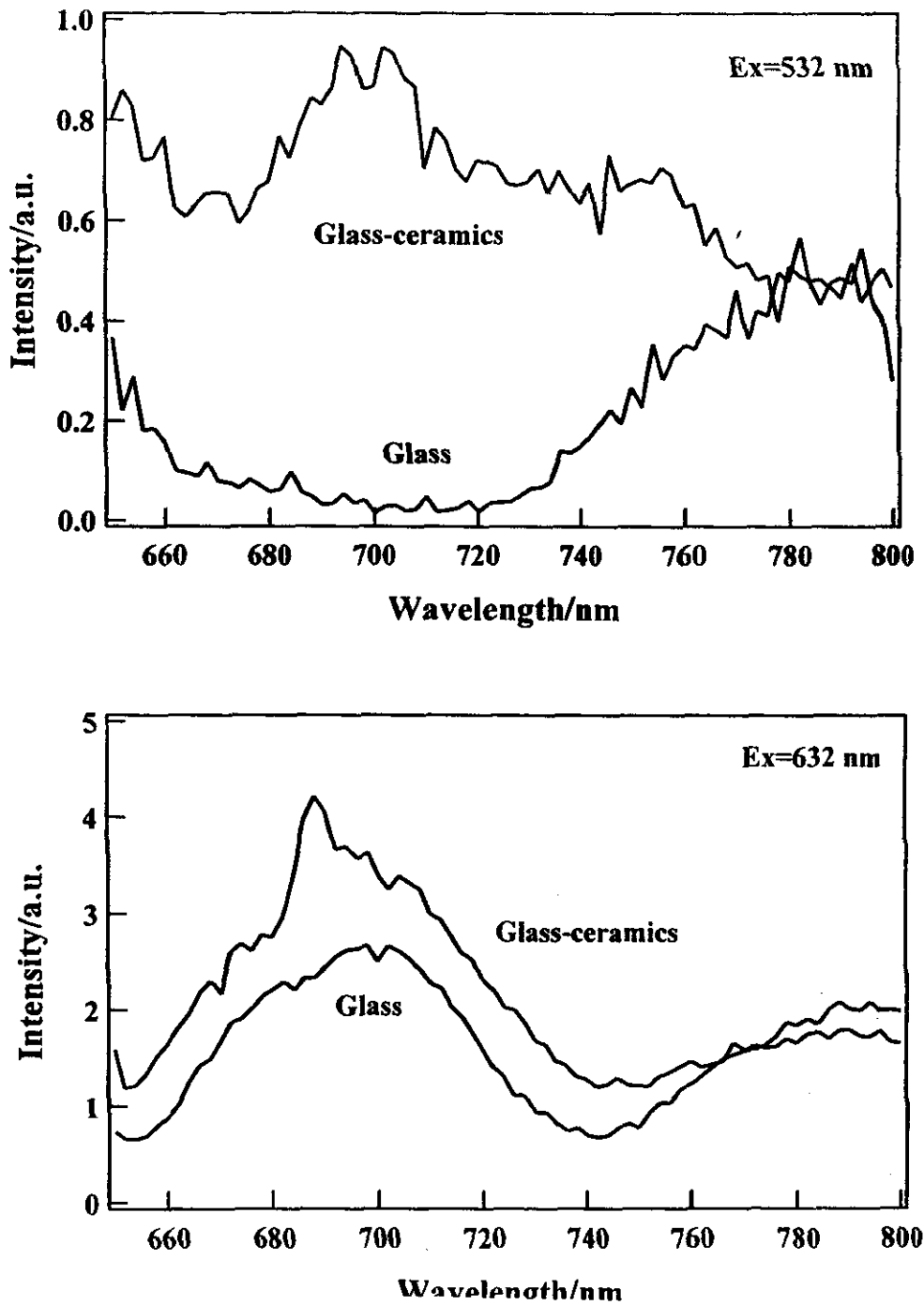


Fig. 13. Emission spectra of glass and glass-ceramics under the excitation of 532 and 632 nm.

On the contrary in glass-ceramics, the absorption bands shift to shorter wavelength at around 390 nm and 545 nm, and the shoulder at around 420 nm is observed, these absorption bands are concluded to be d-d transitions of Cr^{3+} ion. Now assuming that the absorption peak at 386 nm and the shoulder at about 420 nm would be due to the splitting of ${}^4\text{T}_{1g}(\text{F})$ state and their gravity center would be about 400 nm, the ligand field parameters, 10Dq and B , can be estimated to be $\approx 18,350 \text{ cm}^{-1}$ and $\approx 765 \text{ cm}^{-1}$ ($\text{Dq}/\text{B} \approx 2.4$), respectively. This indicates that the Cr^{3+} ions occupy the little strong octahedral sites of spinel crystal $[(\text{Mg},\text{Zn})\text{Al}_2\text{O}_4]$ by the crystallization.

Fig. 13 shows the emission spectra of glass and glass-ceramics under CW(continuous wave) excitation at 532 and 632 nm. The broad emission bands appear at around 680~700 nm and 780~800 nm under the excitation at 632 nm for glass. In contrast for glass-ceramics, the rather sharp structured band can be observed at around 680~720 nm in addition to above broad emission bands⁽⁴³⁾. In particular, it is quite noticeable under excitation at 632 nm. However, the emission at around 780~800 nm is not clear under excitation at 532 nm.

The Cr^{3+} ions usually enter octahedral sites of crystals and glasses, and the ${}^4\text{T}_2$ and ${}^4\text{T}_1$ states of the ${}^4\text{F}$ term undergo considerable interaction of the ligand field. Thus for Cr^{3+} ions in the strong octahedral field such as Al_2O_3 the ${}^4\text{T}_2$ level is located above the ${}^2\text{E}$ state. Therefore, only the ${}^2\text{E} \rightarrow {}^4\text{A}_2$ transition appears in this case. This resonance transition, which is doubly forbidden (by both parity and spin), is characterized by narrow R-line emission⁽⁴⁴⁾.

From above discussion and the result of absorption spectra, the emission at around 680~700 nm might be due to ${}^2\text{E}_g \rightarrow {}^4\text{A}_{2g}$ transition (R-line) of Cr^{3+} ion in strong ligand field, and the broad band centered at around 775 nm can be assigned to ${}^4\text{T}_{2g} \rightarrow {}^4\text{A}_{2g}$ transition of Cr^{3+} ions in weak ligand field. In conclusion, it is estimated that the major part of Cr^{3+} ions occupy the strong octahedral field of spinel crystals $[(\text{Mg},\text{Zn})\text{Al}_2\text{O}_4]$.

4. Conclusion

The absorption and emission spectra of Cr^{3+} ion-containing spinel type transparent glass-ceramics were investigated.

The remarkable change in color and the shift of absorption bands was observed by the crystallization. This is due to the occupation of Cr^{3+} ions in the little strong octahedral field of nano-scale spinel crystals $[(\text{Mg},\text{Zn})\text{Al}_2\text{O}_4]$. The ligand field parameters were estimated to be, $10\text{Dq} \approx 18,350 \text{ cm}^{-1}$ and $\text{B} \approx 765 \text{ cm}^{-1}$ ($\text{Dq}/\text{B} \approx 2.4$).

The rather sharp structured band can be observed at around 680~720 nm in addition to the broad emission bands. In particular, it is quite noticeable under excitation at 430 and 632 nm. This emission can be estimated to due to ${}^2E_g \rightarrow {}^4A_{2g}$ transition(R-line) of Cr^{3+} ions in strong octahedral field of nano-scale spinel crystals[(Mg,Zn)Al₂O₄].

4. 2. Optical properties of Cr³⁺ ions in lithium metasilicate (Li₂O·SiO₂)

transparent glass-ceramics

1. Introduction

Many researches on the behavior of Cr ions in glass, such as valence state and coordination number, have been carried out in association with color generation^(45,46). The Cr ions existed in glasses were mainly Cr⁶⁺ and Cr³⁺, and the equilibrium between them was discussed with glass composition and melting atmosphere.

Glass-ceramics are two phase systems consisting of a base glass within which crystals are grown by heat treatment. Transparent glass-ceramics, in which nano-scale order crystals precipitated, can be obtained by controlling base glass composition and heat treatment condition. Transparent glass-ceramics are currently being considered as hosts for luminescent ions because the possibilities of crystal site control. Although many researches on the absorption and emission characteristics of active ions doped transparent glass-ceramics have been done, the behavior of Cr ion in spinel type and Li₂O·2SiO₂ type transparent glass-ceramics is particularly interesting.

In spinel glass-ceramics, the color changes to pink/red from emerald green. The Cr³⁺ ion was incorporated into the octahedral site of spinel crystal which provides strong ligand field after the crystallization, and therefore the absorption bands shifted to shorter wavelength and the characteristic sharp emission line (R-line) was observed at around 700 nm^(47,51).

In Li₂O·2SiO₂ transparent glass-ceramics^(52,53), on the other hand, it was found that tetrahedrally coordinated Cr⁴⁺ ion could be formed during crystallization. The color changed drastically to deep blue from yellowish-green after crystallization. Both Cr⁶⁺ and Cr³⁺ ions coexisted at first in the glass melted in air, and Cr⁶⁺ ion have been reduced to Cr⁴⁺ ion during crystallization. In this glass-ceramics, tetrahedrally coordinated Cr⁴⁺ ion existed in residual high SiO₂ glassy phase. However, no attractive changes occur in the glass melted under reducing condition, in which only Cr³⁺ ion existed. Thus, the optical properties of transition metal ion are strongly affected by surroundings, and hence an unexpected result can be sometimes obtained in transparent glass-ceramics.

In this paper the optical properties of Cr ion in Li₂O·SiO₂ transparent glass-ceramics were investigated and the possibility of existence of tetrahedrally coordinated Cr³⁺ in Li₂O·SiO₂ crystal is suggested.

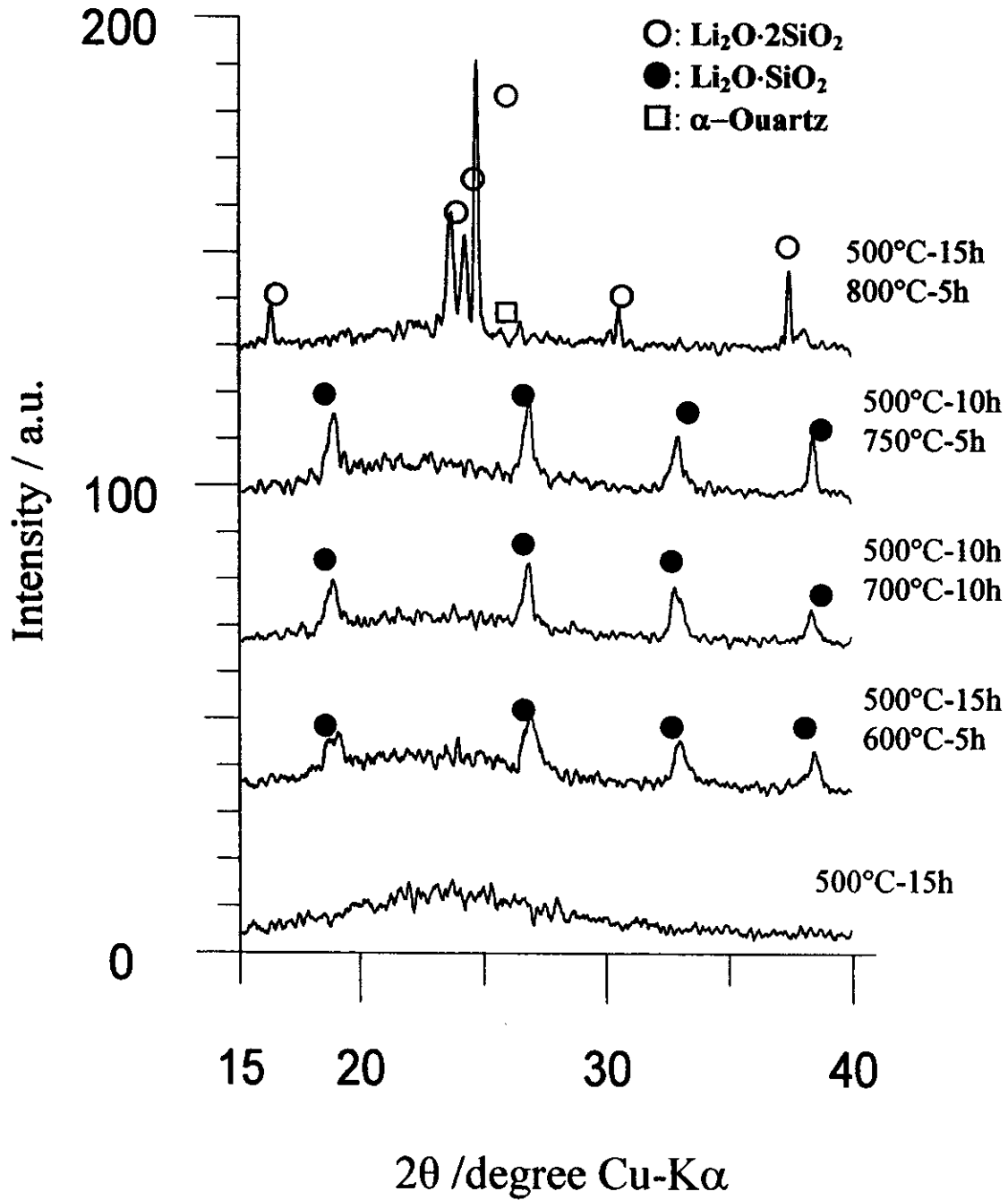


Fig. 14. XRD patterns of $\text{Li}_2\text{O}\cdot\text{SiO}_2$ transparent glass-ceramics.

2. Experiments

2.1. Sample preparation

The base glass composition was $73.0\text{SiO}_2 \cdot 2.15\text{Al}_2\text{O}_3 \cdot 20.7\text{Li}_2\text{O} \cdot 3\text{K}_2\text{O} \cdot 1.15\text{P}_2\text{O}_5$ (mol%) [$77.35\text{SiO}_2 \cdot 3.87\text{Al}_2\text{O}_3 \cdot 10.91\text{Li}_2\text{O} \cdot 4.99\text{K}_2\text{O} \cdot 2.88\text{P}_2\text{O}_5$ (wt%)]. And 0.1 wt% of Cr_2O_3 and 0.5 wt% of Sb_2O_3 were added to 100 g of glass by excess. In this glass the addition of Sb_2O_3 reduced all Cr ion to the 3+ state and eliminated the charge transfer absorption of Cr^{6+} , leaving only the Cr^{3+} ion⁽⁵⁴⁾.

High purity silica sand, alumina and reagent grade of chemicals of Li_2CO_3 , $(\text{NH}_4)_2\text{HPO}_4$, Cr_2O_3 and Sb_2O_3 were used as raw materials. Batch corresponding to 200g of glass was mixed thoroughly and pre-calcined at 300°C overnight to remove NH_3 . It was then melted in a 100 ml Pt/Rh10 crucible at 1450°C for 2 h in an electric furnace. The molten glass was poured onto iron plate and crushed, and melted again at same condition. It was poured onto iron plate and pressed by another iron plate. The glasses were heat treated for crystallization at various conditions after the first heat treatment at 500°C for 10 h for nucleation.

2.2. XRD

Crystalline phases, amount of crystal and crystalline size were examined by powder XRD (Bruker, AXS Model D5005) under the condition of Cu-K α radiation, 40KV-40mA, 0.01° step, 1 sec/step. Amount of crystal was determined using Ohlberg and Strickler's method⁽⁵⁵⁾, and was calculated by

$$100 \times [I_g - I_x] / [I_g - I_c] = \text{percent crystallinity (\%C)} \quad 2)$$

where I_g is the background intensity of glass, I_x that of specimens and I_c that of α -Quartz at $2\theta = 23^\circ$. The calibration curve was obtained using parent glass and α -Quartz at various ratios, and showed good linearity. The percent crystallinity can be obtained by wt%.

The crystal size was calculated using Scherrer's equation.

$$d = 0.9 \cdot \lambda / \beta \cdot \cos \theta \quad 1)$$

where λ is the wavelength of X-ray radiation (1.54 \AA), β the true half width (radian) and θ the diffraction angle (degree). True half width was determined by Jones method⁽⁵⁶⁾, and α -Quartz was used as a standard.

2.3. Optical absorption and emission spectra

The glass and glass-ceramics were optically polished into about 1.5 mm in thickness. The absorption spectra were measured at room temperature with Varian Cary 5E UV-VIS-NIR spectrophotometer in the range of 350-2000nm. The emission spectra were measured at room temperature with Perkin-Elmer LS50B luminescence spectrometer in the range of 300-900 nm.

3. Results and discussion

3.1. Properties of glass-ceramics

The glass-ceramics appeared to be transparent to translucent by the heat treatment below 800°C, and completely opaque above 800°C.

Figure 14 shows XRD patterns of glass-ceramics heat treated under various conditions. Only lithium metasilicate($\text{Li}_2\text{O}\cdot\text{SiO}_2$, hereafter L·S) crystal precipitates below 800°C, and above which a lithium disilicate($\text{Li}_2\text{O}\cdot 2\text{SiO}_2$) crystal precipitates as a major crystalline phase with a small amount of α -Quartz crystal.

Table 6 shows percent crystallinity and crystal size of transparent glass-ceramics. The percent crystallinity was ranging 16.5~33.3% and the crystallite size was ranging 20.1~33.7 nm. Both the percent crystallinity and the crystallite size increased with increase in heating temperature and time. If all of Li_2O (10.9 wt%) would be spent for the crystallization of L·S crystal, the amount of L·S crystal would be about 33 wt%. The measured values may be reasonable.

3.2. Absorption spectra

The glass appeared to be emerald green in color, and turned to pink color by the crystallization below 800°C. However, the pink color disappeared and turned to greenish opaque after the heat treatment Table 6. Crystalline phase, percent crystallinity and crystallite size of transparent glass-ceramics.

Heat treatment (°C – h)*	Appearance	Crystalline phase	Percent crystallinity (%C, by wt)	Crystallite size (nm)
650-10	Transparent	$\text{Li}_2\text{O}\cdot\text{SiO}_2$	16.5	20.1
700-5	Transparent	$\text{Li}_2\text{O}\cdot\text{SiO}_2$	28.8	22.5
700-10	Slightly translucent	$\text{Li}_2\text{O}\cdot\text{SiO}_2$	28.8	27.5
750-5	Slightly translucent	$\text{Li}_2\text{O}\cdot\text{SiO}_2$	33.7	34.0

*: 2nd heat treatment, 1st heat treatment: 500°C – 10 h.

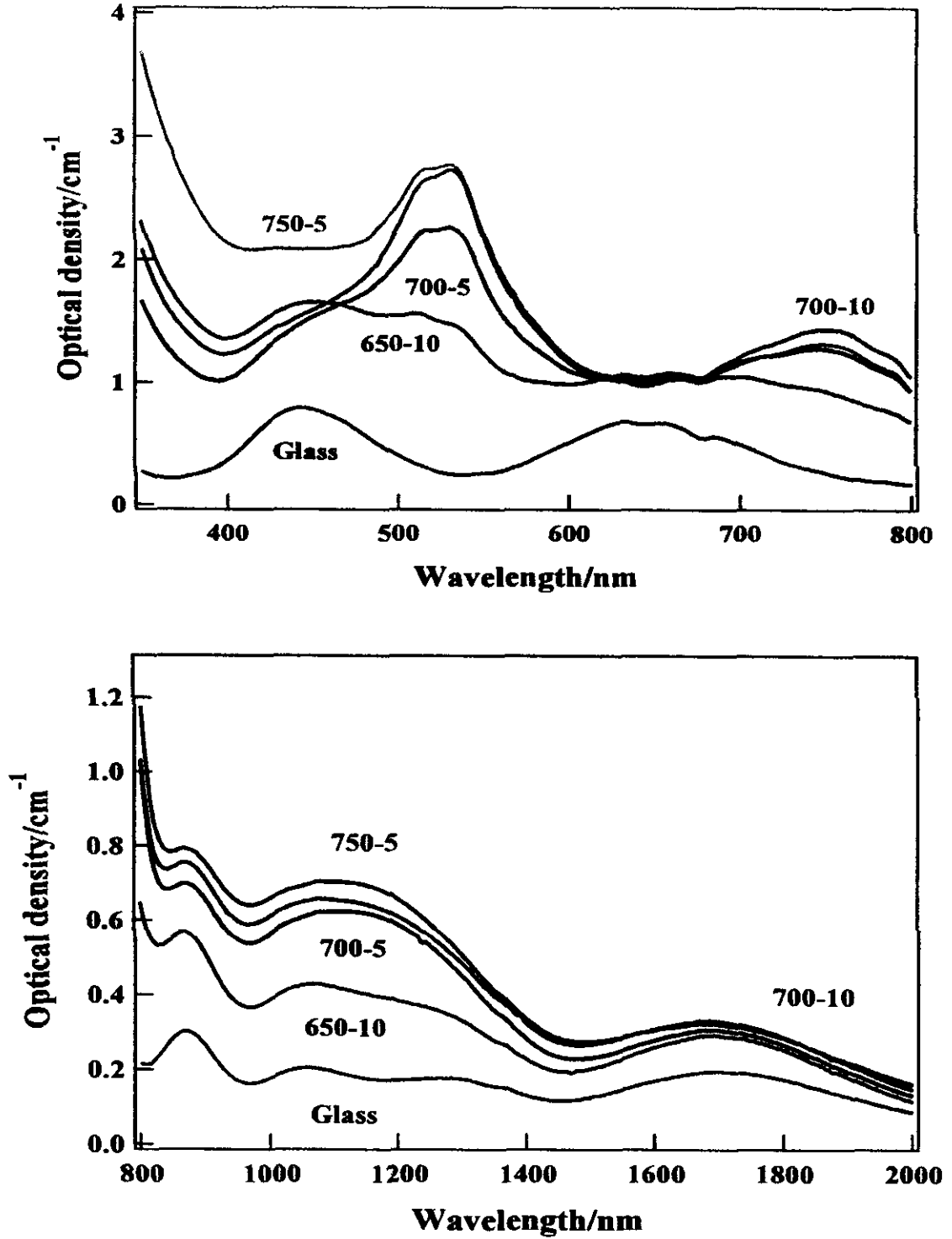


Fig. 15. Absorption spectra of glass and glass-ceramics.

Glass-ceramics: 1st heat treatment: 500°C-10h.

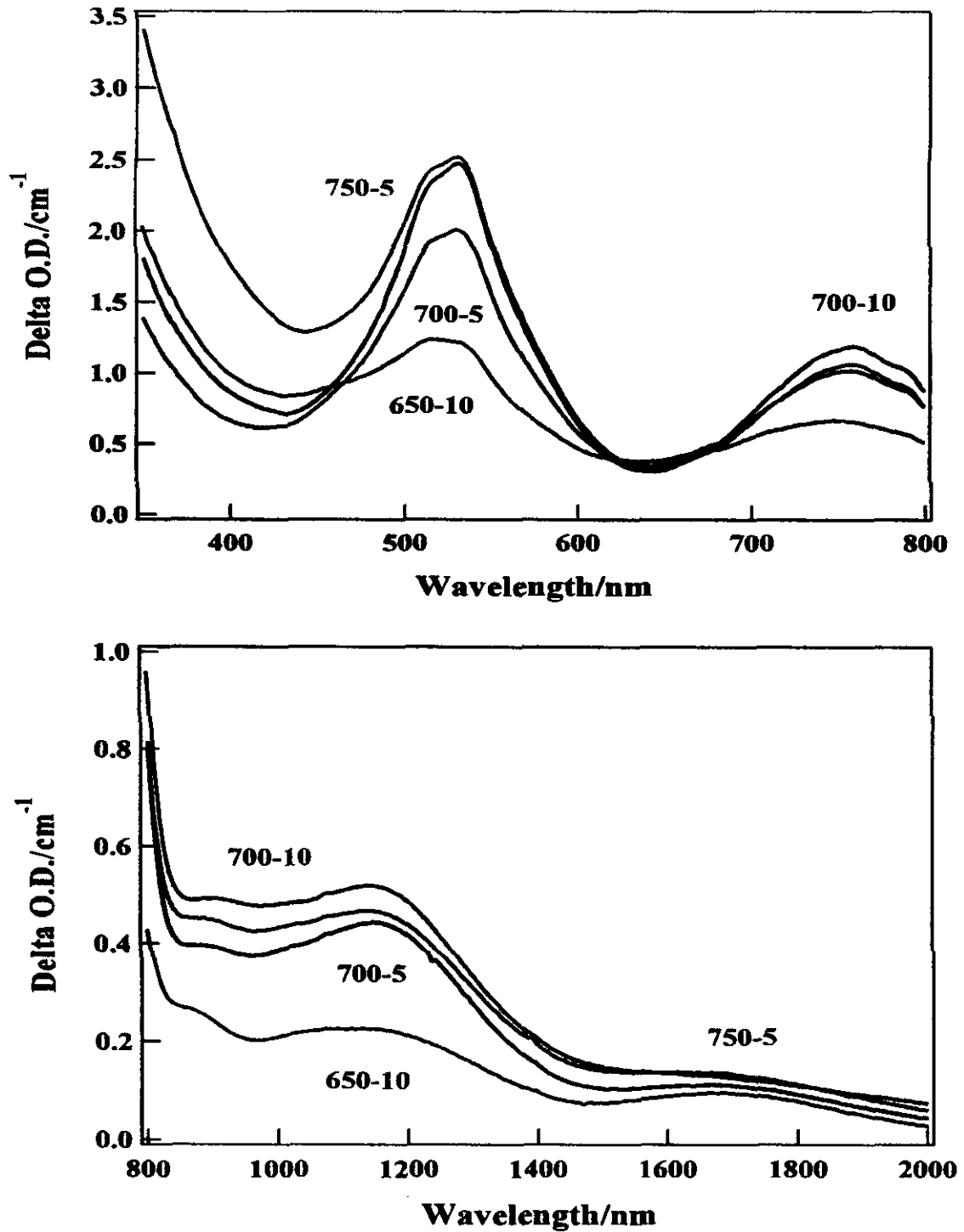


Fig. 16. Differential spectra of glass and glass-ceramics.

Glass-ceramics: 1st heat treatment: 500°C-10h.

$$\Delta[\text{O.D.}(\text{cm}^{-1})] = [\text{O.D.}(\text{cm}^{-1})]_{\text{glass-ceramics}} - [\text{O.D.}(\text{cm}^{-1})]_{\text{glass}}$$

above 800°C.

Figure 15 shows the absorption spectra of glass and glass-ceramics. The weak absorption bands at around 450 and 650 nm in VIS region due to d-d transition of Cr³⁺ ion are observed in glass. In NIR region, weak absorption bands at around 1070 and 1300 nm are observed in glass. This spectrum pattern is a typical Cr³⁺ ion in octahedral coordination, no other absorption bands can be observed, and hence it seems that only Cr³⁺ ion exists in this glass. The absorption bands in VIS region can be assigned to ⁴A₂→⁴T₁ and ⁴A₂→⁴T₂ transition, respectively.

The new and strong bands appear at around 520 and 750 nm in VIS region and the broad band at around 1150 nm appears in NIR region after the crystallization. It seems that these new absorption bands overlap apparently on an original spectrum of glass. It should be noted that the absorption intensity of new bands increases with increase in heating temperature and time. The absorption intensity in near UV region also increases due to the scattering by the crystallization.

The concentration of Cr³⁺ ion in octahedral site might not change significantly, and hence the concentration of Cr ion corresponding to the appearance of new bands might be low. This indicates that the certain Cr ion corresponding to the appearance of new bands might have higher absorption coefficient.

The differential spectrum may be useful for the demonstration of the appearance and disappearance of certain ion species. Here, the differential spectra may be expressed by:

$$\Delta[\text{O.D.}(cm^{-1})] = [\text{O.D.}(cm^{-1})]_{\text{glass-ceramics}} - [\text{O.D.}(cm^{-1})]_{\text{glass}} \quad (3)$$

and represents the appearance and disappearance of certain absorption band.

Figure 16 shows the differential spectra. It is clearly seen that new bands appear at around 520, 750 and 1150 nm. The former two bands show complicated structure. The relationship between $\Delta[\text{O.D.}(cm^{-1})]$ of these new bands and % crystallinity is shown in Figure 17. The absorption intensity of these new absorption bands increases with increase in the amount of crystal. This indicates that these new absorption bands are produced by the crystallization. In this glass, it seems that the change in valence state does not occur and Cr³⁺ is incorporated into L·S crystal.

The origin of the appearance of new bands will be considered and the assignment of these bands was analyzed based on the below two assumptions:

- (1). Change in ligand field strength [Cr³⁺(octahedral)→Cr³⁺(octahedral)]
- (2). Change in coordination number [Cr³⁺(octahedral)→Cr³⁺(tetrahedral)]

In the first case, if the Cr³⁺ ion would be incorporated into strong ligand field in L·S crystal, an absorption band corresponding to ⁴A₂→⁴T₁ transition should be observed at around 400 nm. However,

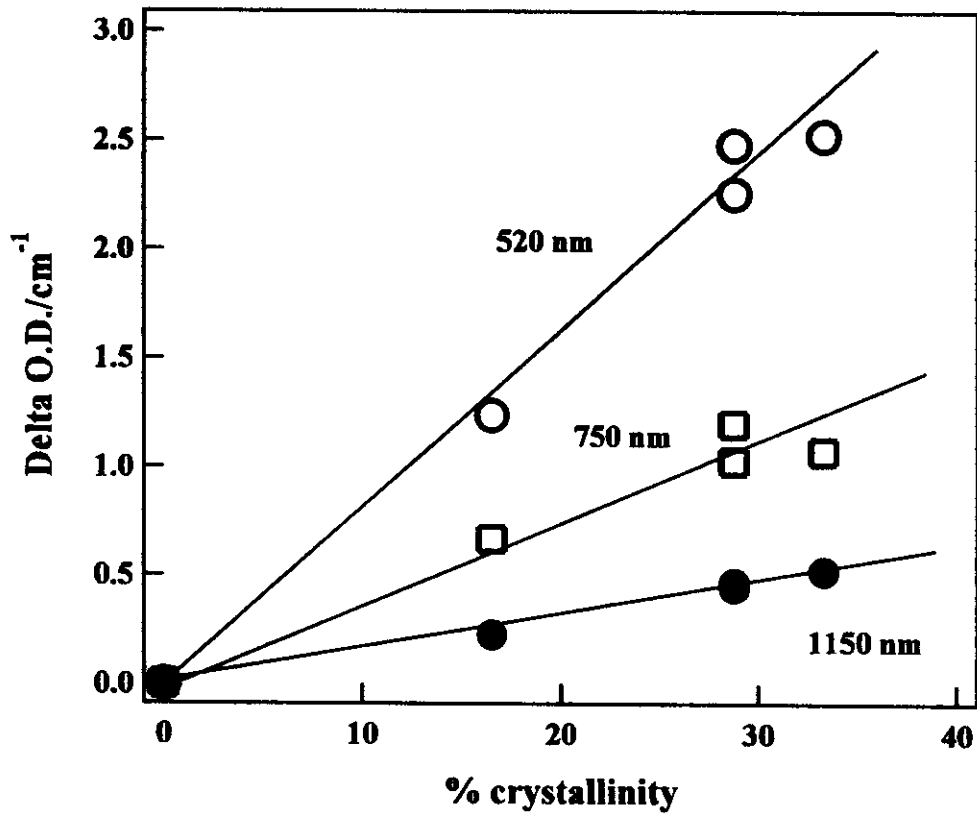


Fig. 17. Relation between absorption intensity of new bands and % crystallinity.

new absorption band can not be observed around that region. Therefore, it is concluded that the bands shift to longer wavelength by the incorporation of Cr^{3+} ion into weak ligand field of L·S crystal unlike ruby and spinel crystals (strong ligand field). In ruby and spinel crystals, the absorption bands of Cr^{3+} ion with octahedral site shifted to shorter wavelength^(50,51). The absorption spectrum of L·S glass-ceramics heat treated at $500^\circ\text{C} - 10\text{ h}$ and $700^\circ\text{C} - 5\text{ h}$ was analyzed by multi-peak fitting method with a Voigtian distribution. By assuming that two absorption peaks, 520 and 750 nm in VIS region, are assigned to ${}^4\text{A}_2 \rightarrow {}^4\text{T}_1$ and ${}^4\text{A}_2 \rightarrow {}^4\text{T}_2$ transition, the ligand field parameters can be estimated to be $10\text{Dq} = 13,197\text{ cm}^{-1}$, Table7. Ligand field parameters of Cr^{3+} ions in glass and glass-ceramics.

Cr^{3+} ion	Transition	Energy center (cm^{-1})	Intensity O.D./ cm^{-1}	Half width (cm^{-1})	Gravity center (cm^{-1})
6 coordination	${}^4\text{A}_{2g} \rightarrow {}^4\text{T}_{2g}$	21,800	0.34	1,740	19,396
		20,000	0.75	1,500	
		18,750	2.1	1,550	
	${}^4\text{A}_{2g} \rightarrow {}^4\text{T}_{1g}$	14,500	0.05	1,000	13,197 (10Dq)
		13,200	0.95	1,100	
		12,200	0.06	1,145	
$10\text{Dq} = 13,197\text{ cm}^{-1}$, $B = 657\text{ cm}^{-1}$, $\text{Dq}/B = 2.01$					
4 coordination	${}^4\text{T}_{1g}(\text{F}) \rightarrow {}^4\text{T}_{1g}(\text{P})$	21,800	0.34	1,500	20,620
		20,000	0.75	1,550	
	${}^4\text{T}_{1g}(\text{F}) \rightarrow {}^4\text{A}_{2g}(\text{F})$	18,750	2.1	1,550	18,750
	?	14,500	0.05	1,000	?
		13,200	0.95	1,100	
		12,200	0.06	1,145	
${}^4\text{T}_{1g}(\text{F}) \rightarrow {}^4\text{A}_{2g}(\text{F})$	8,390	0.33	1,200	8,390	
$10\text{Dq} = 9,657\text{ cm}^{-1}$, $B = 886\text{ cm}^{-1}$, $\text{Dq}/B = 1.09$					
Glass 6 coordination	$10\text{Dq} = 15,385\text{ cm}^{-1}$, $B = 705\text{ cm}^{-1}$, $\text{Dq}/B = 2.18$				
CrCl_3 6 coordination	$10\text{Dq} = 13,600\text{ cm}^{-1}$, $B = 510\text{ cm}^{-1}$, $\text{Dq}/B = 2.67$				

$B = 657 \text{ cm}^{-1}$ and $Dq/B = 2.01$ as shown in Table 7. In Table 7, the ligand field parameters of CrCl_3 are also shown as a typical example of weak ligand field. It should be noticed that $10Dq$ of Cr^{3+} ion in glass-ceramics is much smaller than that in glass and similar to that of CrCl_3 .

According to spectrochemical series, an oxygen ligand produces higher ligand field strength than chlorine, and therefore, Cr^{3+} ion in this transparent glass-ceramics should indicate stronger ligand field strength than that in CrCl_3 . Further, the crystal usually enhances the ligand field strength. And the strong absorption intensity of new absorption bands can not be interpreted sufficiently by this assumption. Thus, the assumption of case (1) might not be acceptable.

On the contrary in the second case, it is known that the absorption intensity of transition metal ions in tetrahedral site is much greater than that in octahedral site. The d^3 electronic configuration in tetrahedral site can be conducted with that of d^7 in octahedral site [$d^3(\text{Oh}) = d^{10-7}(\text{Td})$]. The overall spectral patterns of glass-ceramics, especially differential spectra, are similar to that of Co^{2+} ion in octahedral site [d^7] despite the peak position are different. Now assuming that Cr^{3+} ion occupies tetrahedral site in L·S crystal, three absorption bands may be assigned to ${}^4T_{1g}(\text{F}) \rightarrow {}^4T_{2g}(\text{F})$ (1150 nm), ${}^4T_{1g}(\text{F}) \rightarrow {}^4A_{2g}(\text{F})$ (532 nm) and ${}^4T_{1g}(\text{F}) \rightarrow {}^4T_{2g}(\text{P})$ (510 nm), respectively, and ligand field parameters can be estimated and is shown in Table 2. The $10Dq$ is little greater than that expected by $(4/9)Dq(\text{octahedral})$. By using these values, the absorption band of ${}^4T_{1g}(\text{F}) \rightarrow {}^4A_{2g}(\text{F})$ transition is estimated to be $18,659 \text{ cm}^{-1}$, which is agreed with experimental result ($18,750 \text{ cm}^{-1}$) very well.

Although the some bands can not be assigned, these assignments may satisfy the experimental result. Furthermore, the increase in absorption intensity can be explained by the presence of tetrahedrally coordinated Cr^{3+} ion. The existence of tetrahedrally coordinated Cr^{3+} is suggested in some single crystals^(57,58). Thus, the possibility of existence of tetrahedrally coordinated Cr^{3+} ion in L·S crystal is suggested.

3.3. Emission spectra

Usually Cr^{3+} ion in strong ligand field (octahedral) exhibits the characteristic weak pink to red fluorescence under sun light and also the characteristic sharp line emission around 700 nm can be observed under the excitation of shorter wavelength of light. However, these behaviors were not observed for glass-ceramics.

Figure 18 shows the emission spectra of glass and glass-ceramics under the excitation of 450 and 520 nm. Two broad emission bands centered at around 620 and 720 nm were observed in glass-ceramics,

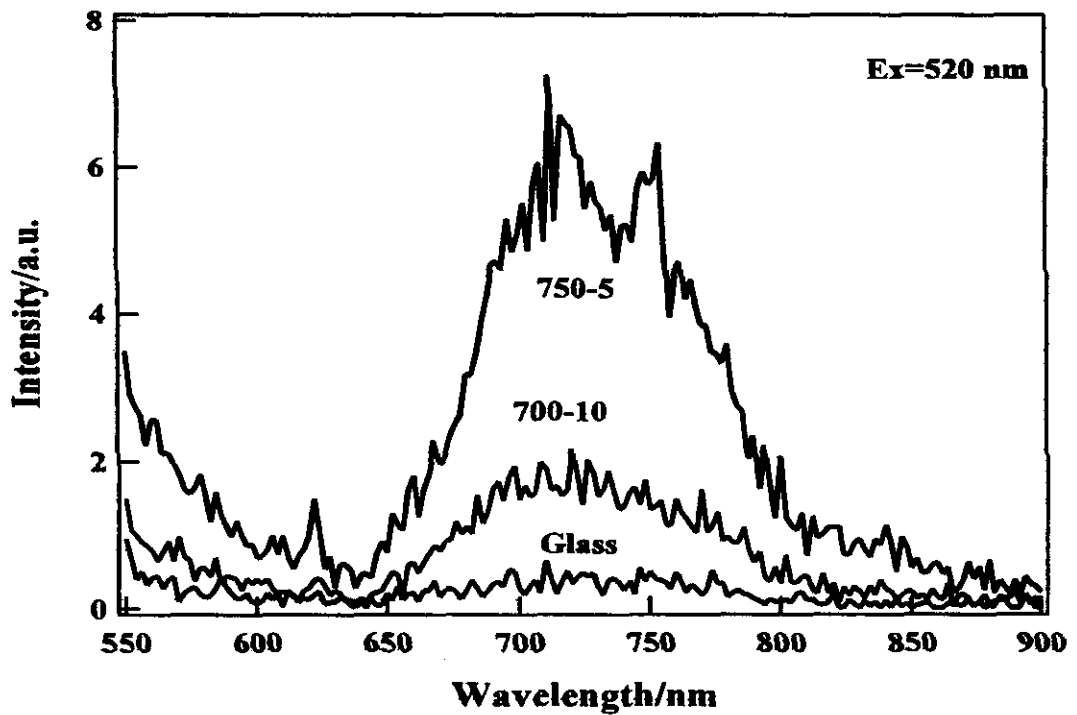
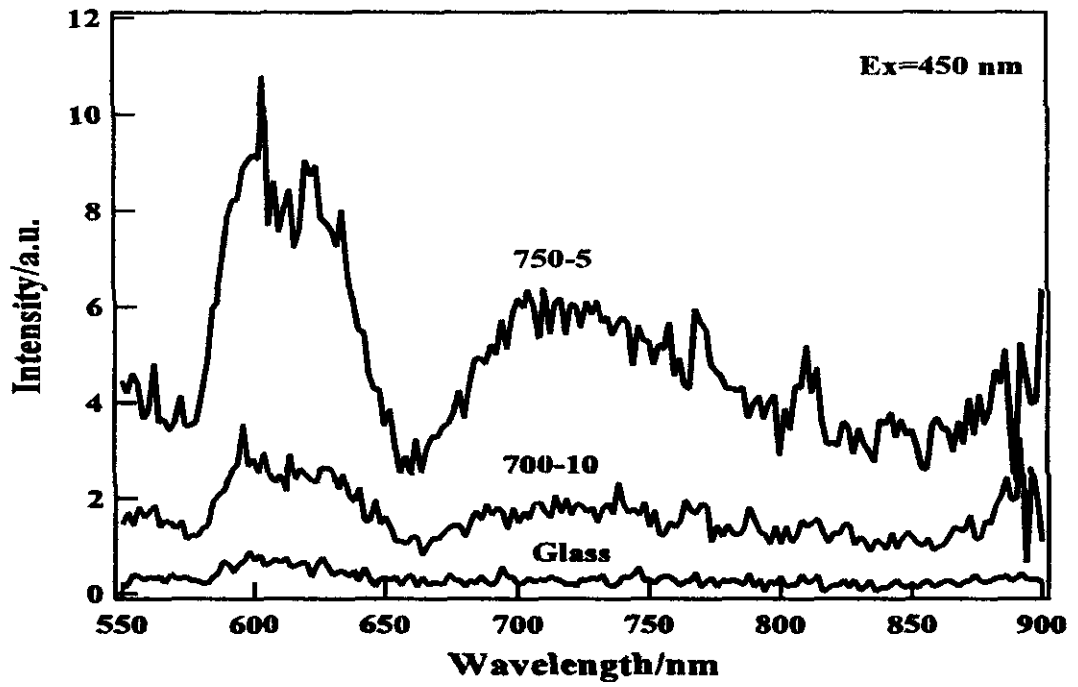


Fig. 18. Emission spectra of glass and glass-ceramics at room temperature.

whilst only former emission band was observed in glass under the excitation of 450 nm. The former emission band disappears and only latter emission band is observed under the excitation of 520 nm for glass-ceramics. The emission intensity increases with progress of crystallization, and that of glass-ceramics heat treated at 500°C–15h, 750°C–5h increases by about 10 times of glass. The emission band ranging 650 – 800 nm might be the characteristic band of tetrahedrally coordinated Cr³⁺ in L·S crystal. However, it is quite difficult to assign these emission bands to certain transition, because there are many emission bands around 0.7-1.0 μm region from octahedrally coordinated Cr³⁺ ion.

4. Conclusion

The optical properties of Cr³⁺ in lithium metasilicate(Li₂O·SiO₂) transparent glass-ceramics was investigated.

Only Li₂O·SiO₂ crystal precipitated in glass-ceramics by the heat treatment below 800°C, and the percent crystallinity was ranging 16.5~33.3% and the crystallite size was ranging 20.1~33.7 nm. The color changed to pink from emerald green of glass, and new and strong bands appeared at around 520, 760 and 1150 nm by the crystallization. The absorption intensity increases with increase in heating temperature and time for crystallization. The assignments of these bands were analyzed by the assumptions based on (1). Change in ligand field strength[octahedral → tetrahedral] and (2). Change in coordination number[6→4].

In the former case, the calculated ligand field parameters were $10Dq = 13,197 \text{ cm}^{-1}$, $B = 657 \text{ cm}^{-1}$ and $Dq/B = 2.01$, respectively. The $10Dq$ value is too small compared with that in glass, further the increase in absorption intensity can not be interpreted by this assumption. Therefore, this assumption can not be acceptable.

On the other hand in latter case, the ligand field parameters can be estimated to be $10Dq = 9,657 \text{ cm}^{-1}$, $B = 886 \text{ cm}^{-1}$ and $Dq/B = 1.09$, respectively. These values seem to be reasonable for tetrahedrally coordinated Cr³⁺ ion in Li₂O·SiO₂ crystal. And the increase in absorption intensity can be explained by this assumption.

Broad emission bands at around 620 and 720 nm were observed under the excitation of 450 nm light in glass-ceramics, and only latter band was observed under the excitation of 520 nm light. The emission intensity increased with the increase in crystallization temperature. The latter band ranging 650 – 800 nm might be the characteristic band of tetrahedrally coordinated Cr³⁺ in L·S crystal. Thus the existence of tetrahedrally coordinated Cr³⁺ ion in Li₂O·SiO₂ crystal is suggested.

4.3. Cr³⁺ ion in AlPO₄ transparent glass-ceramics

1. Introduction

The electronic configuration of transition metal ions is strongly influenced by their ligands. This causes the change in optical properties, such as color change, etc. As mentioned previous sections, the typical ligand field absorption has been observed^(59,60). In spinel type transparent glass-ceramics containing Cr³⁺ ion, the color changes to pink/red from emerald green, and the absorption bands shifted to shorter wavelength by crystallization. It was confirmed that Cr³⁺ ion occupies strong ligand field site in spinel crystal. On the contrary, in Li₂O·SiO₂ transparent glass-ceramics, though the color changes to pink from emerald green, the absorption band shifted to longer wavelength. This indicated that Cr³⁺ ion in this transparent glass-ceramics occupied in weak ligand field site.

AlPO₄ crystal or AlPO₄(-SiO₂) solid solution differs from above crystals, spinel and Li₂O·SiO₂, because these crystals consist of glass formers. From the structural point of view, the optical properties of Cr³⁺ in AlPO₄ crystal or solid solution are particularly interesting. Here the optical properties of Cr³⁺ ion in AlPO₄ transparent glass-ceramics are investigated.

2. Experiments

2.1. Sample preparation

The base glass composition used was 40SiO₂·20Al₂O₃·20P₂O₅·5B₂O₃·15Na₂O (mol%) [28.07SiO₂·23.82Al₂O₃·33.17P₂O₅·4.07B₂O₃·10.86Na₂O·0.4Cr₂O₃ (wt%)]. High purity silica sand, alumina, reagent grade chemicals of (NaPO₃)₆, H₃BO₃, Na₂CO₃ and Cr₂O₃ (Carlo Erba) were used as raw materials. A batch corresponding to 200 g of glass was mixed thoroughly and melted in 100 ml Pt/Rh crucible according to schedule, 1550°C – 3 h and 1500°C – 1 h, in an electric furnace in air. Then the molten glass was poured onto iron plate and pressed by another iron plate. The glass was annealed at about 500°C for 30 min and cooled to room temperature in the furnace.

The glass samples were heat treated at 510°C – 10 h for nucleation and 600~650°C – 5~10 h for crystallization. The glass and glass-ceramics were optically polished into about 2 mm in thickness.

2.2. XRD

The crystalline phases precipitated, amount of crystal and crystal size were examined by powder X-ray diffraction analysis⁽⁶¹⁾

2.3. Absorption and emission spectra

The absorption spectra of glass and glass-ceramics was measured using Variant Carry 5E UV-VIS-NIR spectrometer in the range of 300~1500 nm. The emission spectra were measured using with Perkin-Elmer Luminescence Spectrometer LS50B in the range of 300~900 nm at room temperature.

3. Results and discussion

The highly transparent glass-ceramics can be obtained by the heat treatment, 510°C – 10 h and 600°C – 10 h. The transparency of glass-ceramics was is nearly equal to that of glass.

The main crystalline phase, amount of crystal and crystal size were tridymite type AlPO_4 , 48% and 34 nm, respectively.

Figure 19 shows the absorption spectra of glass and glass-ceramics. The color of both samples was emerald green. Three absorption bands were observed. The band at around 350 nm is assigned to charge transfer band of four coordinated Cr^{6+} ion. And bands at around 450 nm and 650 nm are assigned to ${}^4A_{2g} \rightarrow {}^4T_{2g}$ and ${}^4A_{2g} \rightarrow {}^4T_{1g}$ transition of six coordinated Cr^{3+} ion.

Absorption bands of Cr^{3+} ion shifted to shorter wavelength slightly by the crystallization, and the color did not change. The differential spectrum is effective to clarify the phenomenon happened by crystallization, and it may be expressed by $\Delta \text{O.D. (cm}^{-1}\text{)} = [\text{O.D. (cm}^{-1}\text{)}]_{\text{glass-ceramics}} - \text{O.D. (cm}^{-1}\text{)}_{\text{glass}}$.

Table 8. Ligand field parameters of Cr^{3+} ion in various hosts.

Materials	$10Dq/\text{cm}^{-1}$	B/cm^{-1}	Dq/B
Soda-lime silicate glass	15,291	750	2.04
Spinel TPGC* ⁽⁶²⁾	18,349	765	2.40
$\text{Li}_2\text{O}\cdot\text{SiO}_2$ TPGC* ⁽⁶⁰⁾ [Tetrahedral]	9,657	886	1.09
AlPO_4 TPGC*	16,611	687	2.42
Alexandrite	—	—	2.15
Ruby	—	—	2.8
Crossing point			2.3

*: TPGC=transparent glass-ceramics

Fig. 19 (b) shows the differential spectrum. It is clearly seen that new absorption bands appeared

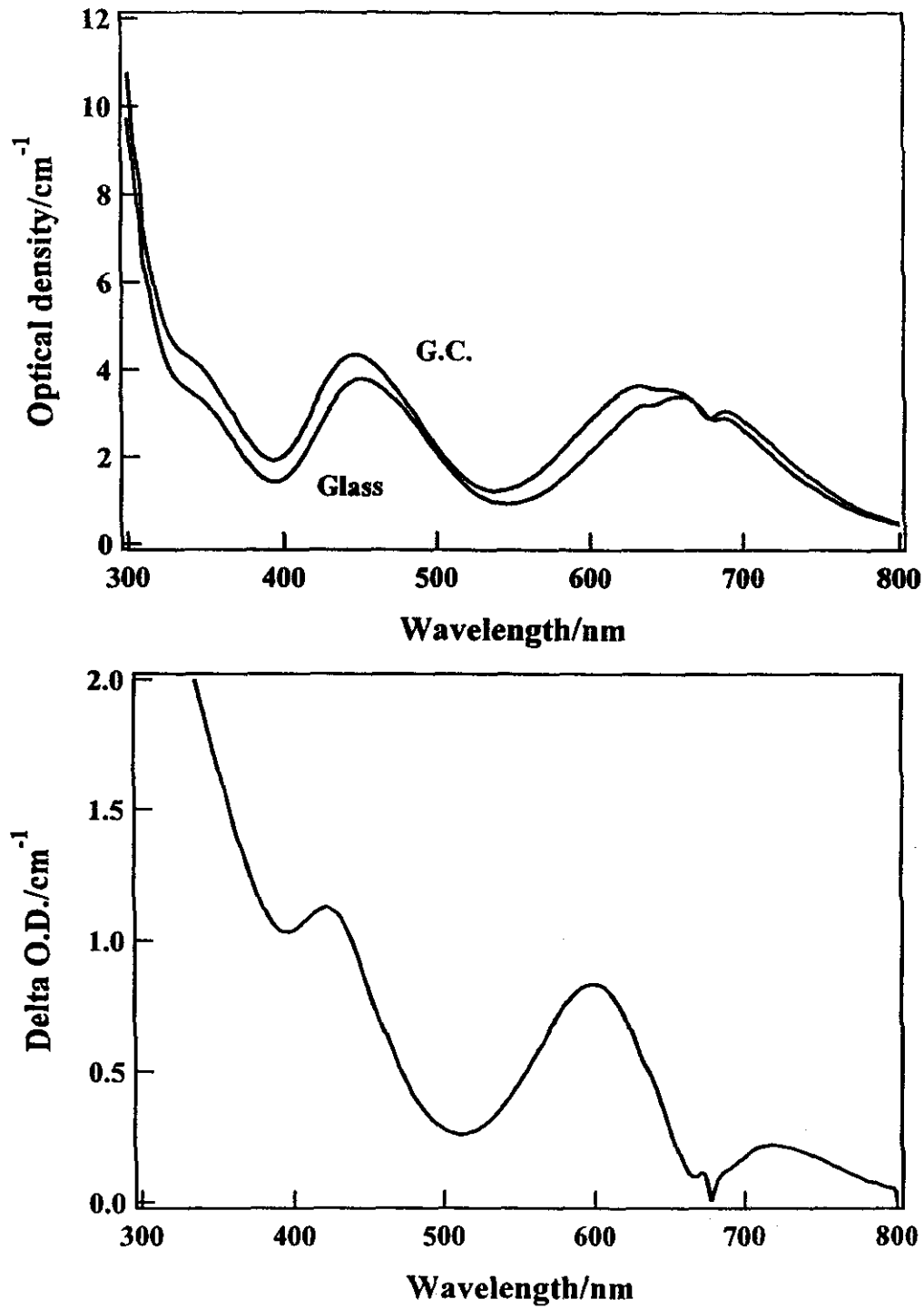


Fig. 19. Absorption and differential spectra of glass and glass-ceramics.

$$\Delta[\text{O.D.}(\text{cm}^{-1})] = [\text{O.D.}(\text{cm}^{-1})]_{\text{glass-ceramics}} - [\text{O.D.}(\text{cm}^{-1})]_{\text{glass}}$$

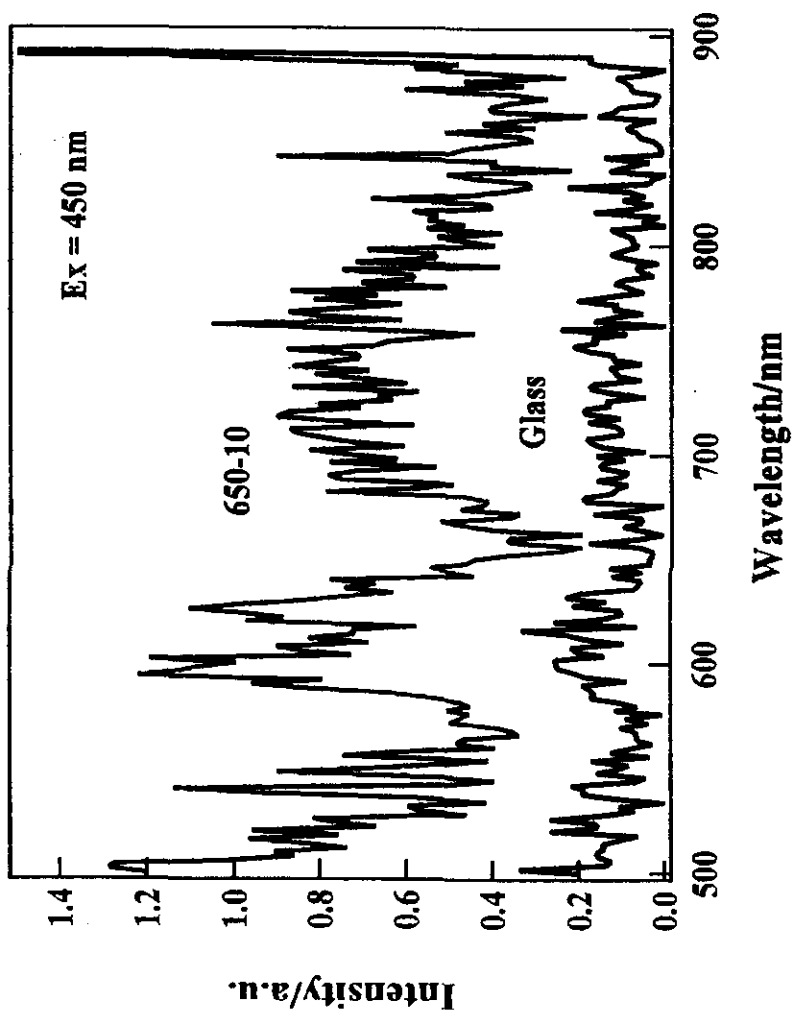


Fig. 20. Emission spectra of glass and glass-ceramics under the excitation of 450 nm.
Glass-ceramics: 510°C-10h, 650°C-5h.

at around 426 nm and 602 nm. These bands assigned to ${}^4A_{2g} \rightarrow {}^4T_{2g}$ and ${}^4A_{2g} \rightarrow {}^4T_{1g}$ transition of six coordinated Cr^{3+} ion in $AlPO_4$ crystal. However, the change in intensity is small, and hence, the amount of Cr^{3+} ion in $AlPO_4$ crystal might be small. From this result, the ligand field parameters, $10Dq$ and B , can be estimated to be $10Dq = 16,611 \text{ cm}^{-1}$ and $B = 687 \text{ cm}^{-1}$,

Respectively⁽⁶²⁾. These values are listed in Table 8 with other materials. The splitting is slightly larger than that in glass, and Cr^{3+} ion occupies little strong ligand field site in $AlPO_4$ crystal. It is well known that the Cr^{3+} site ion in various materials can be classified into two sites, one is strong ligand field site ($Dq/B > 2.3$) and another is weak ligand field site ($Dq/B < 2.3$). Cr^{3+} ion in strong ligand field site can emit sharp line around 700 nm by the excitation of UV light, this line is called R-line and dues to ${}^2E_g \rightarrow {}^4A_{2g}$ transition. On the contrary, Cr^{3+} ion in weak ligand field emits only broad emission near IR region.

Figure 20 shows emission spectra of glass and glass-ceramics under the excitation of 450 nm. The emission intensity of glass-ceramics is little higher than that of glass, especially at around 500 ~ 600nm. This is the typical emission spectra of Cr^{3+} ions in intermediate ligand field.

4. Conclusion

The absorption and emission characteristics of Cr^{3+} ion in $AlPO_4$ transparent glass-ceramics were investigated.

The absorption bands shifted to shorter wavelength by the crystallization. However, the amount of Cr^{3+} ion in $AlPO_4$ crystal is estimated to be small. The new bands appeared at 426 and 602 nm, which were assigned to be ${}^4A_{2g} \rightarrow {}^4T_{2g}$ and ${}^4A_{2g} \rightarrow {}^4T_{1g}$ transition. The ligand field parameters can be calculated: $10Dq = 16,611 \text{ cm}^{-1}$ and $B = 687 \text{ cm}^{-1}$, respectively. The Dq/B was 2.42, and it was found that Cr^{3+} occupies in intermediate ligand field in $AlPO_4$ crystal.

4.4. Cr⁴⁺ ion in Li₂O·2SiO₂ transparent glass-ceramics

1. Introduction

Many researches on the behavior of Cr ions in glasses, such as valence state, coordination number and redox equilibrium, have been carried out in association with color generation⁽⁶³⁻⁶⁵⁾. The Cr ions existed in glasses were usually Cr³⁺ and Cr⁶⁺, and the redox equilibrium between them was discussed with glass composition and melting atmosphere^(66,67). However, since the existence of Cr⁴⁺ ions in glasses⁽⁶⁸⁻⁷¹⁾ and single crystals⁽⁷²⁻⁷⁴⁾ has been reported, the researches on Cr⁴⁺ ions in glasses and single crystals, especially in laser materials and photonics devices, are actively taking place. It has been found that stable Cr⁴⁺ ions were formed only in aluminate, gallate and aluminosilicate glasses with high modifier oxides, and their spectroscopic properties have already been measured^(7,8). The formation of Cr⁴⁺ ions is strongly related to the interaction between Cr³⁺ ions and oxygen excess defects, such as super oxide ion radicals and peroxy linkage, in these glass systems⁽⁶⁸⁻⁷¹⁾.

Transition metal ions are notoriously inefficient when incorporated into glass host, due to the difficulty of controlling the local environment, to which they are very sensitive. However, the properties of Cr⁴⁺ doped glass-ceramics have received little attention, despite the apparent advantages of crystal site control^(75,76).

The authors investigate the behavior of Cr ions in transparent glass-ceramics and found that the Cr⁴⁺ ion can be formed in Li₂O-SiO₂ system transparent glass-ceramics and the characteristic emission of Cr⁴⁺ ion in near infra red region appeared. The formation mechanism of Cr⁴⁺ ions in Li₂O-SiO₂ system transparent glass-ceramics will be discussed here.

2. Experiments

2.1. Sample preparation

Li₂O-SiO₂ system transparent glass-ceramics were prepared and its glass composition was 80SiO₂·4Al₂O₃·13Li₂O·3P₂O₅·0.1~0.4Cr₂O₃ (wt%). High purity silica sand, alumina, and reagent grade chemicals of Li₂CO₃, (NH₄)₂HPO₄, and Cr₂O₃ (Carlo Erba) were used as raw materials. Batches corresponding to 100g of glass were mixed thoroughly and pre-calcined at 400°C for overnight to remove NH₃. They were then melted at 1450°C for 2 h in 100cc Pt/Rh10 crucible in air. The glasses were heat treated at 500°C—15 h for nucleation, and subsequently heat treated at higher temperature for crystallization. They were then cut and polished optically into about 1.0 mm in thickness.

2.2. XRD

The crystalline phases, crystal size and percent crystallinity were determined by XRD⁽⁷⁷⁾.

2.3. Absorption and emission spectra

The absorption spectra were measured with Cary 5E UV-VIS-NIR spectrometer in the range of 300~1600 nm at room temperature. The emission spectra of Cr⁴⁺ ions were measured in accordance with Feng and Tanabe method⁽⁷¹⁾ in the range of 800~1600 nm under the excitation of 792 nm laser diode at room temperature.

3. Results and Discussion

The main crystalline phase is Li₂O·2SiO₂ with a small amount of Li₂O·SiO₂ and α -quartz. The crystal sizes were ranging from 20 to 40 nm and the percent crystallinity was ranging from 60 to 80 nm.

The remarkable change in color was observed by the crystallization, from light green to deep blue. Figure 21 shows the absorption spectra of glass and glass-ceramics. The strong absorption band due to the charge transfer transition of Cr⁶⁺ and a weak absorption bands due to d-d transition of Cr³⁺ appear at around 370 nm and 650 nm, respectively, in glass. On the contrary, in glass-ceramics, the new strong absorption band appears at around 550~750 nm. It should be noted that its absorption intensity increases markedly and the absorption intensity due to Cr⁶⁺ ions decreases. Figure 22 shows the relation between absorption intensity at around 650 nm and second heating temperature. The absorption intensity increases significantly with increase in heating temperature, reaches the maximum at 750°C and decreases again at higher temperature. Especially, the absorption intensity of glass-ceramics, 750°C – 5 h, increases by 15 times that of glass. This new and strong absorption band can not be ascribed to Cr³⁺ and Cr⁶⁺ ions, it might be due to a certain ions formed during crystallization. The spectral pattern of glass-ceramics is similar to that of tetrahedrally coordinated Cr⁴⁺ ions in single crystal⁽⁷³⁾. According to ligand field theory⁽⁷⁸⁾, the absorption intensity of transition metal ions with tetrahedral coordination is much greater than that with octahedral coordination. Accordingly, the appearance of this new absorption band might possibly be due to the tetrahedrally coordinated Cr⁴⁺ ions in transparent glass-ceramics.

Figure 23 shows the emission spectra of glass and glass-ceramics under excitation at 792 nm laser light. The emission at shorter wavelength than 1000 nm due to Cr³⁺ ion was observed in glass, whilst in glass-ceramics both the emission due to Cr³⁺ and the new emission band centered at 1300 nm appear. It is well known that the latter emission band is due to the ³T₂→³A₂ transition of Cr⁴⁺ ions in tetrahedral sites^(71,73,74), and it is confirmed that the Cr⁴⁺ ions exist in this transparent glass-ceramics.

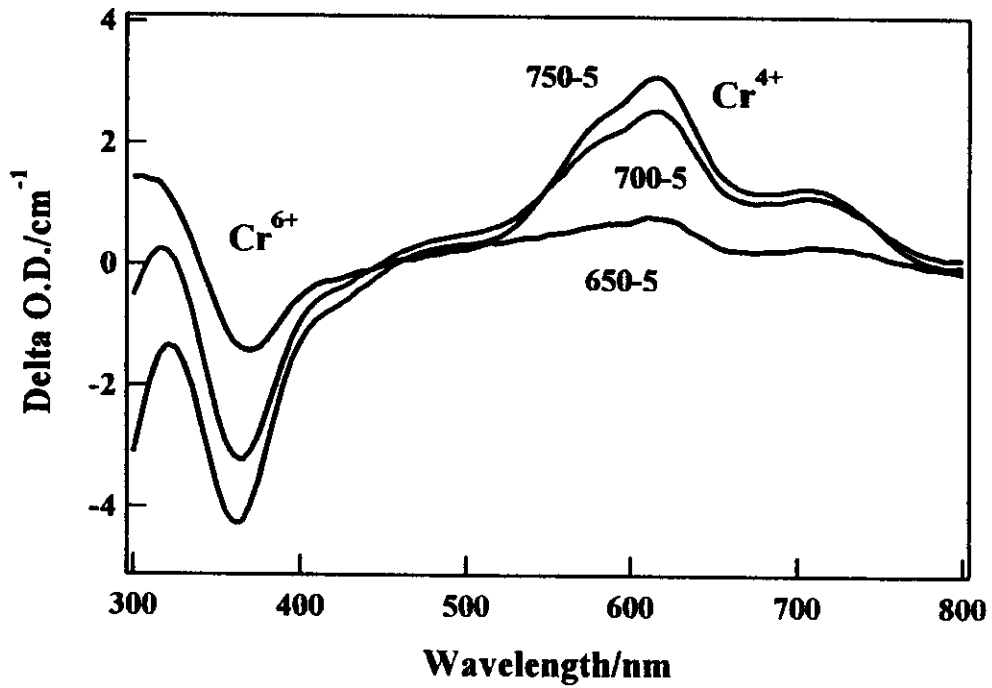
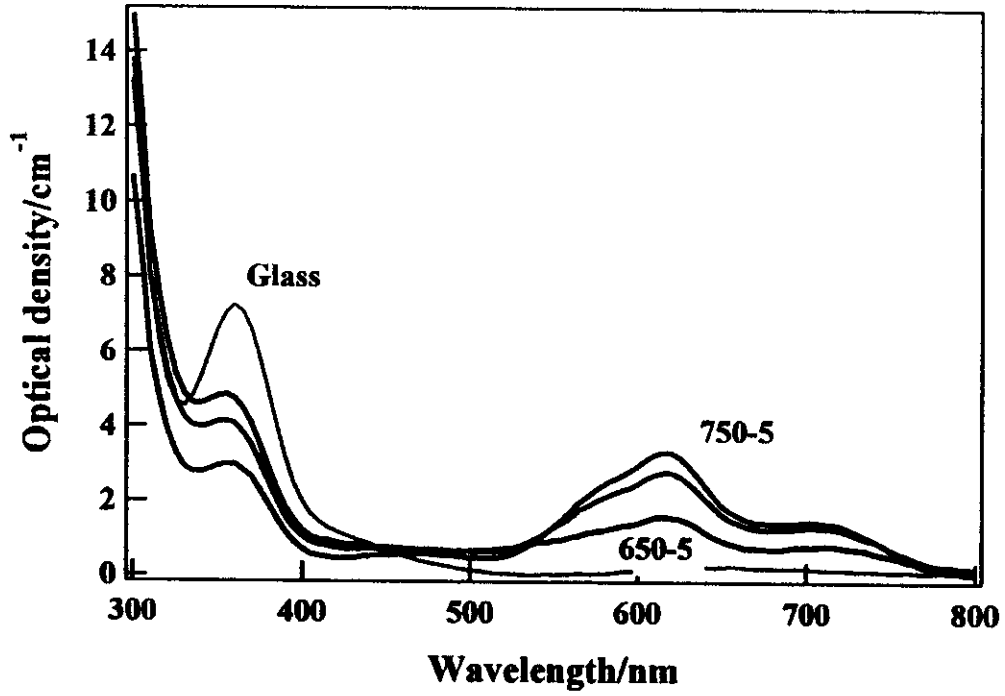


Fig. 21. Absorption and differential spectra of glass and glass-ceramics.

1st heat treatment: 500°C-15h.

$$\Delta[\text{O.D.}(\text{cm}^{-1})] = [\text{O.D.}(\text{cm}^{-1})]_{\text{glass-ceramics}} - [\text{O.D.}(\text{cm}^{-1})]_{\text{glass}}$$

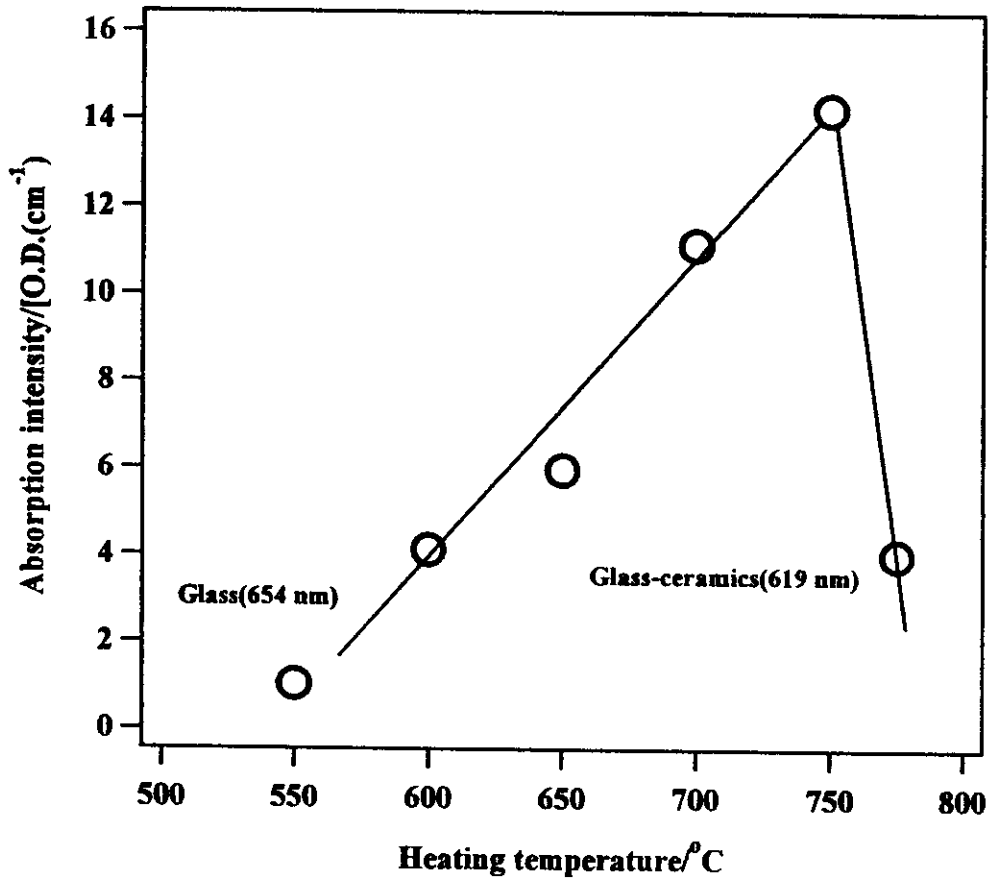


Fig. 22. Relationship between absorption intensity and heating temperature. Heating time: 5 h at various temperature. 1st heat treatment: 500°C-15h. Cr₂O₃=0.4%.

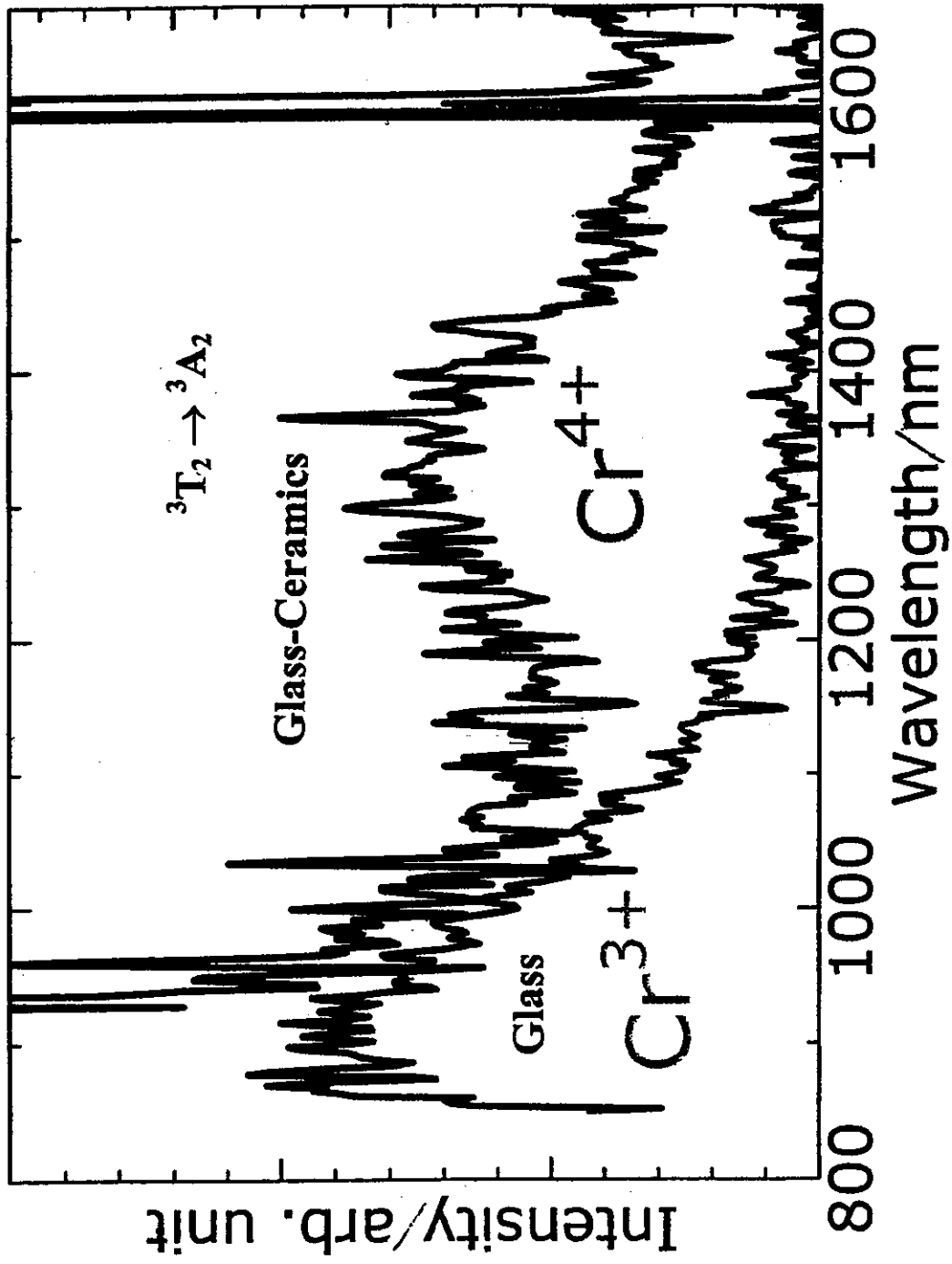


Fig. 23. Emission spectra of glass and glass-ceramics under the excitation at 792 nm laser diode.

It is not clear yet that Cr^{4+} ions can enter into either nano-crystalline $\text{Li}_2\text{O}\cdot 2\text{SiO}_2$ or residual glassy phase. The existence of Cr^{4+} ions in $\text{Li}_2\text{O}\cdot 2\text{SiO}_2$ crystal has never been reported. Then, the authors prepared polycrystalline $\text{Li}_2\text{O}\cdot 2\text{SiO}_2\text{:Cr}$ by sintering method, and the formation of Cr^{4+} ions in this crystal can not be confirmed. Therefore, it is concluded that the Cr^{4+} ions occupy the favorable tetrahedral sites in residual glassy phase. Here, the ligand field strength of tetrahedrally coordinated Cr^{4+} ions was analyzed by multi-peak fitting method with Voigt distribution, and the result is summarized in Table 1. Assuming that the three peaks in visible and NIR region would be ascribed to ${}^3\text{A}_2 \rightarrow {}^3\text{T}_1$ and ${}^3\text{A}_2 \rightarrow {}^3\text{T}_2$ transition, respectively, the ligand field parameters can be estimated to be: $10\text{Dq}=10,610 \text{ cm}^{-1}$, $\text{B}=690 \text{ cm}^{-1}$ and $\text{Dq/B}=1.54$. This Dq/B value is just below the crossing point of ${}^3\text{T}_2$ and ${}^1\text{E}$ levels ($\text{Dq/B}=1.6$). And the Cr^{4+} ions occupy the little stronger sites than those in aluminate glasses reported previously⁽⁷¹⁾, in residual glassy phase.

Table 9. Multi-peak fitting for absorption spectrum of Cr^{4+} ions in transparent glass-ceramics.

Transition	Energy Center (cm^{-1})	Band width (cm^{-1})	Band area (cm^{-1}) ²	Gravity center (cm^{-1})
Cr^{4+} in $\text{Li}_2\text{O-SiO}_2$ system /0.4mass% Cr_2O_3 melted in air, $500^\circ\text{C}-15 \text{ h}$ and $750^\circ\text{C}-5 \text{ h}$.				
${}^3\text{A}_2 \rightarrow {}^3\text{T}_2$	8,658	1,175	4,666	10,610
	10,050	1,120	7,246	(=10Dq)
	11,429	1,082	16,117	
${}^3\text{A}_2 \rightarrow {}^3\text{T}_1$	14,085	810	19,994	16,150
	16,129	958	68,329	
	17,544	952	38,318	

The authors reported previously⁽⁷⁹⁾ that the glass melted under reducing atmosphere, in which only Cr^{3+} ions exist, does not show this phenomena. This result indicates that the Cr^{4+} ions can not be formed by the oxidation of Cr^{3+} ions in analogy with aluminate glasses^(70,71) and hence the Cr^{4+} ions seem to be formed by the reduction of higher valence state of Cr ions. Figure 21 shows that the Cr^{6+} ions decrease with the formation of Cr^{4+} ions. The difference spectrum between glass and glass-ceramics was investigated, and these difference spectra demonstrate the appearance and disappearance of certain Cr ions. The difference spectra may be expressed by: $\Delta[\text{O.D.}(\text{cm}^{-1})] = [\text{O.D.}(\text{cm}^{-1})]_{\text{Glass-ceramics}} - [\text{O.D.}(\text{cm}^{-1})]_{\text{Glass}}$. Figure 21 shows the difference spectra and Figure 24 shows the relationship between the

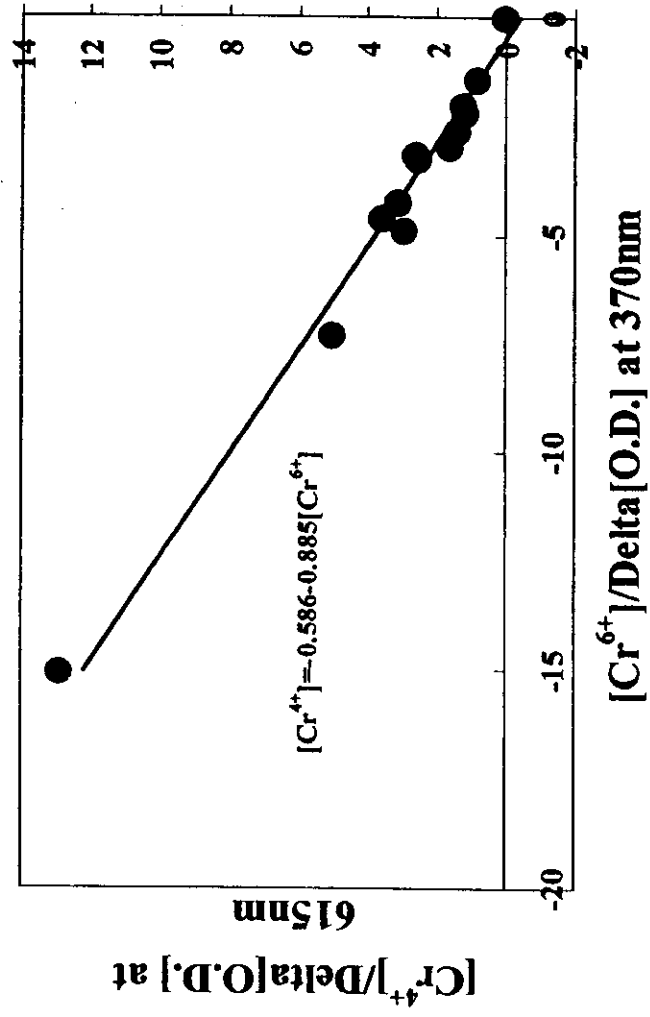
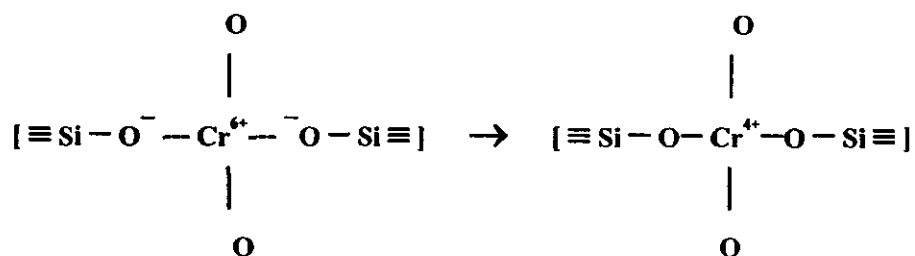


Fig. 24. Relation between decrease in $[\text{Cr}^{6+}]$ and increase in $[\text{Cr}^{4+}]$ in $\text{Li}_2\text{O} \cdot 2\text{SiO}_2$ transparent glass-ceramics.

decrease in Cr^{6+} ions and the increase in Cr^{4+} ions. A good linearity is observed between them and the Cr^{4+} ions increase with decreasing Cr^{6+} ions. This shows the strong correlation between them, consequently, the Cr^{4+} ion is believed to be formed by the reduction of Cr^{6+} ions in the crystallization process. According to Nath and Douglas⁽⁸⁰⁾, $\text{Cr}^{6+}/\sum\text{Cr}$ ratio decreases with decreasing amount of R_2O in $\text{R}_2\text{O-SiO}_2$ glass systems. In the crystallization process, the $\text{Li}_2\text{O}\cdot 2\text{SiO}_2$ crystal precipitates at first, remaining residual high SiO_2 glassy phase. In this situation, the amount of Li_2O decreases



in glassy phase and the Cr^{6+} ions should convert to lower valence state ions, then the redox reaction takes place between Cr^{6+} ions (chromate ions, $[\text{CrO}_4]^{2-}$) and non-bridging oxygen ions, forming Cr^{4+} ions $[\text{CrO}_4]$. $[\text{CrO}_4]$ is equivalent to $[\text{SiO}_4]$ and substitutes $[\text{SiO}_4]$ sites in residual high SiO_2 glassy phase. It is considered that the crystallization is dominant process and acts as important role for the formation of Cr^{4+} ions.

4. Conclusion

The absorption and emission spectra of Cr ions-containing transparent $\text{Li}_2\text{O-SiO}_2$ system glass-ceramics was investigated. The $\text{Li}_2\text{O-SiO}_2$ system transparent glass-ceramics melted in air exhibits significant change in color and absorption spectra by crystallization. It is confirmed that this change is due to the tetrahedrally coordinated Cr^{4+} ions incorporated in residual high- SiO_2 glassy phase. And the emission near infrared region ($\approx 1300\text{nm}$) caused by tetrahedrally coordinated Cr^{4+} ions also was identified. It was found that the Cr^{4+} ions can be formed by the redox reaction between Cr^{6+} ions (chromate ions, $[\text{CrO}_4]^{2-}$) and non-bridging oxygen ions, forming Cr^{4+} ions $[\text{CrO}_4]$, during crystallization. $[\text{CrO}_4]$ is equivalent to $[\text{SiO}_4]$ and substitutes $[\text{SiO}_4]$ sites in residual high SiO_2 glassy phase.

Chapter V

Absorption and emission behavior of rare-earth ions in transparent glass-ceramics

5. 1. Nd³⁺ and Er³⁺ ions in Li₂O·2SiO₂ and AlPO₄ system transparent glass-ceramics

1. Introduction

There has been a growing interest in strong luminescence of rare-earth ions-doped nano-particles because of their practical applications such as high brightness displays. In particular, Bhargaba et al. showed strong orange luminescence from Mn²⁺ ions doped ZnS nano-particles⁽⁸¹⁾. They discussed this enhanced luminescence which occurs through the recombination of photogenerated carriers confined in nano-particles and subsequent energy transfer to rare-earth ions. Nano-particles serve to create a quantum confinement effect of carriers. Since their reports, there are many reports on the optical properties of the active ions doped nano-particles⁽⁸²⁻⁸⁷⁾, and the enhanced fluorescence and the up-conversion were reported⁽⁸⁸⁻⁹⁰⁾.

Here, I demonstrate the preparation of various transparent glass-ceramics doped with Nd³⁺ and Er³⁺ ions by conventional melt quenching method, and also the emission characteristics, especially up-conversion emission, of these ions are discussed.

2. Experiments

2.1. Sample preparation

The compositions of glasses used are shown in Table 10. The sample preparation method was described elsewhere⁽⁹¹⁾. The glasses were melted in 100 ml Pt/Rh10 crucible at 1450^o–2 h (No.1 and 3) and 1550^oC for 2 h (No.2 and 4) in an electric furnace, respectively. Then molten glasses were poured onto iron plate and annealed at 450^oC-30 min for No.1/3 glass and 510^oC–30 min for No.2/4, respectively, and cooled to room temperature in an electric furnace. The glasses were heat treated at 500^oC–15 h for nucleation and subsequently heat treated at 600^oC–10 h for crystallization for No.1/3 glasses and 510^oC–10 h for nucleation and 550^oC–20 h for crystallization for No.2/4 glasses.

2.2. XRD

The crystalline phase, amount of crystal and crystal size were examined by powder X-ray diffraction analysis (XRD, Bruker, AXS Model D5005)⁽⁹¹⁾.

Table 10. Composition of glasses in $\text{Li}_2\text{O}\cdot 2\text{SiO}_2$ and AlPO_4 transparent glass-ceramics (wt %).

No.	SiO_2	Al_2O_3	B_2O_3	P_2O_5	Na_2O	Li_2O	Nd_2O_3^*	Er_2O_3^*
1	80	4	-	3	-	13	1.0	
2	28.07	23.82	4.07	33.17	10.86	-	2.0	
3	80	4	-	3	-	13	—	1.0
4	28.07	23.82	4.07	33.17	10.86	-	—	2.0

*: excess wt %.

2.3. Absorption and emission spectra

The glass samples were optically polished into about 2 mm in thickness. The absorption spectra were measured using Varian Cary 5E spectrometer in the range of 300–1500 nm. The emission spectra were measured at room temperature with Perkin-Elmer LS50B Luminescence spectrometer in the range of 300–900 nm.

3. Results and discussion

Glass-ceramics appeared to be transparent. The main crystal was $\text{Li}_2\text{O}\cdot 2\text{SiO}_2$ with small amount of $\text{Li}_2\text{O}\cdot \text{SiO}_2$ and α -quartz, and the amount and size of $\text{Li}_2\text{O}\cdot 2\text{SiO}_2$ crystal were 70% and 30 nm, respectively (No. 1/3 glass-ceramics). Similarly, AlPO_4 crystal (tridymite type), 50% and 30 nm, respectively (No. 2/4 glass-ceramics).

Figure 25 and 26 show the absorption spectra of glass and glass-ceramics of Nd^{3+} and Er^{3+} doped transparent glass-ceramics. The intensity and positions of absorption bands do not change with composition and by crystallization. This is the characteristics optical properties of rare earth ions because the 4f electrons are shielded by outer 5s or 5p electrons. The absorption in UV region increases with the progress of crystallization due to scattering.

Three strong absorption peaks appeared at around 590, 740 and 800 nm, which are assigned to ${}^4\text{F}_{3/2} \rightarrow {}^4\text{G}_{5/2}$, ${}^4\text{F}_{3/2} \rightarrow {}^4\text{F}_{7/2}$ and ${}^4\text{F}_{3/2} \rightarrow {}^4\text{F}_{5/2}$ for Nd^{3+} ion⁽⁸⁹⁾. And also three strong absorption peaks appeared at around 370, 520 and 640 nm, which are assigned to ${}^4\text{I}_{15/2} \rightarrow {}^4\text{G}_{11/2}$, ${}^4\text{I}_{15/2} \rightarrow {}^2\text{H}_{11/2}$ and ${}^4\text{I}_{15/2} \rightarrow {}^4\text{F}_{9/2}$ for Er^{3+} ion⁽⁹²⁾.

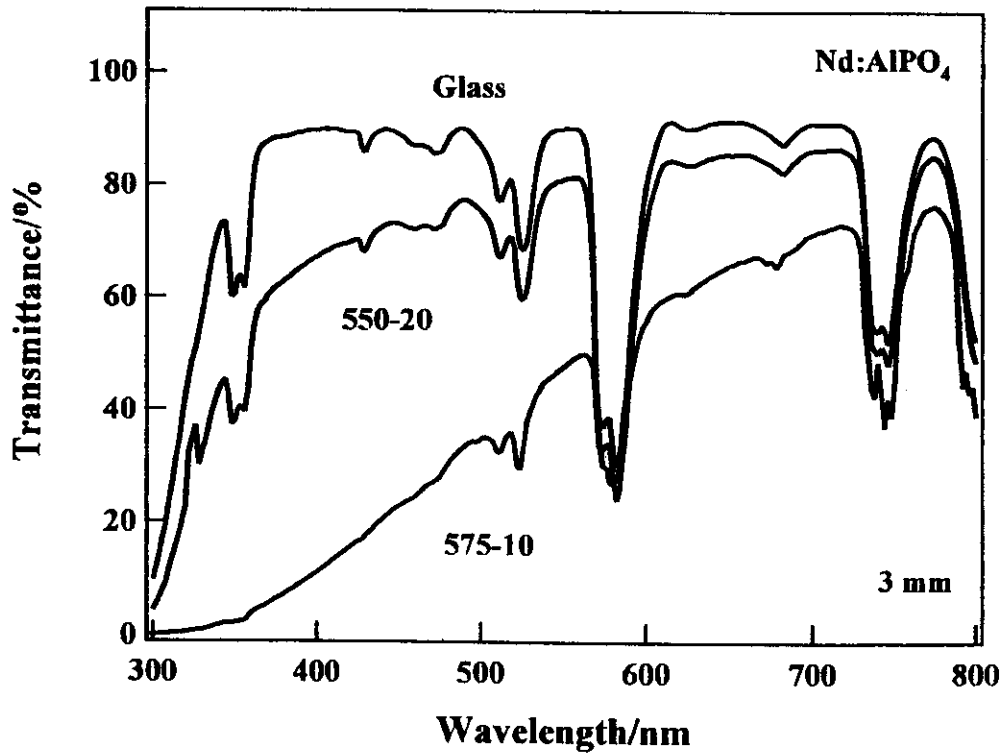
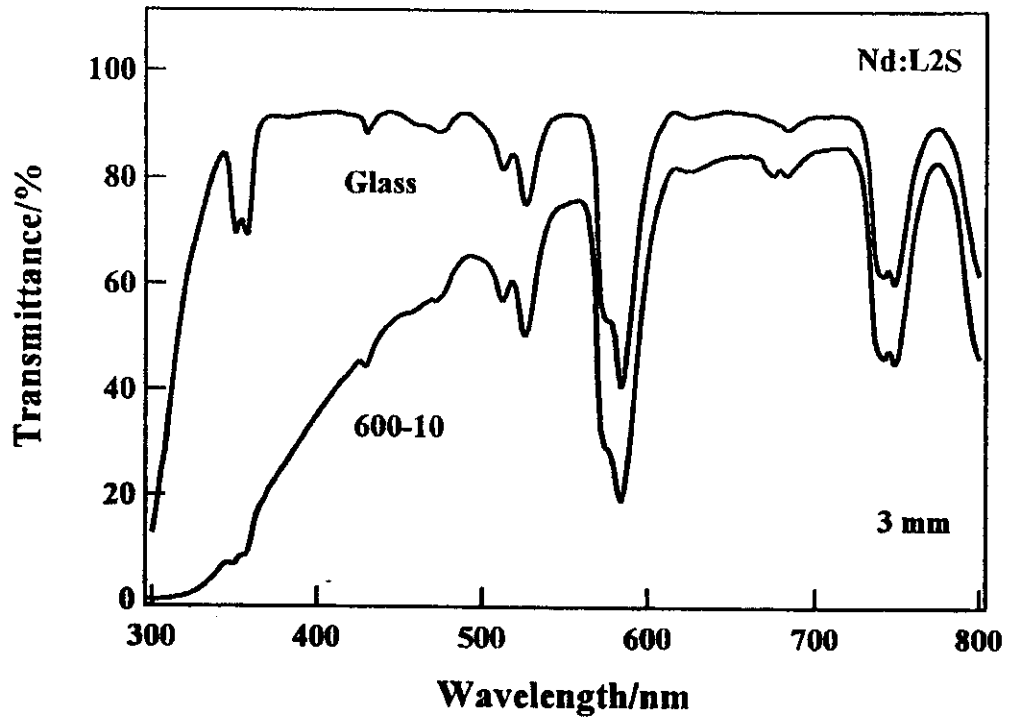


Fig. 25. Transmission spectra of Nd³⁺ doped Li₂O·2SiO₂[L·2S] and AlPO₄ glass-ceramics.

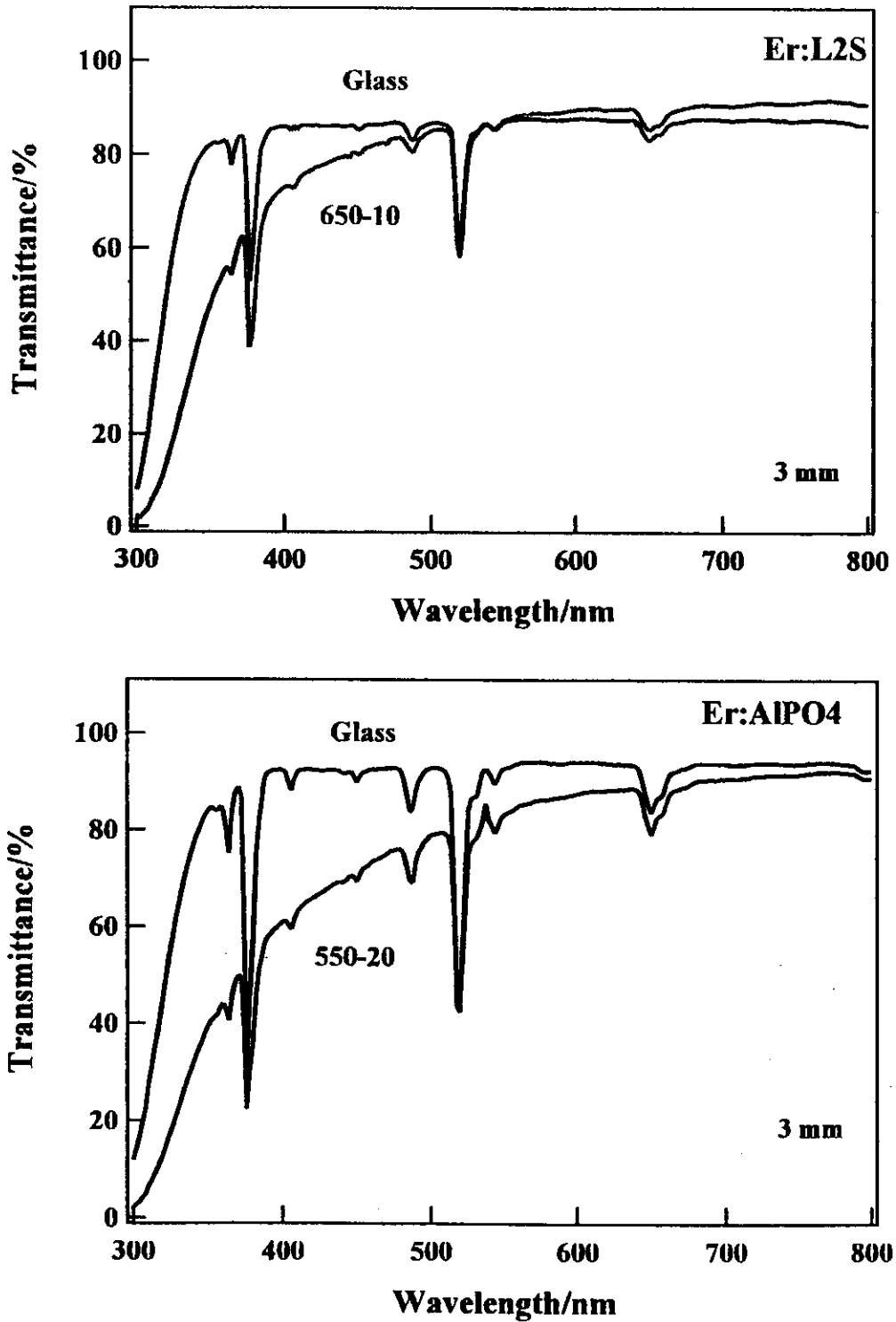


Fig. 26. Transmission spectra of Er³⁺ doped Li₂O·2SiO₂[L·2S] and AlPO₄ glass-ceramics.

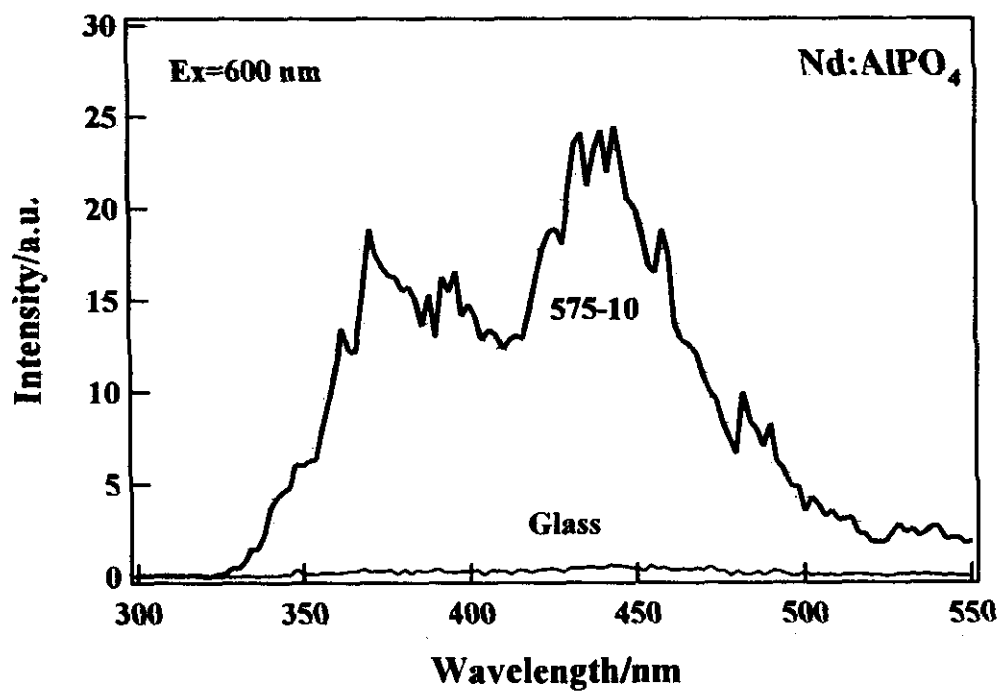
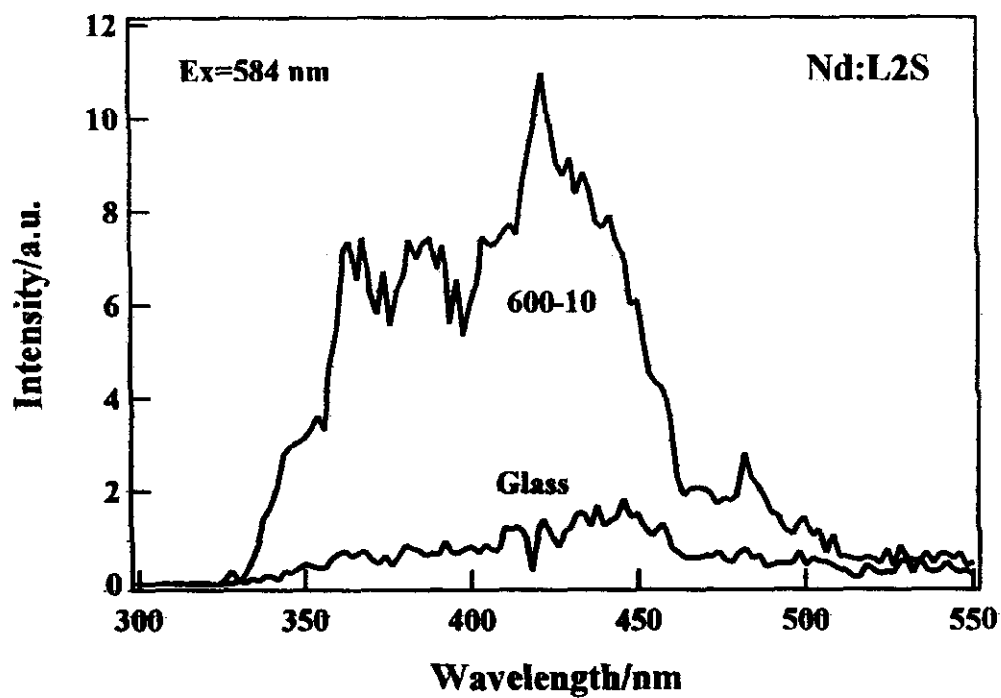


Fig. 27. Up-conversion spectra of Nd³⁺ doped Li₂O·2SiO₂[L·2S] and AlPO₄ glass-ceramics.

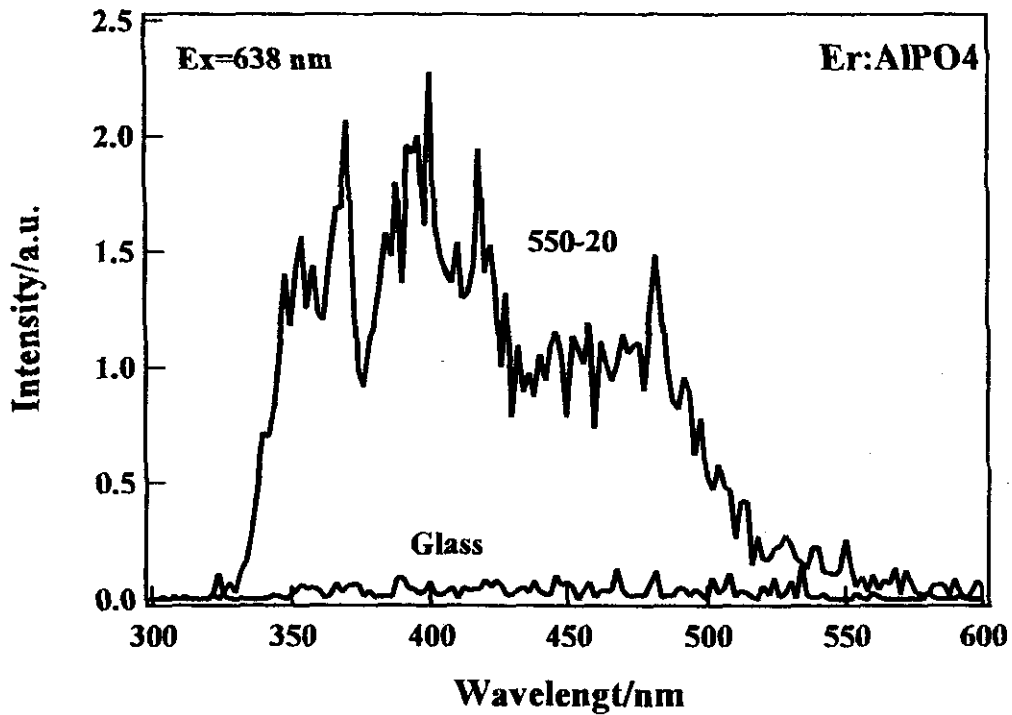
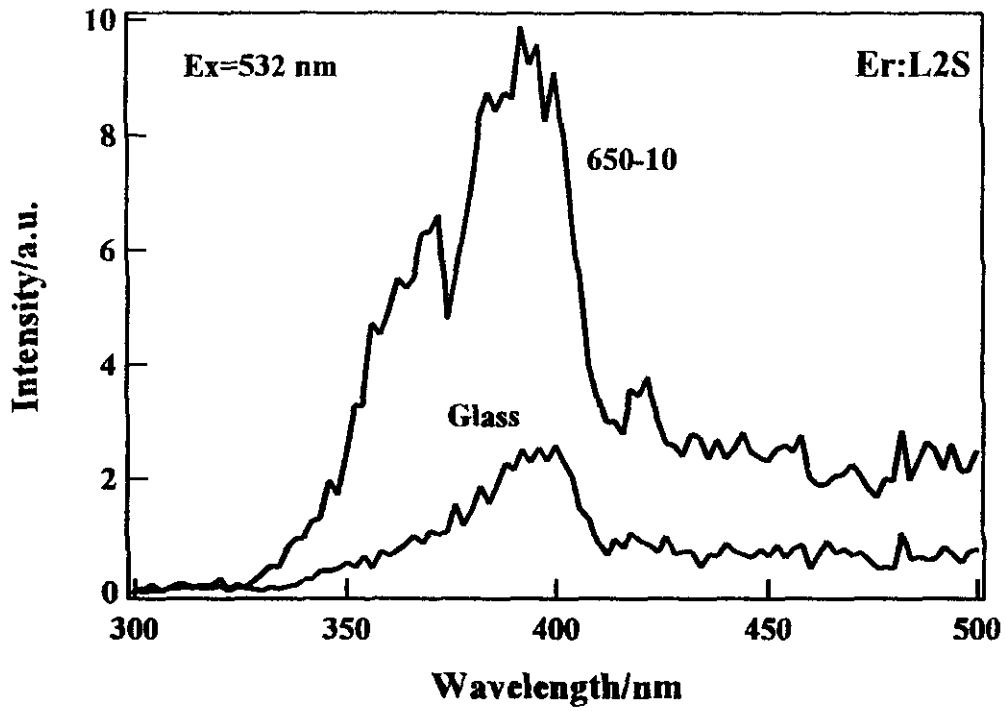


Fig. 28. Up-conversion spectra of Er^{3+} doped $\text{Li}_2\text{O}\cdot 2\text{SiO}_2$ [L·2S] and AlPO_4 glass-ceramics.

Figure 27 and 28 show the emission spectra of Nd^{3+} and Er^{3+} doped transparent glass-ceramics. In this case, the emission was observed by the excitation of longer wavelength of light. This is called "Up-converted emission, up-conversion". The emission bands at around 370 and 440 nm were observed for both Nd^{3+} doped $\text{Li}_2\text{O}\cdot 2\text{SiO}_2$ and AlPO_4 transparent glass-ceramics. These emission bands can be assigned to ${}^4\text{D}_{3/2} \rightarrow {}^4\text{I}_{11/2}$ (${}^2\text{P}_{3/2} \rightarrow {}^4\text{I}_{9/2}$) and ${}^4\text{D}_{3/2} \rightarrow {}^4\text{I}_{15/2}$ (${}^2\text{P}_{3/2} \rightarrow {}^4\text{I}_{13/2}$)⁽⁸⁹⁾. The emission intensity is 10~20 times greater than that of glass.

In Er^{3+} doped transparent glass-ceramics, the emission bands appeared at around 360 and 400 nm. The latter emission band can be assigned to ${}^2\text{P}_{3/2} \rightarrow {}^4\text{I}_{13/2}$ ⁽⁹²⁾. The emission intensity does not increase so much by crystallization unlike Nd^{3+} doped glass-ceramics.

4. Conclusion

The absorption and the emission characteristics, especially up-conversion emission, of Nd^{3+} and Er^{3+} ions doped $\text{Li}_2\text{O}\cdot 2\text{SiO}_2$ and AlPO_4 transparent glass-ceramics, were investigated.

The position and intensity of absorption spectra of Nd^{3+} and Er^{3+} ions does not change before and after crystallization. The up-conversion emission was observed for both the Nd^{3+} and the Er^{3+} ions doped transparent glass-ceramics. Their intensity is much higher than those of glass.

5. 2. Pr³⁺ in Li₂O·2SiO₂ transparent glass-ceramics

1. Introduction

There has been a growing interest in strong luminescence of rare-earth ions-doped nano-particles because of their practical applications such as high brightness displays. In particular, Bhargaba et al. showed strong orange luminescence from Mn²⁺ ions doped ZnS nano-particles⁽⁸¹⁾. They discussed this enhanced luminescence which occurs through the recombination of photogenerated carriers confined in nano-particles and subsequent energy transfer to rare-earth ions. Nano-particles serve to create a quantum confinement effect of carriers. Since their reports, there are many reports on the optical properties of the active ions doped nano-particles⁽⁸²⁻⁸⁷⁾, and the enhanced fluorescence and the up-conversion were reported⁽⁸⁸⁻⁹⁰⁾.

Here, I demonstrate the preparation of various transparent glass-ceramics doped with Pr³⁺ ion by conventional melt quenching method, and also the emission characteristics, especially up-conversion emission, are discussed.

2. Experiments

2.1. Sample preparation

The composition of glass was 80SiO₂·4Al₂O₃·13Li₂O·3P₂O₅·1.4Pr₂O₃ (wt %). The sample preparation method was described elsewhere⁽⁹¹⁾. The glass was melted in 100 ml Pt/Rh10 crucible at 1450°C for 2 h 2 times to improve homogeneity.

The glass was heat treated at 500°C—15 h for nucleation and subsequently heat treated at higher temperature for crystallization.

2.2. XRD

The crystalline phase, amount of crystal and crystal size were examined by powder X-ray diffraction analysis(XRD, Bruker, AXS Model D5005)⁽⁹¹⁾.

2.3. Absorption and emission spectra

The glass samples were optically polished into about 2 mm in thickness. The absorption spectra were measured using Varian Cary 5E spectrometer in the range of 300—1500 nm. The

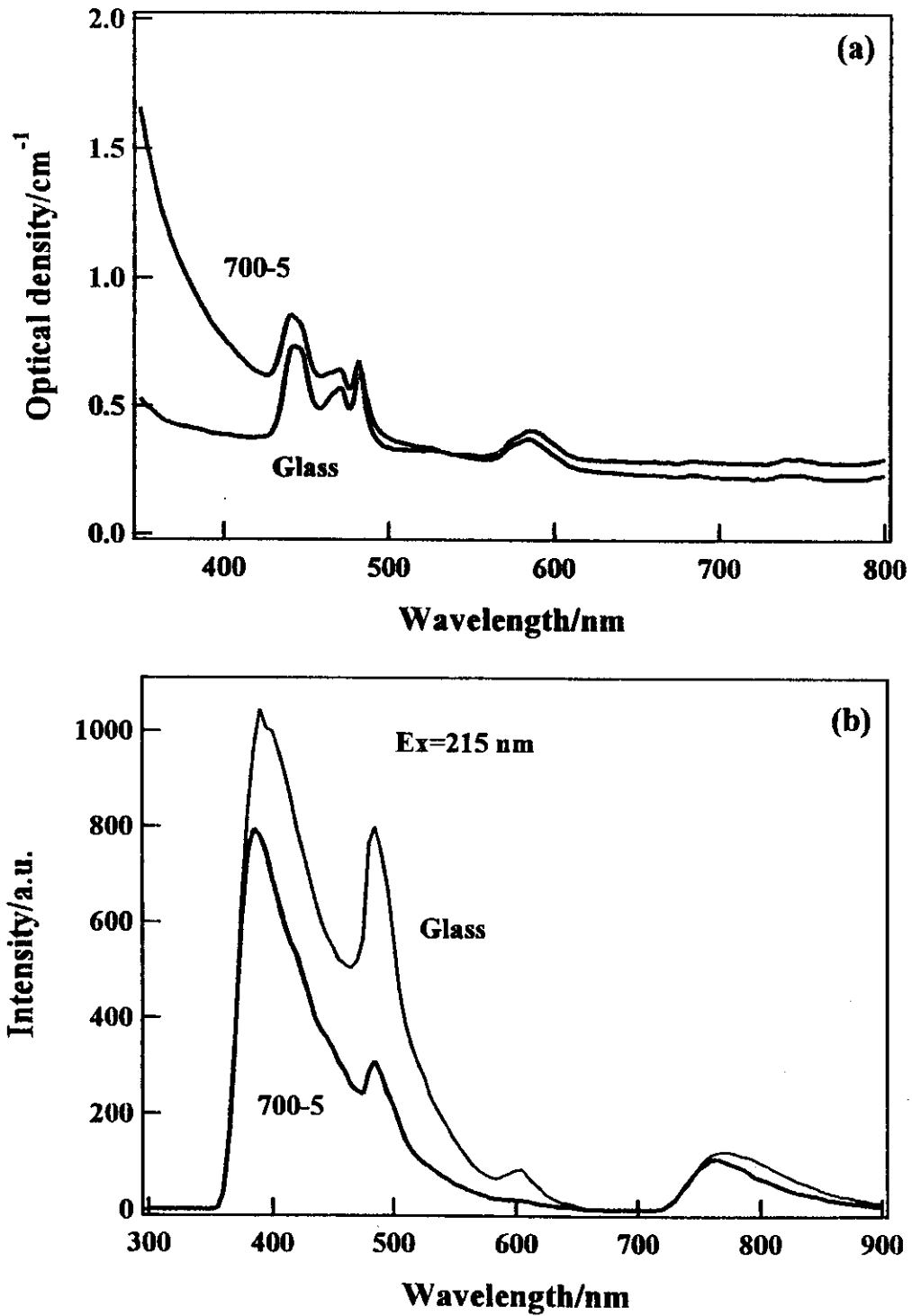
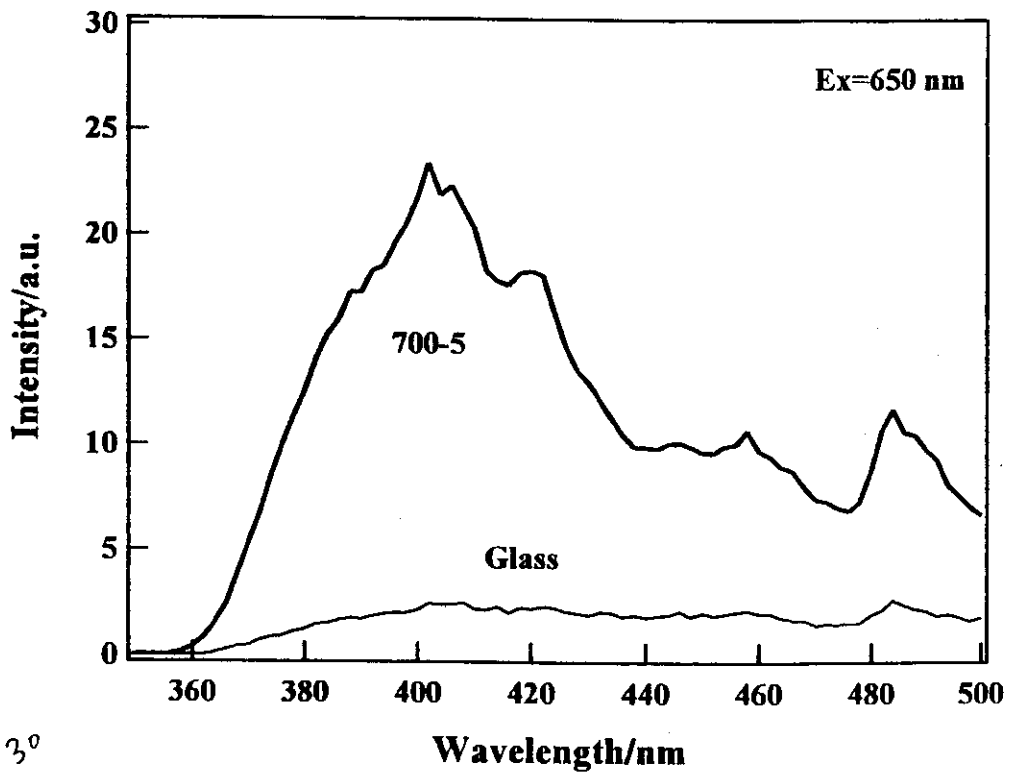
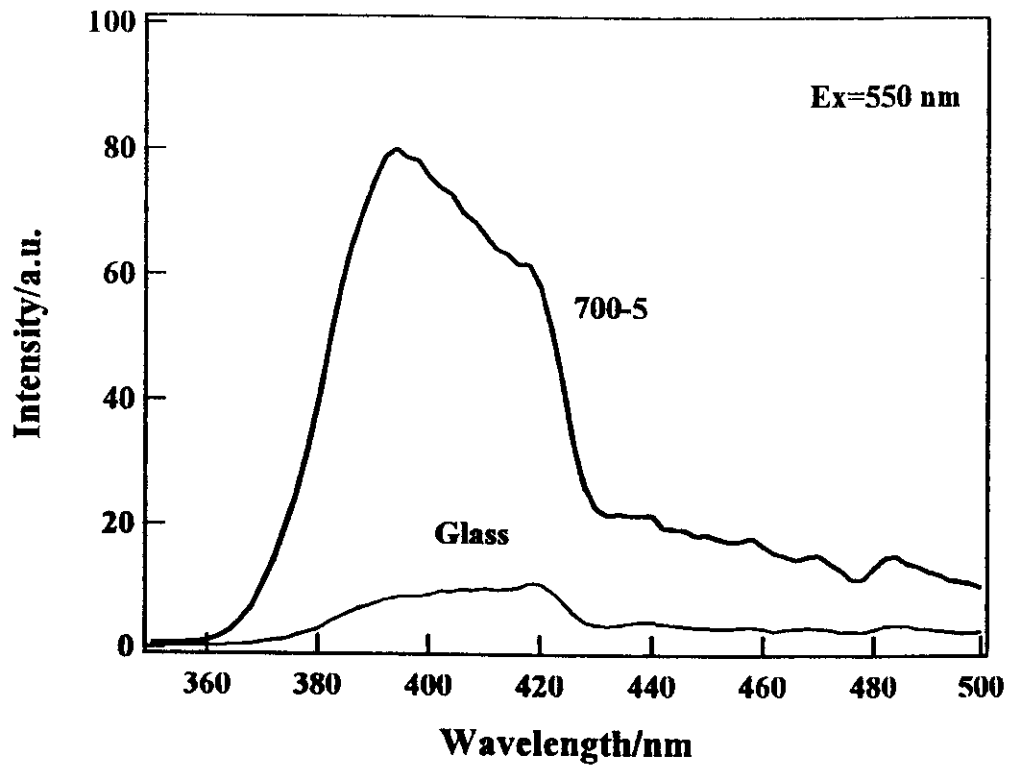


Fig. 29. Absorption and emission spectra of Pr³⁺ doped glass and glass-ceramics.

(a). Absorption spectra

(b). Emission spectra under the excitation at 215 nm.



3°

Fig. 30. Emission spectra of Pr³⁺ doped glass and glass-ceramics at room temperature.

emission spectra were measured at room temperature with Perkin-Elmer LS50B Luminescence spectrometer in the range of 300-900 nm.

3. Results and discussion

Glass-ceramics appeared to be transparent. The main crystal was $\text{Li}_2\text{O}\cdot 2\text{SiO}_2$ with small amount of $\text{Li}_2\text{O}\cdot \text{SiO}_2$ and α -quartz, and the amount and size of $\text{Li}_2\text{O}\cdot 2\text{SiO}_2$ crystal were 70% and 30 nm, respectively.

Fig. 29(a) shows the absorption spectra of Pr^{3+} doped glass and glass-ceramics. The relatively strong four absorption bands are observed, they are assigned to $^3\text{H}_4 \rightarrow ^3\text{P}_2$ (440 nm), $^3\text{H}_4 \rightarrow ^3\text{P}_1$ (470 nm), $^3\text{H}_4 \rightarrow ^3\text{P}_0$ (490 nm) and $^3\text{H}_4 \rightarrow ^1\text{D}_2$ (590 nm), respectively. The peak position and intensity does not change before and after crystallization⁽⁹³⁾. The absorption intensity in near UV region increases by the scattering.

Fig. 29(b) shows the emission spectra of Pr^{3+} doped glass and glass-ceramics under the excitation of 215 nm light. The four emission bands are observed, and they can be assigned to $^1\text{S}_0 \rightarrow ^1\text{I}_6$ (400 nm), $^3\text{P}_0 \rightarrow ^3\text{H}_4$ (490 nm), $^3\text{P}_0 \rightarrow ^3\text{H}_6$ (600 nm) and $^3\text{P}_0 \rightarrow ^3\text{F}_4$ (770 nm), respectively. The emission intensity of Pr^{3+} in glass is higher than that in glass-ceramics. Fig. 30. shows the up-conversion emission spectra of Pr^{3+} doped glass and glass-ceramics under the excitation of 550 and 650 nm light. Two strong emission peaks are observed, and they can be assigned to $^1\text{S}_0 \rightarrow ^1\text{I}_6$ (400 nm) and $^3\text{P}_0 \rightarrow ^3\text{H}_4$ (480 nm)⁽⁹⁴⁾. It is interesting to note that the emission intensity of Pr^{3+} ion in glass-ceramics is much higher than that in glass unlike under the excitation of shorter wavelength of light. This indicates that Pr^{3+} ion might enter into L·2S nano-particles.

4. Conclusion

The absorption and the emission characteristics, especially up-conversion emission, of Pr^{3+} ion doped $\text{Li}_2\text{O}\cdot 2\text{SiO}_2$ transparent glass-ceramics, were investigated.

The position and intensity of absorption spectra of Pr^{3+} ion does not change before and after crystallization. The up-conversion emission was observed for both the Pr^{3+} ion doped transparent glass-ceramics. It is interesting to note that the emission intensity of Pr^{3+} ion in glass-ceramics is much higher than that in glass unlike under the excitation of shorter wavelength of light. This indicates that Pr^{3+} ion might enter into L·2S nano-particles.

Chapter VI

Summary

The preparation of new type transparent glass-ceramics was investigated, and the absorption and emission characteristics of active ions such as transition metal ions and rare earth ions in transparent glass-ceramics were also investigated.

The new type transparent glass-ceramics based on $\text{Li}_2\text{O}\cdot 2\text{SiO}_2$, $\text{Li}_2\text{O}\cdot \text{SiO}_2$, BPO_4 and AlPO_4 crystals can be prepared using corresponding base glass composition. The size and amount of these crystals are 20-40 nm and 30-70 %, respectively. Highly transparent glass-ceramics also were obtained by controlling heat treatment for nucleation and crystallization, and their transparency is comparable with that of glass.

However, the mechanical strength of very fine grained transparent glass-ceramics is not so different from that of conventional glass, usually 50-100 MPa. Higher mechanical strength of transparent glass-ceramics is required for certain application area. Although ion exchange method is a favorable method to increase the mechanical strength keeping surface flatness of transparent glass-ceramics, it is found that this method can not be applied for Li_2O -containing glass and glass-ceramics.

The absorption and emission characteristics of Cr ion in various transparent glass-ceramics were investigated. The Cr^{3+} ion in spinel glass-ceramics occupies strong octahedral site and appears to be pink color, and emits strong sharp red light(R-line). On the contrary, in AlPO_4 glass-ceramics, Cr^{3+} ion is in intermediate ligand field strength, and hence color does not change and an usual emission is observed in NIR region. It should be noted that Cr ion in $\text{Li}_2\text{O}\cdot \text{SiO}_2$ and $\text{Li}_2\text{O}\cdot 2\text{SiO}_2$ crystals based transparent glass-ceramics exhibits anomalous behavior. It is found that Cr^{3+} ion occupies tetrahedral site in $\text{Li}_2\text{O}\cdot \text{SiO}_2$ crystal, the color changes from green of glass to pink. The emission near NIR is observed under the excitation of around 500 nm light. In $\text{Li}_2\text{O}\cdot 2\text{SiO}_2$ transparent glass-ceramics, the existence of Cr^{4+} ion is confirmed. The Cr^{4+} ion was formed by the reduction of Cr^{6+} during crystallization of $\text{Li}_2\text{O}\cdot 2\text{SiO}_2$ crystal, and it occupies tetrahedral site in residual high SiO_2 glassy phase. The characteristic emission around NIR region(1000-1500 nm) was observed under the excitation of 792 nm laser diode.

The absorption and emission characteristics rare earth ions such as Nd^{3+} , Er^{3+} , Pr^{3+} in transparent glass-ceramics were investigated. The absorption intensity and position of these ions in glass-ceramics do not change unlike transition metal ions. The up-conversion emission was observed for these ions in glass-ceramics.

Thus the absorption and emission characteristics of actives ions in transparent glass-ceramics are quite interesting. The more detailed research on this behavior could be required and continued along with

the finding of new type transparent glass-ceramics.

References

1. G. H. Beall et al., US Patent 4 239 519(1980).
2. G.H. Beall and L. R. Pinckney, *J. Am. Ceram. Soc.*, Vol.82, pp.5-18(1999).
3. L. J. Andrews et al., DE-AC02-78ER-04996 Final Report, Dep. Energy, Washington D.C.(1982).
4. G. H. Beall et al., US Patent 4 396 720(1983).
5. K.E. Downey et al., *Proc. CLEO 2001, CtuP1*, Vol.1, Chiba, Japan(2001)211-12.
6. L. Lavin et al., *Opt. Mater.* 25(2004)201-08.
7. M. Mortier and F. Auzul, *J. Non-Cryst. Solids*, 256&257(1999)361-65.
8. S. Morimoto and W. Emem, *J. Ceram. Soc. Japan*, 112(2004)486-90.
9. H. Zheng et al., *J. Luminescence*, 108(2004)395-399.
10. G. H. Beall and D.A. Duke, *J. Mater. Sci.*, 4(1969)340-52.
11. T. Kokubo and M. Tashiro, *J. Non-Cryst. Solids*, 13(1974)328.
12. K. Shioya et al., *J. Non-Cryst. Solids*, 189(1995)16-24.
13. P.A. Tick, N.F. Borrelli and I. M. Reaney, *Opt. Mater.*, 15(2001)81-91.
14. J.M. Jewel, E.J. Friebe and I.D. Aggarwal., *J. Non-Cryst. Solids*, 188(1995)285-88.
15. T. Aboud and L. Stoch, *J. Non-Cryst. Solids*, 219(1997)149-54.
16. S. Morimoto, *J. Ceram. Soc. Japan*, 98(1990)1029-33.
17. S. Morimoto, *Proc. Smart-Mat, '04*, 3-1-5, Chiang Mai, Thailand(2004).
18. E. Philippot, A. Goiffon and A. Ibanez, *J. Crystal Growth*, 160(1996)268-78.
19. K.C. Mishra et al., *J. Luminescence*, 72-74(1997)144-45.
20. S. Morimoto and W. Emem, *J. Ceram. Soc. Japan*, 111(2004)259-62.
21. Ch. Striebel, K. Hoffmann and F. Marlow, *Microporous Mater.*, 9(1997)43-50.
22. A.A. Griffith, *Phil. Trans. Roy. Soc.*, 221A (1920) 163-198.
23. M. Tashiro and S. Sakka, *J. Ceram. Soc. Japan*, 68 (1960) 158-163.[in Japanese].
24. Y. Utsumi, *J. Ceram. Soc. Japan*, 79 (1971) 30-39.[in Japanese].
25. F.J.P. Clarke, *Acta. Met.*, 12 (1964) 139-144.
26. R.W. Davidge and G. Tappin, *J. Mater. Sci.*, 3 (1968) 297-297.
27. E. Orowan, *Repts. Progr. Phys.*, 12 (1949) 185-189.
28. I. Nitta, "X-ray Crystallography, Vol. I", Maruzen, Tokyo (1975) 489-495. [in Japanese].
29. S.M. Ohlberg and D.W. Stricjler, *J. Am. Ceram. Soc.*, 45 (1962) 170-171.
30. D.P.H. Hasselman and R.M. Fulrath, *J. Am. Ceram. Soc.*, 49 (1966) 68-72.
31. S. Morimoto, *J. Ceram. Soc. Japan*, 112(2004)486-90.
32. X. Wu, H. Yuan, W.M. Yen and B.G. Aitken, *J. Luminescence*, 66&67(1996)285-89.
33. K.E. Downey et al., *Proc. Cleo 2001, CuP1*, Vol.1, PP.211-12, Chiba, Japan(2001).

34. J.M. Jewell, E.J. Friebe and I.D. Aggarwal, *J. Non-Cryst.Solids*, 188(1995)285-88.
35. McMillan, P.W., "Glass-Ceramics", Academic Press, London(1979).
36. Morimoto, S., *J. Luminescence*, submitted.
37. S. Morimoto and W. Emem, *J. Ceram. Soc. Japan*, 112(2004)259-62.
38. S.S. Kistler, *J. Amer. Ceram. Soc.*, 45(1962)59-64.
39. G.H. Beall, B.R. Karstetter and H.L. Rittler, *J. Amer. Ceram. Soc.*, 45(1967)181-86.
40. M.B. Volf, "Mathematical Approach to Glass", Elsevier, Amsterdam(1988).
41. G.H. Beall, *J. Non-Cryst. Solids*, 73(1985)413-19.
42. T. Bates, "Ligand field theory and absorption spectra of transition metal ions in glass", in "Modern Aspects of Vitreous State, Vol.2", Ed. Mackenzie, J. D., Butterworth, London(1962)pp.195-254.
43. F. Rossi, G. Pucker, M. Montagna, M. Ferrari and A. Boukenter, *Opt. Mater.*, 3(2000) 373-379.
44. Kaminskii, A. A., "Crystalline Lasers", CRC Press, Boca Laton(1996).
45. T. Bates, "Modern Aspects of Vitreous State, Vol.2", Ed. J. D. Mackenzie, Butterworth, London(1962)195-254.
46. G.H. Sigel Jr., "Treatise of Materials Science and Technology, Vol.12", Eds. M. Tomozawa and R.H. Doremus, Academic Press, New York(1977)5-89.
47. F. Durville et al., *Phys. Chem. Glasses*, 25(1984)126-133.
48. P. Reisfeld, A. Kisilev, A. Buch and M. Ish-Shalom, *J. Non-Cryst. Solids*, 91(1987)333-350.
49. C. Mai, C. Esnouf, R. Xu and J. Zarzycki, *J. Non-Cryst. Solids*, 121(1990)282-287.
50. T. Ishihara et al., *J. Soc. Mat. Sci. Japan*, 42(1993)484-489.
51. H. Nomura et al., *J. Ceram. Soc. Japan*, Supplement 112-1, PacRim5 Special Issue, 112(2005)s1206-1209.
52. S. Morimoto, *J. Ceram. Soc. Japan*, 112(2004)130-132.
53. S. Morimoto, *J. Ceram. Soc. Japan*, 112(2004)486-490.
54. J.S. Stroud, *J. Amer. Ceram. Soc.*, 54(1971)401.
55. S.M. Ohlberg and D.W. Strickler, *J. Amer. Ceram. Soc.*, 45(1962)170-171.
56. I. Nitta, "X-ray Crystallography, Vol. 1", Maruzen, Tokyo(1975)pp.489-495. [in Japanes].
57. V. Tassev, M. Gospodinov and M. Veleva, *Opt. Materials*, 13(1999)249-253.
58. L. Jastrabik et al., *J. Luminescence*, 102-103(2003)657-662.
59. H. Nomura et. al., *J. Ceram. Soc. Japan*, Supplemen 112-1, PacRim5 Special Issue, 112(2004)s1206-1209.
60. S. Morimoto, Submitted to *J. Luminescence*(2005).
61. S. Morimoto and W. Emem, *J. Ceram. Soc. Japan*, 112(2004)259-262.
62. I. Nikolov, et al., *Opt. Materials*, 25(2004)53-58.

63. T. Bates, "Modern Aspects of Vitreous State, Vo. 2", Ed. By J.D. Mackenzie, Butterworth, London(1962)pp. 195-254.
64. S. Morimoto, Unpublished result.
65. T. Bates, "Ligand field theory and absorption spectra of transition-metal ions in glasses", in "Modern Aspects of Vitreous State-Vol.2", Ed. J.D. Mackenzie, Butterworth, London,(1962)pp.195-254.
66. G.H. Sigel Jr., "Optical absorption of Glasses", in "Treatise on Materials Science and Technology-Vol.12", Eds. Tomozawa, M and Doremus, R. H., Academic Press, New York(1977)pp.5-89.
67. H. Rawson, "Properties and Application of Glass", Elsevier, Amsterdam(1980)pp.193-235.
68. P. Nath and R.W. Douglas, Phys. Chem. Glasses, 6(1965)197-202.
69. A. Paul, J. Non-Cryst. Solids, 15(1974)517-25.
70. S.P. Lunkin, D.G. Gamilov and D.M. Yundin, Opt. Spektrosk(USSR), 25(1969)583.
71. X. Wu, U. Hommerrich, W.M. Yen, B.G. Aitken and M. Newhouse, Chem. Phys. Lett., 233 (1995)28-32.
72. T. Murata, M. Torisaka, H. Takebe and K. Morinaga, J. Non-Cryst. Solids, 220(1997)139-46.
73. X. Feng and S. Tanabe, Opt. Mater. 20(2002)63-72.
74. A. Belletti, R. Borromei and L. Oleari, Inorg. Chim. Act., 235(1995)349-355.
75. S. Kuck, K. Petermann, U. Pohlmann, and Huber, G., J. Luminescence, 68(1996)1-14.
76. S. Kuck and S. Hartung, Chem. Phys., 240(1999)387-401.
77. G.H. Beall, J. Non-Cryst. Solids, 73(1985)413-19.
77. K.E. Downey et al., Proc. CLEO 2001, CtuP1, Vol. 1, Chiba, Japan(2001)pp.211-212.
78. S. Morimoto, J. Ceram. Soc. Japan., 112(2004)130-32.
79. Figgis, B. N., "Introduction to Ligand Field Theory", Interscience Publishers, New York(1966).
80. S. Morimoto, J. Ceram. Soc. Japan., 112(2004)486-90.
81. P. Nath and R.W. Douglas, Phys. Chem. Glasses, 6(1965)197-202.
82. P.J. Deren, M. Malinowski and W. Streck, J. Luminescence, 68(1996)91-103.
83. R.N. Bhargava, J. Luminescence, 70(1996)85-94.
84. A.A. Boll and A. Meijerink, J. Luminescence, 87-89(2000)315-318.
85. R.Y. Wang, J. Luminescence, 106(2004)211-217.
86. M. Nogami, T. Enomoto and T. Hayakawa, J. Luminescence, 97(2002)147-152.
87. M. Mortier and F. Auzel, J. Non-Cryst. Solids, 256&257(1999)361-365.
88. W. Glass, J. Toulouse and P.A. Tick, J. Non-Cryst. Solids, 222(1997)258-265.
89. M.J. Dejneka, J. Non-Cryst. Solids, 239(1998)149-155.
90. H.X. Zhang et al., Opt. Materials, 15(2000)47-50.
91. S.Morimoto and W.Emem, J. Ceram. Soc. Japan, 112(2004)259-262.
92. X. Zhang et al., Opt. Materials, 20(2002)21-25.

93. R. Balda et al., *J. Luminescence*, 97(2002)190-197.

94. H. Zheng et al., *J. Luminescence*, 108(2004)395-399.

Appendix A

Determination of percent crystallinity by XRD

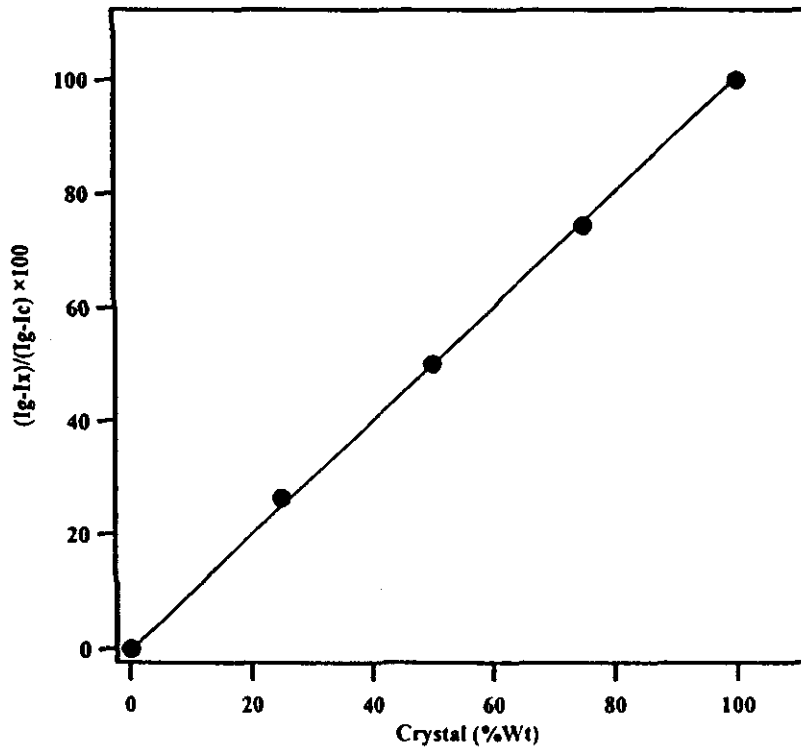
Determination of percent crystallinity by XRD

Percent crystallinity is using Ohlberg and Strickler's method ⁽⁵⁵⁾.

$$\text{Percent crystallinity} = 100x (I_g - I_x)/(I_g - I_c)$$

Where I_g is the background intensity of glass, I_x that of the specimen and I_c that of the crystal at $2\theta = 23^\circ$. The calibration curve is obtained using mixtures of α -Quartz and parent glass at various ratios. Results are shown below. The good linearity is obtained.

Mixture		I_g	I_c	I_x	$(I_g - I_x)/(I_g - I_c) \times 100$
Glass	α -Quartz				
100	0	66.7	3.5	66.7	0
75	25	66.7	3.5	19.6	74.53
50	50	66.7	3.5	35	50.16
25	75	66.7	3.5	50	26.42
0	100	66.7	3.5	3.5	100



Appendix B

Publication

Optical Absorption of Cr-Containing Li₂O-SiO₂ System Transparent Glass-Ceramics

Shigeki MORIMOTO

クローム含有透明結晶化ガラスの光吸収

森本繁樹

School of Ceramic Engineering, Institute of Engineering, Suranaree University of Technology,
111 University Avenue, Muang District, Nakhon Ratchasima 30000, Thailand

The absorption spectra of Cr-containing Li₂O-SiO₂ transparent glass-ceramics was investigated. The crystalline phases precipitated in glass-ceramics are mainly Li₂O·2SiO₂ with a small amount of α-SiO₂. The percent crystallinity and crystal sizes are 40-77 and 20-42 nm, respectively. A strong absorption band ascribed to the charge transfer of Cr⁴⁺ ion and a weak *d-d* absorption band ascribed to Cr³⁺ ion were observed in the glass. However, the new absorption bands appeared at around 600-700 nm and the absorption intensity of these bands increased significantly (about 15 times) upon crystallization. It was suggested that the tetrahedrally coordinated Cr⁴⁺ ion might exist in Li₂O-SiO₂ transparent glass-ceramics.

[Received October 14, 2003; Accepted January 23, 2004]

Key-words : Li₂O-SiO₂ system, Transparent glass-ceramics, Cr ions, Absorption spectra

1. Introduction

Many researches on the behavior of Cr ions in glasses, such as valence state and co-ordination number, have been carried out¹⁾⁻³⁾ in association with color generation. The Cr ions existed in glasses were mainly Cr³⁺ and Cr⁶⁺, and the redox equilibrium between them was discussed with glass composition and melting atmosphere. However, since Cr²⁺ ion was found⁴⁾ and recent years it was reported the existence of Cr⁴⁺ in glasses,⁵⁾⁻⁷⁾ the researches on Cr²⁺ and Cr⁴⁺ ions in glasses and single crystals, especially in laser oscillation materials and opto-electronic devices, is actively taking place. Furthermore, the research on Cr doped transparent glass-ceramics is attempted for the application in various field.^{8),9)} In these field, glasses have many advantages comparing with crystalline materials. They are: flexibility and ease of forming to any shape, uniformity and reproducibility and process economy in high-volume manufacturing, etc.

Li₂O-SiO₂ system is well known as a base glass for glass-ceramics, such as chemically machinable glass-ceramics or high strength glass-ceramics. A transparent glass-ceramics can be readily obtained from this system, in which the transparency is substantially comparable to that of glass in NIR region.¹⁰⁾

The author investigates various properties of Li₂O-SiO₂ system transparent glass-ceramics. Here the absorption spectra of Cr ion containing Li₂O-SiO₂ system transparent glass-ceramics were investigated, and the possibility of the existence of Cr⁴⁺ is suggested.

2. Experiment

2.1. Sample preparation

The composition of glass used is 80SiO₂-4Al₂O₃-13Li₂O-3P₂O₅-0.4Cr₂O₃(mass%). High purity silica sand, alumina and reagent grade chemicals of Li₂CO₃, (NH₄)₂HPO₄ (Carlo Erba) and Cr₂O₃ (Carlo Erba) were used as raw materials. A batch corresponding to 100 g of glass was mixed thoroughly and pre-calcined at 400°C for overnight to remove NH₃. Then it was melted in 100 cc Pt/Rh10 crucible at 1450°C for 3 h in an electric furnace in air, and poured onto iron plate. They

were then annealed at 450°C for 30 min and cooled to room temperature in the furnace. The glasses were heat treated for crystallization at various conditions after the first heat treatment at 500°C for 15 h.

The glass and glass-ceramics were cut and polished into the plate of about 0.8 mm in thickness.

2.2. Absorption measurement

Absorption spectra of glass and glass-ceramics were measured at room temperature with Cary 5E UV-VIS-NIR spectrophotometer in the range of 300-1500 nm.

2.3. XRD

Crystalline phases was examined by powder XRD (Bruker, AXS Model D5005). The crystalline size was calculated by Scherrer's equation:

$$d = 0.9\lambda / \beta \cdot \cos\theta \quad (1)$$

where *d* is the crystalline size (Å), λ the wavelength of X-ray (1.54 Å), β true half width (radian) and θ diffraction angle (degree). The true half width was determined by Jones method,¹¹⁾ and α-quartz was used as a standard.

The percent crystallinity was determined by Ohlberg and Strickler's method¹²⁾ and was calculated by below equation:

$$\text{Percent crystallinity} = 100 \times (I_g - I_x) / (I_g - I_c) \quad (2)$$

where *I_g* is the background intensity of glass, *I_x* the background intensity of specimens and *I_c* the background intensity of crystal at 2θ = 23°. The calibration curve was obtained by mixtures of parent glass and α-quartz with various ratio, and showed a good linearity.

3. Results and discussion

The glass exhibits light green in color. The color of transparent glass-ceramics changes from light green to green-blue, blue, deep blue, and greenish blue depending on heat treatment condition. The crystalline phases precipitated in glass-ceramics are mainly Li₂O·2SiO₂ with a slight amount of Li₂O-SiO₂ crystal at lower temperature. At higher temperature, a small amount of α-quartz crystal also starts to precipitate. Figure 1 shows XRD patterns of glass-ceramics,

Strength of Li₂O-SiO₂-System Transparent Glass-Ceramics

Shigeki MORIMOTO and Waraporn EMEM

School of Ceramic Engineering, Institute of Engineering, Suranaree University of Technology,
111 University Avenue, Muang District, Nakhon Ratchasima 30000, Thailand

Li₂O-SiO₂系透明結晶化ガラスの強度

森本繁樹・Waraporn EMEM

School of Ceramic Engineering, Institute of Engineering, Suranaree University of Technology,
111 University Avenue, Muang District, Nakhon Ratchasima 30000, Thailand

The relationship between fracture strength and crystal size in the Li₂O-SiO₂-system transparent glass-ceramics was investigated. The precipitated crystal phase, percent crystallinity and crystal size were Li₂O·2SiO₂, 60-80% and 20-60 nm, respectively, following heat treatment below 800°C for 5-144 h. It is found that fracture strength increases linearly with increasing crystal size in the range of 20-60 nm for both non abraded and abraded specimens. Fracture strength can be expressed as a function of crystal size, *d* (nm), by

$$\sigma = 100.5 + 2.32d \text{ (MPa) [Non-abraded]}$$

$$\sigma = 56.3 + 0.99d \text{ (MPa) [Abraded]}$$

This result shows the opposite tendency for previous result of glass-ceramics of micrometer order crystals. This indicates that very fine crystals cannot effectively interrupt crack propagation, and hence, the stress required for changing the direction of propagation might be small. It can be considered that a critical crystal size may exist for the attainment of the maximum strength. [Received November 17, 2003; Accepted February 5, 2004]

Key-words : Li₂O-SiO₂ system, Transparent glass-ceramics, Nanocrystals, Fracture strength

1. Introduction

One of the significant characteristics of glass-ceramics is that they are stronger than that of glass. Although glass is a typical brittle material that readily fractures, its theoretical strength is quite high (≈ 10 GPa). However, the practical strength of glass is below 50-100 Mpa. Griffith¹⁾ introduced the "Griffith flaw theory" to explain this phenomena. On the reason is that various kind of flaw existing on the surface act as stress concentrator. A higher strength close to the theoretical strength could be obtained by thin fiber or by removing surface flaws.

Generally, the high strength of glass-ceramics represents practical strength. It is recognized that crystals dispersed in glass-ceramics prevent flaw generation or crack propagation.

Many studies on the relationship between fracture strength and crystal size have carried out for glass-ceramics^{2),3)} and sintered polycrystalline materials.^{4),5)} It is confirmed that fracture strength increases with decreasing crystal size on the basis of Griffith's equation assuming that the crystal size is equal to the crack size in a micrometer-order crystal [$\sigma \propto d^{-1/2}$].⁶⁾ According to this idea, the fracture strength of very fine grained sintered polycrystalline materials and glass-ceramics, e.g., transparent glass-ceramics, should be very high. However, the fracture strength of very fine grained transparent glass-ceramics is not so different from that of conventional glass, hence, this idea is not applicable to these materials.

We investigated the relationship between the fracture strength and crystal size of Li₂O-SiO₂-system transparent glass-ceramics and found that fracture strength increases with increasing crystal size up to 100 nm.

2. Experiment

2.1 Sample preparation

The composition of the glass used is 80SiO₂·4Al₂O₃·

13Li₂O·3P₂O₅ (mass%)[77.7SiO₂·2.3Al₂O₃·18.8Li₂O·1.2P₂O₅ (mol%)]. High-purity silica sand, alumina and reagent grade chemicals of Li₂CO₃ and (NH₄)₂HPO₄ (Carlo Erba) were used as raw materials. A batch corresponding to 200 g of glass was mixed thoroughly and precalcined at 400°C overnight to remove NH₃. Then it was melted in a 100 ml Pt/Rh10 crucible at 1450°C for 3 h in an electric furnace.

A rod about 5 mm diameter was freshly drawn and cut into about 7 cm long sample for strength measurement. The samples were then annealed at 450°C for 30 min and cooled to room temperature in the furnace. They were then heat-treated for crystallization under various conditions.

The densities of glass and glass-ceramics were measured by the He-gas substitution method using Accupyc 1330 (Micromeritics).

2.2 DTA, XRD, SEM

A differential thermal analysis (DTA) was carried out routinely to determine the crystallization temperature at a heating rate of 10 K/min using a Perkin-Elmer DTA-7.

Crystalline phases were examined by powder X-ray diffraction analysis (XRD) (Bruker, AXS Model D5005). Crystalline size was calculated using Scherrer's equation.

$$d = 0.9 \cdot \lambda / \beta \cdot \cos \theta \quad (1)$$

Where *d* is the crystalline size (Å), λ the wavelength of X-ray (1.54Å), β the true half width (radian) and θ the diffraction angle (degree). True half width was determined by the Jones method,⁷⁾ and α -quartz was used as a standard.

Percent crystallinity was determined using Ohlberg and Strickler's method,⁸⁾ and was calculated using by:

$$\text{Percent crystallinity (\%C)} = 100 \times (I_g - I_x) / (I_g - I_c) \quad (2)$$

where *I_g* is the background intensity of glass, *I_x* that of the

Formation, Absorption and Emission Spectra of Cr^{4+} Ions in $\text{Li}_2\text{O}-\text{SiO}_2$ System Transparent Glass-Ceramics

Shigeki MORIMOTO

School of Ceramic Engineering, Institute of Engineering, Suranaree University of Technology,
111 University Avenue, Muang District, Nakhon Ratchasima 30000, Thailand

$\text{Li}_2\text{O}-\text{SiO}_2$ 系透明結晶化ガラス中での Cr^{4+} イオンの生成と光吸収及び発光スペクトル

森本繁樹

School of Ceramic Engineering, Institute of Engineering, Suranaree University of Technology,
111 University Avenue, Muang District, Nakhon Ratchasima 30000, Thailand

The formation mechanism, optical absorption and emission spectra of Cr^{4+} ions-containing $\text{Li}_2\text{O}-\text{SiO}_2$ system transparent glass-ceramics were investigated. In this material, the main crystalline phase was $\text{Li}_2\text{O} \cdot 2\text{SiO}_2$, and the percent crystallinity and crystal size were 67–72 and 20–33 nm, respectively. The remarkable change in color and absorption spectra was observed upon crystallization. The characteristic emission of tetrahedrally coordinated Cr^{4+} ions was identified in the near infrared region, 1000–1600 nm. It was found that tetrahedrally coordinated Cr^{4+} ions exist in this transparent glass-ceramics from absorption and emission measurement. The Cr^{4+} ions exist in residual high SiO_2 glassy phase, and their ligand field parameters are estimated to be: $10Dq = 10,610 \text{ cm}^{-1}$, $B = 690 \text{ cm}^{-1}$ and $Dq/B = 1.54$. This Dq/B value is just below the crossing point of 3T_2 and 1E levels ($Dq/B = 1.6$). The Cr^{4+} ions in $\text{Li}_2\text{O}-\text{SiO}_2$ system transparent glass-ceramics occupy the little stronger ligand field sites than those in aluminate glass reported previously ($Dq/B = 1.2$). It is considered that the Cr^{4+} ions can be formed by the reduction of Cr^{6+} ions (chromate ion $[\text{CrO}_4]^{2-}$) associated with decreasing the basicity of residual glassy phase during crystallization. In this process the behavior of Li^+ ions plays a significant role. The $[\text{CrO}_4]$ formed is equivalent to $[\text{SiO}_4]$ and substitutes $[\text{SiO}_4]$ sites in the residual high SiO_2 glassy phase.

[Received February 16, 2004; Accepted July 30, 2004]

Key-words: $\text{Li}_2\text{O}-\text{SiO}_2$ system, Transparent glass-ceramics, Tetrahedrally coordinated Cr^{4+} ions, Emission spectra

1. Introduction

Nowadays many researches on crystals^{1)–4)} and glasses^{5)–8)} with Cr^{4+} ions in tetrahedral coordination are being done because they are able to produce tunable laser emission at longer wavelength. In the area of telecommunications such materials hold the promise of broad-band optical gain at the 1.3 and 1.5 μm optical communication wavelength.

It has been found that the stable Cr^{4+} ions can be formed only in aluminate, alumino-silicate and gallate system with higher modifier oxides, and their spectroscopic properties have already been measured.^{5)–7)} According to their results, the formation of tetrahedrally coordinated Cr^{4+} ions is related to the interaction between Cr^{3+} ions and oxygen excess defects, such as super oxide ion radicals and peroxy linkage.⁸⁾ Due to the disorder of glass structure the inhomogeneous line-broadening of transition metal ions is caused by site multiplicity. On the other hand, the properties of Cr^{4+} doped glass-ceramics have received little attention, despite the possibilities of crystal site control.⁹⁾ The glass-ceramics, as well as glasses, has many advantages comparing with single crystals: flexibility and ease of forming to any shape, uniformity and reproducibility and process economy in high-volume manufacturing, etc.

The author has investigated the behavior of Cr ions in $\text{Li}_2\text{O}-\text{SiO}_2$ system transparent glass-ceramics,¹⁰⁾ and the possibility of the existence of Cr^{4+} ions in this glass-ceramics was suggested. In this paper, the formation mechanism, absorption and emission spectra of Cr^{4+} ions in $\text{Li}_2\text{O}-\text{SiO}_2$ system transparent glass-ceramics were discussed.

2. Experiments

2.1 Sample preparation

The glass composition of $80\text{SiO}_2 \cdot 4\text{Al}_2\text{O}_3 \cdot 13\text{Li}_2\text{O} \cdot 3\text{P}_2\text{O}_5 \cdot 0.4\text{Cr}_2\text{O}_3$ (mass%) was used. Three glasses were melted under various conditions. (1). A-glass (Oxy): a half of Li_2O was introduced by LiNO_3 and melted in 100 ml Pt/Rh10 crucible in air, (2). B-glass (Air): melted in 100 ml Pt/Rh crucible in air and (3). C-glass: 1.5 mass% carbon was added to batch and melted in covered alumina crucible in air.

High purity silica sand, alumina and reagent grade chemicals of Li_2CO_3 , LiNO_3 , $(\text{NH}_3)_2\text{HPO}_4$ and Cr_2O_3 (Carlo Erba) were used as raw materials. Batches corresponding to 100 g of glass were mixed thoroughly and melted at 1450°C for 2 h under various conditions described above. The molten glasses were poured onto iron plate and pressed by another plate. They were then annealed at 450°C for 30 min. and cooled to room temperature in the furnace.

The glasses were heat treated at 500°C for 15 h for nucleation and subsequently heat treated at various conditions for crystallization. The glasses and glass-ceramics were optically polished into 0.8 mm in thickness.

Crystalline phases, percent crystallinity and crystal size were determined by X-ray diffraction method (XRD). The detail of measurement is given elsewhere.¹¹⁾

2.2 Preparation of polycrystalline $\text{Li}_2\text{O} \cdot 2\text{SiO}_2$: Cr

The polycrystalline $\text{Li}_2\text{O} \cdot 2\text{SiO}_2$: Cr was prepared by a solid state reaction to investigate whether Cr^{4+} ions exist in this crystal. A mixture of high purity silica sand, $(1/2\text{Li}_2\text{CO}_3 + 1/2\text{LiNO}_3)$ and Cr_2O_3 (Carlo Erba) corresponding to $\text{Li}_2\text{O} \cdot 2\text{SiO}_2$: Cr_2O_3 (1 mass%) composition was heat treated at 900°C

Effect of K₂O on Crystallization of Li₂O-SiO₂ Glass

Shigeki MORIMOTO

Li₂O-SiO₂ 系ガラスの結晶化に及ぼす K₂O の効果

森本繁樹

School of Ceramic Engineering, Institute of Engineering, Suranaree University of Technology, 111 University Avenue, Muang District, Nakhon Ratchasima 30000, Thailand

The effect of a small amount of K₂O on the crystallization behavior of the system of Li₂O-SiO₂ glass was investigated. Lithium disilicate (Li₂O·2SiO₂; L·2S) and lithium metasilicate (Li₂O·SiO₂; L·S) crystals precipitate simultaneously, but only L·2S crystals grow upon further heat treatment in the glass without K₂O (Li glass). In the glass containing K₂O (K3 glass), only L·S crystals precipitate and grow. The stable crystalline phases are L·2S and SiO₂ crystals in both glasses. Phase separation was observed before crystallization; a Li₂O-rich phase formed an isolated droplet phase in Li glass and the continuous phase in K3 glass. The Li⁺-K⁺ ion exchange test confirmed these structures. [SEM-EDX] analysis confirmed that K₂O exists in the Li₂O rich phase after phase separation in K3 glass. Thus, K3 glass separates into two phases, one of which is a continuous phase rich in Li₂O and containing considerable amount of K₂O. The L·S crystal precipitates and grows in this phase upon further heat treatment. Consequently, K₂O suppresses the crystallization of L·2S and promotes the precipitation of L·S crystals.

[Received September 12, 2005; Accepted November 17, 2005]

Key-words: Li₂O-SiO₂ glass, Phase separation, Crystallization, Lithium disilicate, Lithium metasilicate, K₂O

1. Introduction

It is well known that the Li₂O-SiO₂ system is a base glass for glass ceramics, and much research on the crystallization process has been carried out.¹⁾⁻⁴⁾ According to the phase diagram of this system, the immiscible region is located between the Li₂O·2SiO₂ and SiO₂ end members, and the glass containing more SiO₂ than the Li₂O·2SiO₂ composition separates into two phases; one is an isolated droplet phase rich in SiO₂ and the other is a matrix phase close to the Li₂O·2SiO₂ composition. Li₂O·2SiO₂ crystals precipitate homogeneously in matrix phase upon the heat treatment.³⁾ Recently, Soares et al.⁴⁾ confirmed that both Li₂O·SiO₂ and Li₂O·2SiO₂ crystals precipitate simultaneously at first, but only Li₂O·2SiO₂ grows. Also Li₂O·SiO₂ disappears upon further heat treatment in glass with Li₂O·2SiO₂ composition.

From a practical point of view, high-hardness and high-fracture strength glass ceramics composed of lithium disilicate crystal can be obtained from modified Li₂O-SiO₂ glass. On the contrary, a modified Li₂O-SiO₂ glass containing a small percentage of K₂O has been applied as a chemically machinable photosensitive glass or glass ceramic.⁶⁾ In this case, Li₂O·SiO₂ crystal precipitates as a metastable initial phase and converts to Li₂O·2SiO₂ and quartz crystals upon heat treatment above 800°C. The solubility of Li₂O·SiO₂ crystal in HF solution is much higher than that of glass, and therefore, chemical machining can be achieved. Although the amount of K₂O added is usually 3-4 mass% and the SiO₂/Li₂O ratio is kept higher than 2.5, lithium metasilicate crystal precipitates as an initial phase. The Li₂O·2SiO₂ crystal should precipitate according to the phase diagram.⁷⁾ This behavior is well known, however, the reason behind it is not yet clear.

The author investigated the effect of K₂O on crystallization behavior of the system of Li₂O-SiO₂. The results are reported here.

2. Experimental

2.1 Sample preparation

Two types of glass were prepared, as shown in Table 1. Li₂O of 3 mol% was replaced by equimolar K₂O (K3 glass).

High-purity silica sand and alumina, and reagent-grade chemicals of Li₂CO₃, K₂CO₃, (NH₄)₂HPO₄ were used as raw materials. Batches corresponding to 150 g of glass were mixed thoroughly and precalcined at 300°C overnight to remove NH₃. They were melted in a 100 ml Pt/Rh10 crucible at 1450°C for 2 h in an electric furnace in air. The molten glasses were poured onto an iron plate and crushed, and melted again under the same conditions. They were then poured onto the iron plate and pressed by another iron plate. The glasses were heat treated for crystallization under various conditions after an initial heat treatment at 500°C for 15 h for nucleation.

2.2 TDA and DTA

Glass transition temperature (T_g), dilatometric softening point (Y_p) and thermal expansion coefficient of glasses were measured routinely using a fused silica single-push-rod dilatometer (Netzsch 402P) at the heating rate of 5°C/min. The differential thermal analysis (DTA) was carried out using a Perkin-Elmer DTA-7 at the heating rate of 10°C/min.

2.3 XRD and SEM

Crystalline phases were examined by powder X-ray diffraction analysis (XRD, Bruker, AXS Model 5005) under the condition of Cu K α radiation, 40 kV-40 mA, 0.01° step and 1 s/

Table 1. Glass Compositions (mol%) Studied

No.	SiO ₂	Al ₂ O ₃	Li ₂ O	Na ₂ O	K ₂ O	P ₂ O ₅	SiO ₂ /Li ₂ O
Li	73.0	2.15	23.7	-	-	1.15	3.08
K3	73.0	2.15	20.7	-	3.0	1.15	3.53

Strengthening of $\text{Li}_2\text{O} \cdot 2\text{SiO}_2$ Transparent Glass-Ceramics by Ion Exchange

Chokchai YATONGCHAI and Shigeki MORIMOTO

イオン交換法による $\text{Li}_2\text{O} \cdot 2\text{SiO}_2$ 系透明結晶化ガラスの強化

Chokchai Yatongchai · 森本繁樹

School of Ceramic Engineering, Institute of Engineering, Suranaree University of Technology,
111 University Avenue, Muang District Nakhon Ratchasima 30000, Thailand

The chemical strengthening of $\text{Li}_2\text{O} \cdot 2\text{SiO}_2$ transparent glass-ceramics was investigated. The fracture strength of glass and glass-ceramics increased first and then decreased, and the crack formation and peeling of ion exchanged layer were observed for both $\text{Li}^+ \leftrightarrow \text{Na}^+$ and $\text{Li}^+ \leftrightarrow \text{K}^+$ ion exchange. This suggests that the sub-microscopic crack generates perpendicular to the surface when the ion exchanged layer peels off from the surface. The volume change by $\text{Li}^+ \leftrightarrow \text{Na}^+$ and $\text{Li}^+ \leftrightarrow \text{K}^+$ ion exchange is very large, over 10%, this large volume change causes the peeling and crack formation of ion exchanged layer despite in which the compressive stress arise. In the early stage of ion exchange, the compressive stress arisen affects effectively on the increase in strength. However, as increase in the thickness of ion exchanged layer, the volume change of ion exchanged layer can not be neglected, and crack and peeling may generate in that layer. Finally, the fracture strength decreases.

[Received August 8, 2005; Accepted January 19, 2006]

Key-words : Transparent glass-ceramics, Ion exchange, XRD, $\text{Li}_2\text{O} \cdot 2\text{SiO}_2$ crystal, Crowding

1. Introduction

Transparent glass-ceramics comprises the essential group in glass-ceramics, is composed of fine-grained crystallites, usually nano-scale size, and residual glassy phase. The transparent glass-ceramics has been developed and used for many applications, such as transparent cookware, precision optical instruments, ring-laser gyroscope, large telescope mirror blanks, etc. Further, recently, active ions, transition metal ion and rare-earth ion, doped transparent glass-ceramics are developed and many researches on this materials have been carried out.¹⁾⁻⁴⁾

Li_2O - SiO_2 system of glass has well been known as a base glass for glass-ceramics, such as chemically machinable glass-ceramics and high strength glass-ceramics. And also, transparent glass-ceramics based on lithium metasilicate [$\text{Li}_2\text{O} \cdot \text{SiO}_2$] and lithium disilicate [$\text{Li}_2\text{O} \cdot 2\text{SiO}_2$] crystals can be obtained easily in this system of glass.^{5),6)} However, the mechanical strength of transparent glass-ceramics is not so high,⁷⁾ similar to that of glass, and hence the higher mechanical strength is required in special application area.

There are two methods to increase mechanical strength of glasses and glass-ceramics, thermal strengthening and chemical strengthening. The latter is called as ion exchange strengthening method and has many advantages over thermal strengthening, such as easy processing, available for any shapes of articles, available for thin articles, available to maintain the surface flatness and smoothness, capable of applying for low thermal expansion materials, etc. $\text{Li}^+ \leftrightarrow \text{Na}^+$ and $\text{Li}^+ \leftrightarrow \text{K}^+$ ion exchange is expected to increase mechanical strength of these transparent glass-ceramics.

Here the chemical strengthening of $\text{Li}_2\text{O} \cdot 2\text{SiO}_2$ transparent glass-ceramics was investigated.

2. Experiments

2.1 Sample preparation

The composition of glass used is $80\text{SiO}_2 \cdot 4\text{Al}_2\text{O}_3 \cdot 13\text{Li}_2\text{O} \cdot 3\text{P}_2\text{O}_5$ (mass%) [$72.9\text{SiO}_2 \cdot 2.15\text{Al}_2\text{O}_3 \cdot 23.8\text{Li}_2\text{O} \cdot 1.15\text{P}_2\text{O}_5$ (mol%)]. High purity silica sand, alumina and reagent grade

chemicals of Li_2CO_3 and $(\text{NH}_4)_2\text{HPO}_4$ (Aldrich) were used as raw materials. A batch corresponding to 200 g of glass was mixed thoroughly and pre-calcined at 300°C for overnight to remove NH_3 . Then it was melted in a 100 ml Pt/Rh10 crucible at 1450°C for 2 h in an electric furnace. The molten glass was poured onto iron plate and crushed, and then it was melted at the same condition to improve homogeneity.

A rod about 5 mm diameter was freshly drawn and cut into about 7 cm long. The samples were annealed at 450°C for 30 min and cooled to room temperature in the furnace.

The samples were heat treated at 500°C for 15 h for nucleation and 700°C for 10 h for crystallization.

2.2 Ion exchange

The samples were ion exchanged in NaNO_3 and KNO_3 molten bath under various conditions (Salt/glass ratio is 10 by weight).

2.3 XRD and SEM

Crystalline phases and lattice constant were determined by powder X-ray diffraction analysis (XRD) (Bruker, AXS Model D5005). Si powder was used as an internal standard for the measurement of the lattice constant. The surface structure of glasses and glass-ceramics after ion exchange were observed by scanning electron microscopy (SEM; JEOL, JSM 640).

2.4 Strength measurement

The fracture strength was measured using Instron Model 5569 according to ASTM C-158. The three point bending method was employed, and the span length and loading rate were 50 mm and 1 mm/min, respectively.

3. Results and discussion

The glass transition temperature (T_g), dilatometric softening point (Y_p), thermal expansion coefficient (α) and density of glass were 473°C , 541°C , $88.9 \times 10^{-7}/\text{K}$ (30 - 300°C) and 2.354 g/cm^3 , respectively. The main crystal, percent crystallinity and crystallite size of glass-ceramics were $\text{Li}_2\text{O} \cdot 2\text{SiO}_2$ crystal (JCPDS 40-0376), about 70% and 40 nm, respectively. The thermal expansion coefficient and density of transparent glass-ceramics were $90 \times 10^{-7}/\text{K}$ (30 - 300°C) and 2.414 g/cm^3 .

Absorption and Emission Spectra of Ni-Doped Glasses and Glass-Ceramics in Connection with Its Co-Ordination Number

Ni 含有ガラスと透明結晶化ガラスの光吸収及び発光スペクトルとその配位数との関係

Sasithorn KHONTHON, Shigeki MORIMOTO and Yasutake OHISHI*

School of Ceramic Engineering, Institute of Engineering, Suranaree University of Technology,
111 University Avenue, Muang District, Nakhon Ratchasima 30000, Thailand

*Department of Future-oriented Basic Science and Materials, Toyota Technological Institute,
2-12-1, Hisakata, Tempaku-ku, Nagoya-shi 468-8511, Japan

The absorption and emission spectra of Ni-doped glasses and transparent glass-ceramics are discussed in relation to its coordination number. The results evidenced that the color changed drastically to deep pink from yellow for the lithium metasilicate crystal based transparent glass-ceramics and to blue from brown for the spinel crystal based transparent glass-ceramics after crystallization, respectively. The absorption spectra of lithium metasilicate and Spinel glasses suggest the existence of a tetrahedral Ni^{2+} ion and a trigonal bipyramid Ni^{2+} ion. On the contrary, tetrahedral Ni^{2+} ions in the lithium metasilicate transparent glass-ceramics and the octahedral Ni^{2+} ion in Spinel transparent glass-ceramics are dominant. The emission at around 580 nm was observed in Spinel transparent glass-ceramics under the excitation of 380 nm, however, a very weak or no emission was observed in the lithium metasilicate glass, lithium metasilicate transparent glass-ceramics and Spinel glass under the excitation of 430 nm. This emission might be due to a ${}^1T_1(D) \rightarrow {}^3A_1(F)$ transition after the excitation from ${}^3A_2(F)$ to ${}^3T_1(P)$ of the octahedral Ni^{2+} ions. In addition, only Spinel transparent glass-ceramics exhibits a broad NIR emission at around 1220 nm under the excitation of a 974 nm laser diode. This emission may be due to ${}^3T_2(F) \rightarrow {}^3A_2(F)$ transition. It is considered that the tetrahedral Ni^{2+} ion is located between the chains in the lithium metasilicate crystal.

[Received May 25, 2006; Accepted July 20, 2006]

Key-words : Ni^{2+} ion, Transparent glass-ceramics, Absorption spectra, VIS-NIR emission spectra, Coordination number

1. Introduction

Ni-doped glasses tend to absorb over the entire visible spectrum typically producing brown colored glasses, and it was concluded that Ni was present as Ni^{2+} in a wide range of compositions in both four-[Ni(4)] and six-coordination[Ni(6)] with oxygen in the past.^{1,2)} Although the Ni^{2+} ion has a clear preference for octahedral coordination, it was well known that tetrahedral Ni^{2+} ion favorably appeared in high-alkali borate and borosilicate glasses and octahedral Ni^{2+} ion existed in low alkali borate and borosilicate glasses, and their color were pink and green-blue, respectively.^{3,4)} Their optical properties have been recognized using ligand field theory.³⁾ However, recently the modern spectroscopic techniques (EXAFS etc.) have confirmed that a trigonal bipyramid Ni^{2+} [Ni(5)] also presented in many glasses and the brown colored glasses contained both [Ni(4)] ion and Ni[(5)]⁵⁻⁸⁾ ion, and Ni was found with three coordination numbers (6, 5 and 4) in some glasses.⁶⁾ The color of glasses changes depending on the fraction of these Ni ions.

The spectroscopy of the Ni^{2+} ion-doped single crystals and glass-ceramics has received much attention in recent years. Much of the present interest focuses on the possibility of Ni^{2+} -doped materials as active media for tunable near infrared lasers.⁹⁻¹²⁾ In these materials, Ni^{2+} ion occupies octahedral sites and exhibits a broad emission in near infrared region (1100-1600 nm). In contrast, no emission of tetrahedrally coordinated Ni^{2+} ion even at cryogenic temperature has been reported.

In this paper the absorption and emission spectra of Ni-doped glasses and glass-ceramics are discussed in relation to its coordination number.

2. Experimental

2.1 Sample preparation

The compositions of glasses studied are shown in Table 1. These glasses are able to convert to transparent glass-ceramics based on $Li_2O \cdot SiO_2$ crystal (LS3) and Spinel crystal [(Mg, Zn) Al_2O_4] (Spinel) by adequate heat treatment.

High purity silica sand, alumina and reagent grade chemicals of Li_2CO_3 , K_2CO_3 , MgO, ZnO, TiO_2 , ZrO_2 and NiO were used as raw materials. Batches corresponding to 50 g of glass were mixed thoroughly and melted in a 50 cc Pt/Rh10 crucible under appropriate condition in an electric furnace in air. After melting they were poured onto iron plate and pressed by another iron plate. Then they were annealed at suitable conditions and cooled slowly in the furnace.

The glasses were heat treated under various conditions for nucleation and crystallization. The glasses and glass-ceramics were cut and polished optically into about 1 mm in thickness for optical measurement.

2.2 XRD

Crystalline phases, percent crystallinity and crystalline size were measured by powder X-ray diffraction analysis (XRD, Bruker, AXS Model D5005) under the condition of Cu K α radiation ($\lambda = 0.154$ nm), 40 kV-40 mA, 0.01°/step and 1 s/step. The percent crystallinity was determined using Ohlberg and Strickler's method.¹³⁾ α -Quartz crystal and parent glasses

Table 1. Glass Compositions (mass%) Studied

Name	SiO ₂	Al ₂ O ₃	Li ₂ O	K ₂ O	MgO	ZnO	TiO ₂	ZrO ₂	NiO*
LS3	65	5	26	4	-	-	-	-	0.4
Spinel	46.9	26.54	-	-	5.25	10.59	1.79	8.93	0.4

* excess wt%

Phase separation and crystallization in the system $\text{SiO}_2\text{--Al}_2\text{O}_3\text{--P}_2\text{O}_5\text{--B}_2\text{O}_3\text{--Na}_2\text{O}$ glasses

Shigeki Morimoto *

*School of Ceramic Engineering, Institute of Engineering, Suranaree University of Technology, 111 University Avenue,
Muang District, Nakhon Ratchasima 30000, Thailand*

Received 12 July 2005; received in revised form 26 January 2006
Available online 24 March 2006

Abstract

The phase separation and crystallization behavior in the system $(80 - X)\text{SiO}_2 \cdot X(\text{Al}_2\text{O}_3 + \text{P}_2\text{O}_5) \cdot 5\text{B}_2\text{O}_3 \cdot 15\text{Na}_2\text{O}$ (mol%) glasses was investigated. Glasses with $X = 20$ and 30 phase separated into two phases, one of which is rich in $\text{Al}_2\text{O}_3\text{--P}_2\text{O}_5\text{--SiO}_2$ and forms a continuous phase. Glasses containing a larger amount of $\text{Al}_2\text{O}_3\text{--P}_2\text{O}_5$ ($X = 40$ and 50) readily crystallize and precipitates tridymite type AlPO_4 crystals. It is estimated that the phase separation occurs forming continuous $\text{Al}_2\text{O}_3\text{--P}_2\text{O}_5\text{--SiO}_2$ phase at first, and then tridymite type AlPO_4 crystals precipitate and grow in this phase. Highly transparent glass–ceramics comparable to glass can be successfully obtained by controlling heat treatment precisely. The crystal size and percent crystallinity of these transparent glass–ceramics are 20–30 nm and about 50%, respectively.

© 2006 Elsevier B.V. All rights reserved.

PACS: 64.75; 61.43; 81.05.P; 78.66.J

Keywords: Crystallization; Glass–ceramics; Nucleation; Crystals; Nanocrystals; Optical properties; Oxide glasses; Alkali silicates; Phases and equilibria

1. Introduction

Glass–ceramics can be defined as a two-phase system comprising crystals that have been controllably grown from a parent glass by precise heat treatment. Optical properties of glass–ceramics have been impaired by the scattering losses. However, the ability of some crystalline phases to partition rare-earth or transition metal ions into the crystal phase during crystallization has suggested that these materials could provide efficient lasing hosts [1–5]. Such systems would be capable of properties that are glass-like in most respects, except for the spectroscopy, which can be crystal-like.

In early 1960s, transparency which was sufficiently good, so that imaging through short pass length was possi-

ble, was observed in certain glass–ceramics materials [6] and this eventually led to a commercial cookware application. This work was instrumental in the subsequent discovery of many new transparent glass–ceramic systems [7–10].

From the structure of glass point of view, network mixed glasses in the system $\text{SiO}_2\text{--Al}_2\text{O}_3\text{--P}_2\text{O}_5\text{--B}_2\text{O}_3$ ($-\text{Na}_2\text{O}$) are also of special interest because all these may act as glass formers [11]. It is well known that AlPO_4 crystal readily precipitates from glasses containing relatively large amount of Al_2O_3 and P_2O_5 [12,13]. AlPO_4 crystal has all the three normal silica structures and has a bulk and surface acoustic wave function similar to α -quartz [14–17].

In order to obtain transparent glass–ceramics based on AlPO_4 crystal, the phase separation and crystallization behavior of glasses in the system $\text{SiO}_2\text{--Al}_2\text{O}_3\text{--P}_2\text{O}_5\text{--B}_2\text{O}_3\text{--Na}_2\text{O}$ was investigated, and highly transparent glass–ceramics could be successfully obtained. These results are reported.

* Tel.: +66 44 22 4475; fax: +66 44 22 4165.
E-mail address: shigeki@ccs.sut.ac.th

Luminescence Characteristics of Ni²⁺ Ion-Doped Glasses and Glass-Ceramics in Relation to Its Coordination Number*

Sasithorn KHONTHON**, Shigeki MORIMOTO** and Yasutake OHISHI***

**School of Ceramic Engineering, Institute of Engineering,
Suranaree University of Technology,
111 University Avenue, Muang District, Nakhon Ratchasima 30000, Thailand
E-mail: shigeki@sut.ac.th

***Department of Future-oriented Basic Science and Materials,
Toyota Technological Institute
2-12-1, Hisakata, Tempaku-ku, Nagoya 468-4511, Japan

Abstract

Ni²⁺ ions occupy the tetrahedral (4), trigonal bipyramid (5) and octahedral (6) sites in glasses and glass-ceramics. The color changes depending on coordination number, typically pink for tetrahedral site, brown for trigonal bipyramid and tetrahedral sites and green to blue for octahedral site, respectively. The broad near infrared (NIR) emission peaking at around 1220 nm was observed for octahedral Ni²⁺ ions. This emission is due to ³T₂(F) → ³A₂(F) transition.

Key words: Ni²⁺ Ion, Transparent Glass-Ceramics, Absorption Spectra, UV-VIS-NIR Emission Spectra, Coordination Number

1. Introduction

Ni-doped glasses tend to absorb over the entire visible spectrum typically producing brown colored glasses, and it was concluded that Ni was present as Ni²⁺ in a wide range of compositions in both four-[Ni(4)] and six-coordination[Ni(6)] with oxygen in the past^(1,2). Although the Ni²⁺ ion has a clear preference for octahedral coordination, it was well known that tetrahedral Ni²⁺ favorably appeared in high-alkali borate and borosilicate glasses and octahedral Ni²⁺ existed in low alkali borate and borosilicate glasses, and their color were pink and green-blue, respectively⁽³⁾. Their optical properties have been recognized using ligand field theory⁽³⁾. However, recently the modern spectroscopic techniques (EXAFS etc.) have confirmed that a trigonal bipyramid Ni²⁺ [Ni(5)] also presented in many glasses and the brown colored glasses contained both [Ni(4)] and Ni[(5)]⁽⁴⁻⁷⁾, and Ni was found with three coordination numbers (6, 5 and 4) in specified glasses⁽⁵⁾. The color of glasses changes depending on the fraction of these Ni ions.

The spectroscopy of the Ni²⁺ ion-doped single crystals and glass-ceramics has received much attention in recent years. Much of the present interest focuses on the possibility of Ni²⁺-doped materials as active media for tunable near infrared lasers⁽⁸⁻¹¹⁾. In these materials, Ni²⁺ ion occupies octahedral sites and exhibits a broad emission in near infrared (NIR) region (1100-1600 nm). In contrast, no emission of tetrahedrally coordinated Ni²⁺ even at cryogenic temperature has been reported.

In this paper the absorption and emission spectra of Ni-doped glasses and glass-ceramics are discussed in relation to its coordination number.

Appendix C

Patents



คำขอรับสิทธิบัตร / อนุสิทธิบัตร

- การประดิษฐ์
 การออกแบบผลิตภัณฑ์
 อนุสิทธิบัตร

ข้าพเจ้าผู้ลงลายมือชื่อในคำขอรับสิทธิบัตร/อนุสิทธิบัตรนี้
 รับสิทธิบัตร/อนุสิทธิบัตร ตามพระราชบัญญัติสิทธิบัตร พ.ศ.2522
 ที่เพิ่มเติมโดยพระราชบัญญัติสิทธิบัตร(ฉบับที่ 2) พ.ศ. 2535
 และ พระราชบัญญัติสิทธิบัตร (ฉบับที่ 3) พ.ศ. 2542

สำหรับเจ้าหน้าที่

วันรับคำขอ	17 ธ.ค. 2557	เลขที่คำขอ	089498
วันยื่นคำขอ			
สัญลักษณ์จำแนกการประดิษฐ์ระหว่างประเทศ			
ใช้กับแบบผลิตภัณฑ์ ประเภทผลิตภัณฑ์			
วันประกาศโฆษณา		เลขที่ประกาศโฆษณา	
วันออกสิทธิบัตร/อนุสิทธิบัตร		เลขที่สิทธิบัตร/อนุสิทธิบัตร	
ลายมือชื่อเจ้าหน้าที่			

ชื่อที่แสดงถึงการประดิษฐ์/การออกแบบผลิตภัณฑ์

กรรมวิธีการผลิตกระดาษ-เซรามิก ชนิดเบตา-แคลเซียมไฮดรอกไซด์เพื่อใช้ทำอุปกรณ์ในร่างกายและสามารถตัดและเจาะได้ควม
 คำขอรับสิทธิบัตรการออกแบบผลิตภัณฑ์นี้เป็นคำขอสำหรับผลิตภัณฑ์อย่างเดียวกันและเป็นคำขอลำดับที่
 ในจำนวน คำขอ ที่ยื่นในคราวเดียวกัน **เครื่องจักรกล**

ผู้ขอรับสิทธิบัตร/อนุสิทธิบัตร และที่อยู่(เลขที่ ถนน ประเทศ)

มหาวิทยาลัยเทคโนโลยีสุรนารี

111 ถนนมหาวิทยาลัย ตำบลสุรนารี อำเภอเมือง จ.นครราชสีมา 30000 ประเทศไทย

3.1 สัญชาติ ไทย

3.2 โทรศัพท์ (044) 224-043-4

3.3 โทรสาร (044) 224-070

3.4 อีเมล

สิทธิในการขอรับสิทธิบัตร/อนุสิทธิบัตร

- ผู้ประดิษฐ์/ผู้ออกแบบ ผู้รับโอน ผู้ขอรับสิทธิโดยเหตุอื่น

ตัวแทน (ถ้ามี) ที่อยู่ (เลขที่ ถนน จังหวัด รหัสไปรษณีย์)

นายราชูย์ อิศ์เวศน

623 หมู่ 4 ถนนมหาวิทยาลัย ตำบลหนองจะบก อำเภอเมือง
จังหวัดนครราชสีมา 30000

5.1 ตัวแทนเลขที่ 1238

5.2 โทรศัพท์ (044) 224043-4, 224047-8

5.3 โทรสาร (044) 224043, 224070

5.4 อีเมล

ผู้ประดิษฐ์/ผู้ออกแบบผลิตภัณฑ์ และที่อยู่ (เลขที่ ถนน ประเทศ)

ปรากฏตามเอกสารแนบท้าย

คำขอรับสิทธิบัตร/อนุสิทธิบัตรนี้แยกจากหรือเกี่ยวข้องกับคำขอเดิม

ผู้ขอรับสิทธิบัตร/อนุสิทธิบัตร ขอให้ออกว่าคำขอรับสิทธิบัตร/อนุสิทธิบัตรนี้ ในวันเดียวกับคำขอรับสิทธิบัตร

ที่ วันยื่น เพราะคำขอรับสิทธิบัตร/อนุสิทธิบัตรนี้แยกจากหรือเกี่ยวข้องกับคำขอเดิมเพราะ

- คำขอเดิมมีการประดิษฐ์หลายอย่าง ถูกคัดค้านเนื่องจากผู้ขอไม่มีสิทธิ ขอเปลี่ยนแปลงประเภทของสิทธิ

หมายเหตุ ในกรณีที่ไมอาจระบุรายละเอียดครบถ้วน ให้จัดทำเป็นเอกสารแนบท้ายแบบพิมพ์นี้โดยระบุหมายเลข คำกับขอและหัวข้อที่แสดงรายละเอียด
 เพิ่มเติมดังกล่าวด้วย

Appendix D
Curriculum Vitae

Curriculum Vitae

Name-Surname (in Thai)
(in English) Shigeki Morimoto
Gender Male Date of Birth 19/March/1949
Place of Birth Tottori-City, Tottori-Prefecture, Japan Age 57
Title: (e.g. Lecturer, Assist. Prof., Assoc. Prof., Prof.) Assistant Professor
Educational Qualification Ph.D. (Engineering), Tokyo University, Japan(1991)
Contact Address:
Office: School of Ceramic Engineering, Institute of Engineering, Suranaree University of
Technology
Telephone/Fax 66-44-22-4475/4612
E-mail-address shigeki@ccs.sut.ac.th
Home: SUT (Campus)
Telephone/Fax 66-44-22-5680 Mobile Phone None

Research Experience

A. National and International Publication

- (1). **Morimoto, S., "Optical Absorption of Cr-Containing Li₂O-SiO₂ System Transparent Glass-Ceramics", *Journal of Ceramic Society of Japan*, Vol. 112, (2004) pp.130-132.**
- (2). **Morimoto, S. and Emem, W., "Strength of Li₂O-SiO₂ System Transparent Glass-Ceramics", *Journal of Ceramic Society of Japan*, Vol. 112, (2004) pp.259-262.**
- (3). **Morimoto, S., "Formation, Absorption and Emission Spectra of Cr⁴⁺ Ions in Li₂O-SiO₂ System Transparent Glass-Ceramics", *Journal of Ceramic Society of Japan*, Vol. 112, (2004) pp.486-490.**
- (4). **Morimoto, S., "Effect of K₂O on Crystallization of Li₂O-SiO₂ Glass", *Journal of Ceramic Society of Japan*, Vol. 114, (2006) pp.195-198.**
- (5). **Yatongchai, C. and Morimoto, S., "Strengthening of Li₂O·2SiO₂ Transparent Glass-Ceramics by Ion Exchange", *Journal of Ceramic Society of Japan*, Vol. 114, (2006) pp.227-229.**
- (6). **Morimoto, S., "Phase Separation and Crystallization in the System SiO₂-Al₂O₃-P₂O₅-B₂O₃-Na₂O Glasses", *Journal of Non-Crystalline Solids*, Vol. 352, (2006) pp.756-760.**
- (7). **Khonthon, S. and Morimoto, S., "Absorption and Emission Spectra of Ni-doped Glasses and Glass-Ceramics in Connection with its Coordination Number", *Journal of Ceramic Society of Japan*, Vol. 114, (2006) pp.791-794.**

B. Useful research outputs

Patent for "Preparation of Machinable Glass-ceramics Based on β -Ca₂P₂O₇ Crystal"

C. Others such as textbooks, articles, proceedings, patents, etc.

1. Proceedings

- (1). **Morimoto, S.**, “**Absorption and Emission Spectra of Cr Ion-Containing Transparent Glass-Ceramics**”, *XXth International Congress on Glass*, P-07-100, Kyoto, Japan, 26/Sept.-1/Oct. (2004).
- (2). **Morimoto, S.**, “**Absorption and Emission Spectra of Cr⁴⁺ Ion in Li₂O-SiO₂ System Transparent Glass-Ceramics**”, *International Conference on Smart Materials*, O-3-1-3, Chiang Mai, Thailand, 1-3/Dec. (2004).
- (3). **Morimoto, S.** and **Charussri Lorprayoon** “**Preparation of Machinable Glass-ceramics Based on β -Ca₂P₂O₇ Crystal**”, *International Conference on Smart Materials*, O-3-1-5, Chiang Mai, Thailand, 1-3/Dec. (2004).
- (4). **Morimoto, S.**, “**Effect of K₂O on the Crystallization in the Li₂O-SiO₂ System of Glass**”, *46 th Meeting on Glass and Photonics Materials*, Glass Division of The Ceramic Society of Japan, A03, Hikone, Japan, 21-22/Nov.(2005).
- (5). **Yatongchai, C.** and **Morimoto, S.**, “**Decrystallization/Amotphization of Li₂O-SiO₂ Transparent Glass-Ceramics by Ion Exchange**”, *46 th Meeting on Glass and Photonics Materials*, Glass Division of The Ceramic Society of Japan, A04, Hikone, Japan, 21-22/Nov.(2005).
- (6). **Emem, W.** and **Morimoto, S.**, “**Preparation of Glass-Ceramics Using Fly Ash as a Raw Material**”, *46 th Meeting on Glass and Photonics Materials*, Glass Division of The Ceramic Society of Japan, A05, Hikone, Japan, 21-22/Nov.(2005).
- (7). **Morimoto, S.**, “**Effect of K₂O on the Crystallization in the Li₂O-SiO₂ System of Glass**”, *46th Meeting on Glass and Photonics Materials*, Glass Division of The Ceramic Society of Japan, A03, Hikone, Japan, 21-22/Nov.(2005).
- (8). **Khonthon, S.**, **Morimoto, S.** and **Ohishi. Y.**, “**Luminescence Characteristics of Ni²⁺ Ion-doped Glasses and Glass-Ceramics in relation to its Coordination Number**”, *Asian Symposium on Materials and Processing 2006*, A-16, Bangkok, Thailand, 9-10/Nov. (2006).
- (9). **Morimoto, S.**, **Khonthon, S.** and **Ohishi. Y.**, “**Luminescence Characteristics of Se-, Te- and Bi-doped Glasses and Glass-Ceramics**”, *Asian Symposium on Materials and Processing 2006*, A-17, Bangkok, Thailand, 9-10/Nov. (2006).
- (10). **Morimoto, S.**, **Khonthon, S.** and **Ohishi. Y.**, “**Luminescence Characteristics of Te- and Bi-doped Glasses and Glass-Ceramics**”, *47th Symposium on Glasses and Photonics Materials*, Glass Division of The Ceramic Society of Japan, 2A-09, Chiba, Japan, 21-22//Nov. (2006).

2. Patents

Morimoto, S. and **Charussri Lorprayoon**, “**Preparation of Machinable Glass-ceramics Based on β -Ca₂P₂O₇ Crystal**”, 14/May/2003. Thailand

D. Awarded Awards

None.....

E. Specialized Fields

Glass Science and Technology, Inorganic Chemistry, Materials Science.....

F. Current Job responsibility

■ **Research Work**

- (1). "Preparation of Porous Glass Using Fly Ash as a Raw Material", Co-advisor for Master Student(School of Chemical Engineering, Institute of Engineering, SUT)
- (2). "Luminescence Characteristics of Se-, Te- and Bi-doped Glasses and Glass-Ceramics"